AROMATASE INHIBITORS PRODUCE HYPERSENSITIVITY IN EXPERIMENTAL MODELS OF PAIN: STUDIES *IN VIVO* AND IN ISOLATED SENSORY NEURONS

Jason Dennis Robarge

Submitted to the faculty of the University Graduate School
in partial fulfillment of the requirements
for the degree
Doctor of Philosophy
in the Department of Pharmacology and Toxicology,
Indiana University

September 2014

Accepted by the Graduate Faculty, of Indiana University, in partial fulfillment of the requirements for the degree of Doctor of Philosophy.

_____

David A. Flockhart, M.D., Ph.D., Chair

_____

Jill C. Fehrenbacher, Ph.D.

Doctoral Committee

_____

Rajesh Khanna, Ph.D.

_____

Todd C. Skaar, Ph.D.

June 9, 2014

_____

Michael R. Vasko, Ph.D.

DEDICATION

For Dad

ACKNOWLEDGEMENTS

This scientific endeavor was possible with the support, guidance, and collaboration of many individuals at Indiana University. Foremost, I am grateful for the mentorship of two excellent scientists, Dr. David Flockhart and Dr. Michael Vasko, who encouraged me to pursue scientific questions with thoughtful ambition. For the rest of my scientific career, I will always ask two critical questions: “What’s the clinical impact?” and “What’s the question?”. I am also equally thankful for the friendship and mentorship of many members of the Vasko lab family. I enjoyed so many enlightening conversations about scientific and non-scientific matters alike with Dr. Djane Duarte, Dr. Ramy Habashy, Behzad Shariati, and others. I thank Dr. Todd Skaar, Dr. Rajesh Khanna, and Dr. Jill Fehrenbacher for their encouragement and fair critique as members of my committee.

I would especially like to thank my family. To my parents, who provided me with every opportunity to pursue higher education and were unwavering in their support and confidence in me. Dad would be unquestionably proud and content with this accomplishment. To my wife, Tami, for her love, support, and patience, and her insistence in leading a balanced life. Somehow, in the middle of it all, we’ve started a wonderful family and I look forward to what lies ahead, as a scientist and as a dad.

A special thanks to several agencies for continued financial support throughout my degree. This work was made possible, in part, by a Predoctoral Traineeship Award from the Indiana Clinical and Translational Sciences Institute and a Predoctoral Traineeship Award funded by the Department of Defense Breast Cancer Research Program (W81XWH-10-1-0349).

Jason Dennis Robarge

AROMATASE INHIBITORS PRODUCE HYPERSENSITIVITY IN EXPERIMENTAL MODELS OF PAIN: STUDIES *IN VIVO* AND IN ISOLATED SENSORY NEURONS

Aromatase inhibitors (AIs) are the current standard of care for the treatment of hormone receptor positive breast cancer in postmenopausal women. Nearly one-half of patients receiving AI therapy develop musculoskeletal toxicity that is characterized by joint and/or muscle pain and approximately one-fourth of patients discontinue their therapy as a result of musculoskeletal pain. Since there are no effective strategies for prevention or treatment, insight into the mechanisms of AI-induced pain is critical to improve treatment. However, there are few studies of AI effects in animal models of nociception. To determine whether AIs produce hypersensitivity in animal models of pain, I examined the effects of AI administration on mechanical, thermal, and chemical sensitivity in rats. The results demonstrate that (1) repeated injection of 5 mg/kg letrozole in male rats produces mechanical, but not thermal, hypersensitivity that extinguishes when drug dosing is stopped; (2) administering a single dose of 1 or 5 mg/kg letrozole in ovariectomized (OVX) rats also induces mechanical hypersensitivity, without altering thermal sensitivity and (3) a single dose of 5 mg/kg letrozole or daily dosing of letrozole or exemestane in male rats augments flinching behavior induced by intraplantar ATP injection. To determine whether the effects of AIs on nociceptive behaviors are mediated by activation or sensitization of peptidergic sensory neurons, I determined whether letrozole exposure alters release of calcitonin gene-related peptide (CGRP) from isolated rat sensory neurons and from sensory nerve endings in rat spinal cord slices. No changes in basal, capsaicin-evoked or high extracellular potassium-evoked CGRP release were observed in sensory neuronal cultures acutely or chronically

exposed to letrozole. Furthermore, letrozole exposure did not alter the ability of ATP to augment CGRP release from sensory neurons in culture. Finally, chronic letrozole treatment did not augment neuropeptide release from spinal cord slices. Taken together, these results do not support altered release of this neuropeptide into the spinal cord as mediator of letrozole-induced mechanical hypersensitivity and suggest the involvement of other mechanisms. Results from this dissertation provide a new experimental model for AI-induced hypersensitivity that could be beneficial in delineating mechanisms mediating pain during AI therapy.

David A. Flockhart, M.D., Ph.D., Chair

TABLE OF CONTENTS

LIST OF TABLES

LIST OF FIGURES

LIST OF ABBREVIATIONS

^{3}H-Es	6,7-^{3}H-estrone
^{14}C-An	4-^{14}C-Δ4-androstenedione
α,β-meATP	alpha, beta-methyleneadenosine 5'-triphosphate
AI	aromatase inhibitor
AIMSS	aromatase inhibitor-induced musculoskeletal symptoms
ANA	anastrozole
ATAC	Arimidex, Tamoxifen Alone or in Combination Study
ADP	adenosine diphosphate
ATP	adenosine 5′-triphosphate
AUC	area under the curve
AUFS	absorbance units full scale
BMI	body mass index
cDNA	complimentary deoxyribonucleic acid
CGRP	calcitonin gene-related peptide
CNS	central nervous system
C_T	threshold cycle
CV	coefficient of variation
CYP	cytochrome P450
DMD	desmethyldiazepam
DRG	dorsal root ganglia
ERs	estrogen receptors
EXE	exemestane
GPER	G protein-coupled estrogen receptor 1
GPR30	G protein-coupled receptor 30

HPβCD	2-hydroxypropyl-β-cyclodextrin
HPLC	high pressure liquid chromatography
HPRT	human hypoxanthine phosphoribosyltransferase 1
HRP	horseradish peroxidase
iCGRP	immunoreactive calcitonin gene-related peptide
i.p.	intraperitoneal
KO	knock-out
LET	letrozole
MPL	1-methyl-2-pyrrolidinone
mRNA	messenger ribonucleic acid
MSK	musculoskeletal
NGF	nerve growth factor
NSB	non-specific binding
OVX	ovariectomized
P2X receptors	purinergic cation-permeable ligand gated ion channels
P2Y receptors	purinergic G protein-coupled receptors
PBS	phosphate buffered saline
PCR	polymerase chain reaction
PGE_2	prostaglandin E_2
PMSG	pregnant mare's serum gonadotrophin
PVDF	polyvinylidene difluoride
PWL	paw withdrawal latency
PWT	paw withdrawal threshold
RNA	ribonucleic acid
RIPA	radioimmunoprecipitation assay buffer
RT	real-time

RT-PCR	real-time polymerase chain reaction
s.c.	subcutaneous
SD	standard deviation
TAM	tamoxifen
TBST	tris-buffered saline containing 0.1% Tween 20 (v/v)
TNP-ATP	2′,3′-O-(2,4,6-trinitrophenyl) adenosine-5′-triphosphate
TRP	transient receptor potential cation channel
UDP	uridine diphosphate
UTP	uridine triphosphate

INTRODUCTION

Clinical trials conducted over decades have demonstrated that aromatase inhibitors (AIs) are effective therapies for hormone sensitive breast cancer in postmenopausal women. Therapeutic outcomes have improved as increasingly potent AIs were introduced into clinical use, providing indirect evidence for a relationship between estrogen suppression and clinical efficacy (Geisler and Lonning, 2005a). In many breast cancer patients, therapeutic doses of the third generation aromatase inhibitors anastrozole, exemestane, and letrozole, achieve sufficient suppression of blood estrogen concentrations to inhibit growth of estrogen-sensitive tumors. Consequently, treatment of hormone receptor positive breast cancer with AIs is widely accepted as an effective therapy in postmenopausal women (Aebi et al., 2011; Burstein et al., 2010) and guidance issued by the American Society of Clinical Oncology recommends AIs as first-line therapy or as sequential treatment after tamoxifen.

The occurrence of side effects during chemotherapy with many agents can become a limiting factor for overall drug tolerability. Recent clinical studies describe up to 50% of breast cancer patients developing painful joints and muscles within weeks to months of initiating AI therapy (Crew et al., 2007; Henry et al., 2007). Approximately 25% of all breast cancer patients discontinue AI therapy as a result of intolerable drug-induced musculoskeletal pain (Henry et al., 2012). Although many studies have been conducted to identify clinical factors and biomarkers to predict which patients will develop AI-induced pain, factors with strong associations have not been identified and findings have been largely inconsistent between studies. Furthermore, although the general consensus is that these adverse effects are secondary to reduced estrogens, no conclusive study has addressed this basic mechanistic premise (Felson and Cummings,

2005; Henry et al., 2008). Clinical studies of AI-induced pain in breast cancer patients are complicated by an underlying incidence of musculoskeletal pain in postmenopausal women and by prior treatment with chemotherapy regimens or tamoxifen, which may themselves induce or influence the risk of developing musculoskeletal pain. To date, mechanisms causing AI-induced musculoskeletal pain remain unknown, and consequently, no clearly recognized therapies exist for prevention or treatment.

In spite of the importance of understanding how AIs may alter pain pathways, there are few studies of AI effects using animal assays for nociception that may provide insight into toxicity induced by this widely prescribed class of drugs. The *objective* of this proposal is to establish a model for AI-induced pain and investigate the potential contribution of nociceptive sensory neurons. The *central hypothesis* is that aromatase inhibitors sensitize sensory neurons, resulting in pain during AI treatment.

Aromatase

Discovery and biochemistry of aromatase

The discovery and characterization of aromatase proved to be one of the first characterizations of a molecular drug target for rational development of cancer therapies. Early in the characterization of sex steroids, it was thought that androgens with a 19-carbon backbone may serve as estrogen precursors. The first indirect experimental evidence of the metabolism of androgens into estrogens was shown by Seinach and Kun, who observed enhanced estrogenic activity in urine after administering unlabeled testosterone to men (Sodersten et al., 2014; Steinach and Kun, 1937). This observation was confirmed nearly 20 years later when Baggett and colleagues demonstrated conversion of radiolabeled testosterone to estrogens by the

human ovary (Baggett et al., 1956). The reaction was believed to involve a cytochrome P450 enzyme due to the ability of aminoglutethimidine, a known inhibitor of adrenal P450-mediated hydroxylation, to inhibit the “aromatization” reaction (Chakraborty et al., 1972). However, the enzyme was unique among P450s due to the inability of carbon monoxide to inhibit the reaction, the standard method at that time for determining P450-mediated reactions. Aromatase catalyzes the conversion of C19-androgens to C18-estrogens through a three-step reaction that sequentially generates 19-hydroxy and 19-aldehyde intermediates before the final aromatization step (Ryan, 1959). As shown in Figure 1, endogenous substrates include androstenedione, testosterone, and 16α-androstenedione, which are metabolized to estrone, 17β-estradiol, and estriol, respectively. The formation of estriol is most prominent in human pregnancies, where maternal and fetal liver form 16α-hydroxy-dehydroepiandrosterone sulfate that is converted to 16α-hydroxy-androstenedione by sulfatase and isomerase enzymes and converted to estriol by placental aromatase and 17-hydroxysteroid dehydrogenase. Late in gestation, approximately 90% of the 16α-hydroxy-dehydroepiandrosterone sulfate entering the placenta is derived from the fetal compartment and only 10% from the mother (Siiteri and MacDonald, 1966). Endogenous androgens, such as dihydrotestosterone, and estrogens have been shown to inhibit aromatase activity, however it is unclear whether endogenous concentrations of these steroids modulate enzymatic activity under physiologic conditions (Shimizu et al., 1993; Wozniak and Hutchison, 1993).

Isolation and characterization of the aromatase enzyme and the gene encoding this protein was initially described in human tissues and subsequent studies identified the orthologous molecules in other organisms. Human aromatase is the product of the *CYP19A1* gene residing on chromosome 15q21. Analyses of cDNA libraries from

different tissues revealed complex tissue-specific regulation and expression of *CYP19A1* that is determined by the use of eleven alternative promoters in the 93 kb 5′-noncoding region of the gene. Initiating transcription at one of the tissue-specific promoters generates a unique exon I that is subsequently spliced to the splice acceptor site of exon II, creating tissue-specific messenger ribonucleic acid (mRNA) (Bulun et al., 2003; Chow et al., 2009). However, a common translation start site in exon II results in an identical translated protein produced in all tissues. Comparative genomic analysis of human and mouse *CYP19A1* has demonstrated that the gene structures in humans and rodents are closely related (Chow et al., 2009). Alignments of aromatase amino-acid sequences between human and rats or mice demonstrate 77.3% sequence homology between these species and key substrate binding site and catalytic residues are highly conserved (Ghosh et al., 2009) (Figure 2). Antibodies raised against purified proteins from human placental microsomes suggested aromatase may exist as two isoforms with approximate molecular weights of 50 to 51 and 55 kDa (Harada, 1988; Mendelson et al., 1985). Furthermore, aromatase activity in rat microsomes can be inhibited by antibodies raised against human aromatase, suggesting the *CYP19A1* orthologs encode enzymes with similar isotopes (Osawa et al., 1987).

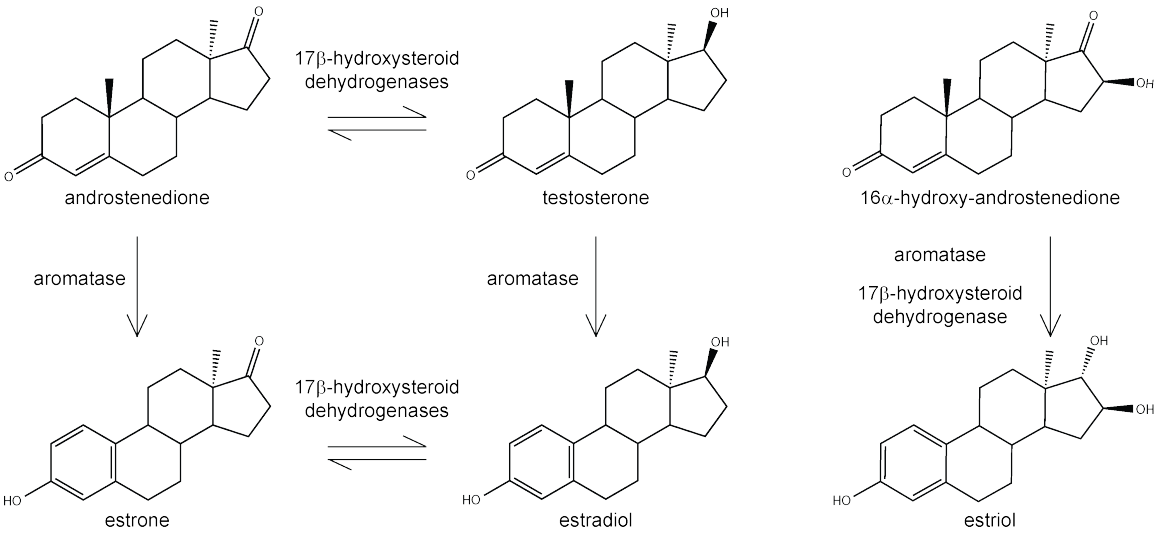

Figure 1. Endogenous substrates and products of aromatase.

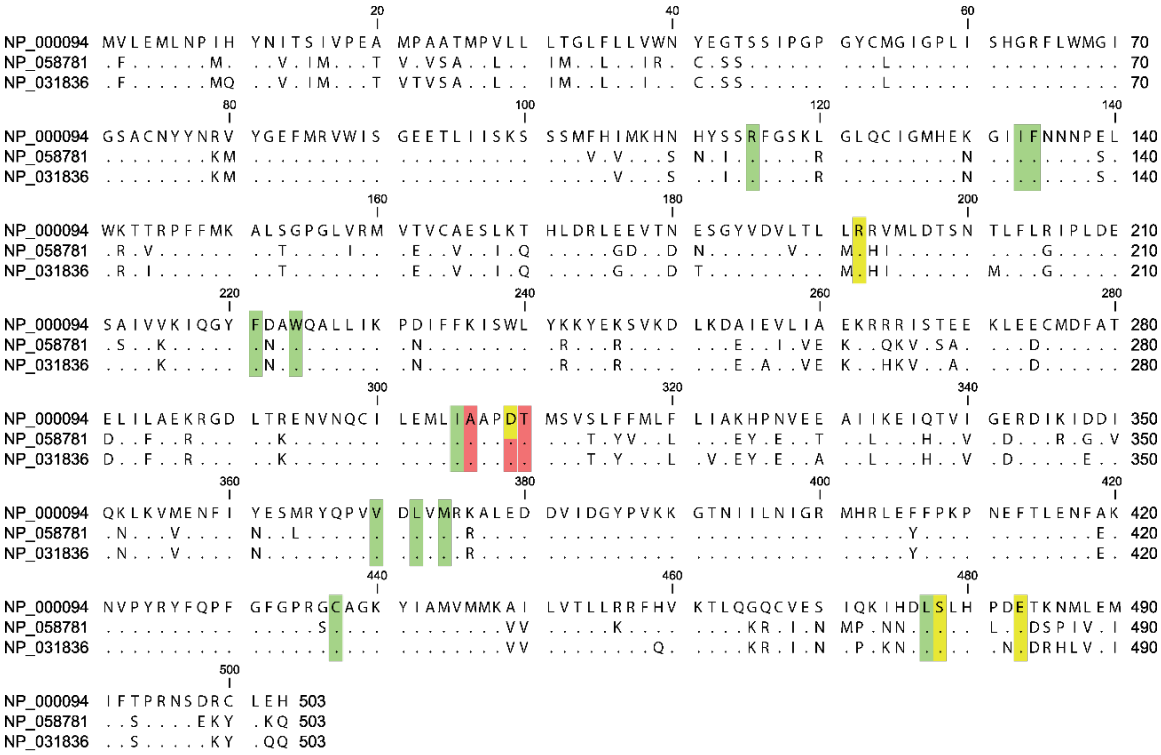

Figure 2. Alignment of amino acid sequences of human, rat and mouse aromatase. Aromatase protein sequences from rat (NP_058781) and mouse (NP_031836) were aligned to the human sequence (NP_000094) using ClustalW. Amino acids residues are depicted by standard one-letter codes. Amino acid residues in the aligned rat and mouse sequences that exactly match those in human aromatase are indicated by dots. Amino acids predicted to form the active site are shaded in green, while residues that form putative active-site access channel are shaded in yellow. Residues predicted to directly contribute to the aromatization reaction are shaded in red (Ala306, Asp309 and Thr310).

Contribution of aromatase activity to tissue estrogen concentrations

Estrogen content in a cell or tissue is the net result of processes that result in new molecules arriving in the cell (*in situ* synthesis by aromatase, diffusion or active transport from the local environment: neighboring cells or blood supply) and processes that eliminate the steroid (*in situ* metabolism, diffusion or active transport out of the cell). The availability of estrogens for uptake into the cell will be determined by the steroid in the blood and extra-cellular metabolism of sex steroids. Oxidative metabolism and conjugative metabolism by glucuronidation, sulfonation, and/or O-methylation in the liver are all processes that mediate the metabolic disposition of estrogens in humans (Lee et al., 2001; Raftogianis et al., 2000; Zhu and Lee, 2005) and rodents (Brooks et al., 1965; Holler et al., 1977). These estrogen metabolites are terminally eliminated in the urine and feces. Routes of metabolic disposition of blood-borne estrogens by the liver have also been identified in organs such as the brain, suggesting *in situ* metabolism of estrogens may be a mechanism to limit or terminate estrogen signaling (Reddy et al., 1981).

While aromatase was first characterized in the ovaries and early studies of estrogens focused on the endocrine actions of these steroids, other tissues are known to synthesize estrogens. Studies led by Christopher Longcope, Paul MacDonald, and Pentti Siiteri challenged the standing dogma that steroid hormones were only produced in endocrine glands such as the adrenals, ovaries, and testes. In order to characterize aromatization *in vivo*, these studies utilized a technique now termed “total body aromatization”, where tracer doses of an androgen (e.g. 4-^{14}C-Δ4-androstenedione or ^{14}C-An) and an estrogen (e.g. 6,7-^{3}H-estrone or ^{3}H-Es), labeled with different radioactive isotopes, are administered simultaneously. The fraction of administered androgen that is converted to a specific estrogen is estimated by taking the ratio of the molar ratio of ^{14}C-

Es / ^{3}H-Es measured in the blood or urine to the molar ratio of ^{14}C-An / ^{3}H-Es administered. In oophorectomized and adrenalectomized young adult females and normal adult males, these investigators observed formation of estrone and estradiol following intravenous dosing of radiolabeled androstenedione, demonstrating extra-ovarian and extra-adrenal sources of aromatase activity (Longcope et al., 1969; MacDonald et al., 1967). Additional studies demonstrated higher conversion of androstenedione to estrogens in obese men and women, suggesting that adipose may be an important contributing source of aromatase activity (Grodin et al., 1973; Kley et al., 1980). Indeed, subsequent experiments demonstrated aromatization of androgens in excised human adipose tissue (Schindler et al., 1972).

In humans and rodents, concentrations of unconjugated estrogens have been shown to be several fold higher in tissue than in the blood; conversely, concentrations of estrone sulfate and other conjugates estrogens are much lower in tissues compared with blood. For example, in women, estradiol and estrone concentrations have been reported to be 1.6 to 12-fold and 2.5 to 5-fold higher in breast tissue than plasma (Geisler et al., 2001; Lonning et al., 2009). These findings are consistent with a study estimating uptake and formation of estrone in the breast from 24 postmenopausal women with breast cancer (Larionov et al., 2002). During steady-state infusions of ^{3}H-labelled androstenedione and ^{14}C-labelled estrone, a median breast tissue:plasma ratio of ^{14}C-estrone of 6 was observed in normal tissue, consistent with diffusion and or active uptake of blood estrone and sequestration by binding (Larionov et al., 2002). By measuring ^{3}H-estrone in breast tissue of these patients, aromatase activity in the breast was estimated to account for a median of 15% of local radiolabeled estrone concentrations (Larionov et al., 2002).

Elevated tissue:blood ratios of estrogens have been observed in additional tissues. Estradiol concentrations in the hippocampus, cortex, and hypothalamus of female Sprague Dawley rats collected on postnatal day 10 were approximately 25, 125, and 833.3-fold higher than plasma concentrations (Konkle and McCarthy, 2011b). Aromatase activity measured in the hypothalamus was 10-fold higher than in the hippocampus and cortex (Konkle and McCarthy, 2011b). These studies suggest AI treatment could alter estrogen content in local tissues by reducing *in situ* aromatization, thereby reducing estrogens in peripheral tissue, including the blood. To understand the mechanism by which AIs alter the physiology of a cell secondary to a change in estrogen content of this tissue, it is important to determine the contribution of *in situ* synthesis by aromatase.

Aromatase inhibitors

Rationalization, discovery, and development of AIs as breast cancer therapies

In a seminal paper published in 1896, Sir George Beatson, M.D. introduced ovariectomy (oophorectomy) of premenopausal women as therapy for breast cancer and identified manipulation of steroid hormones as an effective therapeutic strategy (Beatson, 1896). Others subsequently noticed reduced tumor burdens following surgical adrenalectomy and hypophysectomy (Santen et al., 2009). The recognition that surgical treatment of breast cancer may be effective as a result of estrogen suppression initiated a strong interest in the discovery of new endocrine therapies for breast cancer. Recognizing the therapeutic potential of targeting aromatase prompted a systematic search for selective aromatase inhibitors. Structure-function characterization of over 100 compounds by Harry Brodie and Angela Brodie led to the identification of 1,4,6-androstatrienedione (Schwarzel et al., 1973) and 4-hydroxy-androstenedione as the

most promising candidate inhibitors with selectivity for aromatase (Brodie et al., 1977). The effectiveness of these compounds to treat breast cancer drove the development of additional aromatase inhibitors with increasing selectivity and potency (Geisler and Lonning, 2005b).

Current generation AIs are used to treat early stage, locally advanced, and metastatic breast cancers in which the primary tumors express estrogen receptor alpha and/or the progesterone receptor (Schnitt, 2006). The clinical value of determining hormone-receptor positivity is to determine the likelihood that a patient will respond to endocrine therapy, such as AIs. As a result of improved detection of early stage breast cancers, AIs are most often used in adjuvant (after surgery) treatment regimens in postmenopausal women. Five years of AI therapy, either as monotherapy or following two to three years of tamoxifen, has been shown to reduce the risk of cancer recurrence relative to five years of tamoxifen therapy alone (Dowsett et al., 2010). Anastrozole and exemestane are currently being evaluated for their ability to reduce the development of invasive breast cancer in postmenopausal women at high risk for the disease (Lazzeroni and DeCensi, 2013).

Pharmacology of third-generation AIs: exemestane and letrozole

Exemestane (6-methylenandrosta-1,4-diene-3,17-dione) is an irreversible aromatase inhibitor. Pre-incubation studies using human placental microsomes as a source of aromatase enzyme show exemestane confers time-dependent aromatase inhibition, with a K_i of 26 nmol/L (Giudici et al., 1988). While bioavailability in humans was never determined due to the absence of a suitable formulation for intravenous delivery, approximately 5% of exemestane is bioavailable in rats following an oral dose of 30 mg/kg (U.S. Food and Drug Administration, 1998b). Rapid metabolism likely

accounts for its low bioavailability, as less than 5% of the drug is excreted unchanged in rats (U.S. Food and Drug Administration, 1998b). The drug is also extensively metabolized in humans, as <1% of unchanged drug is recovered in urine and feces after a single oral dose of 25mg in humans (U.S. Food and Drug Administration, 1998a). In human liver microsomes, exemestane undergoes reduction of the 17-keto group by multiple cytochrome P450s to form the most abundant metabolite, 17-hydroexemestane (Kamdem et al., 2011). Although 17-hydroexemestane inhibits aromatase, it is 2.6-times less potent than the parent drug and plasma concentrations in humans are approximately ten percent of the parent, suggesting the metabolite does not substantially contribute to the *in vivo* pharmacologic activity of exemestane at therapeutic doses (U.S. Food and Drug Administration, 1998a). Daily oral dosing of 25mg exemestane in postmenopausal women suppresses aromatization of intravenously administered ^{3}H-androstenedione to ^{3}H-estrone by 97.9%, corresponding to an average suppression of plasma concentrations of estradiol, estrone, and estrone sulfate by 92.2%, 94.5%, and 93.2% respectively (Geisler et al., 1998).

The ability of exemestane to inhibit aromatase in rats was estimated using adult female rats injected with pregnant mare's serum gonadotrophin (PMSG) (Giudici et al., 1988). PMSG contains follicle-stimulating hormone and luteinizing hormone which stimulate the synthesis of enzymes mediating steroidogenesis in the ovaries, including a significant induction of estrogen synthesis by aromatase (Banks et al., 1991; Rowlands, 1944). Twenty-four hours after administering exemestane (0, 0.3, 1, 3, or 10 mg/kg; s.c.) to PMSG-stimulated rats, aromatase activity was significantly inhibited in ovarian microsomes preparations, with the ED_{50} between 1 and 3 mg/kg. Aromatase activity in rats dosed with 10 mg/kg exemestane was 20% of the vehicle-treated controls, suggesting maximum effective doses had not been tested. Results of a similar study

measuring aromatase activity in ovary microsomal preparations from PMSG-stimulated rats, showed aromatase activity was reduced to 43.6% of controls 6 hours after administration of 10 mg/kg exemestane (s.c.) (Zaccheo et al., 1991). In these rats, average plasma estradiol concentrations were reduced to 27.9% of the concentration measured in control animals (Zaccheo et al., 1991).

In contrast to exemestane, letrozole (4-4′-(1H-1,2,4-triazol-1-yl-methylene)-bis-benzonitrile) is a non-steroidal, competitive aromatase inhibitor. Letrozole inhibits aromatase activity in human placental microsomes with an IC_{50} of 11.5 nM and inhibits luteinizing hormone-stimulated production of estradiol in hamster ovaries *in situ* with an EC_{50} of approximately 10 nM, suggesting the drug is a potent aromatase inhibitor (Bhatnagar et al., 1990). In humans, letrozole is almost completely absorbed into circulation after oral dosing of the therapeutic dose of 2.5 mg (Sioufi et al., 1997). Once absorbed, letrozole clearance occurs primarily through cytochrome P450 (CYP) - mediated metabolism to an inactive carbinol (4,4′-methanol-bisbenzonitrile), which is excreted in the urine as a glucuronide conjugate (Pfister et al., 2001). Single doses of 0.1, 0.5, and 2.5 mg letrozole reduce serum estrone and estradiol concentrations within two and eight hours of administration (Iveson et al., 1993). Twenty-four hours after a single dose of 2.5 mg, concentrations of estrone and estradiol are suppressed to at least 10 and 3 pM and remain suppressed for up to fourteen days (Iveson et al., 1993). Daily oral dosing of 2.5mg letrozole in postmenopausal women suppresses aromatization of intravenously administered ^{3}H-androstenedione to ^{3}H-estrone by over 99.1%, and additionally suppresses plasma concentrations of estradiol, estrone, and estrone sulfate by an average of 84.3%, 87.8%, and 98.0%, respectively (Geisler et al., 2002).

Letrozole pharmacokinetics in rats resembles those observed in humans. Letrozole dosed intravenously in female rats has a half-life of 34 to 37 hours (doses of 0.1, 0.5, 1, and 2 mg/kg) and a volume of distribution of approximately 2 liters/kg (Tao et al., 2006). Letrozole readily crosses the blood brain barrier and accumulates in tissue, resulting in tissue concentrations several fold higher than those measured in plasma (Dave et al., 2013; Liu et al., 2000). Gender significantly influences letrozole pharmacokinetics in rats. Cumulative plasma drug exposure following oral dosing in males is between 10% and 60% that of females and can be attributed to a much shorter half-life in males (Liu et al., 2000; U.S. Food and Drug Administration, 1996; Wempe et al., 2007). Akin to metabolism observed in humans, ^{14}C-letrozole administered intravenously to female rats is primarily excreted in urine as a glucuronide conjugate of the carbinol (4,4′-methanol-bisbenzonitrile) metabolite (U.S. Food and Drug Administration, 1996). Similar to exemestane, the *in vivo* potency of letrozole has been determined using several rat models that are sensitive to estrogen concentrations. The estimated ED_{50} for letrozole inhibition of androstenedione-induced uterine hypertrophy in immature female rats (an index of aromatase inhibition *in vivo*) is 1-3 ug/kg (Bhatnagar et al., 1990). Daily oral administration of letrozole to intact, cycling female rats for 14 days results in a dose-dependent reduction in uterine wet weight (Bhatnagar et al., 1990). Uterine weight reduction following administration of 1 mg/kg was equivalent to that observed after ovariectomy.

Aromatase inhibitor-induced musculoskeletal symptoms (AIMSS)

Detection and measurement of AIMSS

Early trials evaluating the efficacy of AIs for treatment of estrogen sensitive metastatic breast cancer showed arthralgia and joint pain were more frequently reported

by patients receiving AIs than several other therapies (Bonneterre et al., 2000; Dombernowsky et al., 1998; Goss et al., 1999; Nabholtz et al., 2000). The first report to highlight the potential clinical importance of increased rates of arthralgia and joint pain during AI therapy was a letter to the editor in the Journal of Clinical Oncology written by Paul Donnellan and colleagues (Donnellan et al., 2001). He reported musculoskeletal symptoms in 77 post-menopausal patients receiving anastrozole who had previously failed on tamoxifen. Importantly, none of these patients had previous arthritis or arthralgia associated with menopause or prior chemotherapy. Within two months of initiating anastrozole, twelve patients (16%) reported new joint pain, primarily in the hands, knees, hips, lower back and shoulders. Early morning stiffness was a common side effect. Four of the 77 patients (5%) discontinued therapy due to arthralgia, which subsequently resolved.

Despite these indications that musculoskeletal toxicity may be a significant side effect of AIs, early observations by oncologists suggested that these drugs were well-tolerated. This view was reinforced by low rates of musculoskeletal adverse events reported in large randomized phase III clinical trials, which demonstrated the efficacy of AIs as adjuvant hormonal therapy for the treatment of early stage breast cancer (Baum et al., 2002; Coombes et al., 2004; Thurlimann et al., 2005; Whelan et al., 2005). In these studies, the incidence of musculoskeletal toxicity (disorder, pain, arthralgia, or aches) was 2-8% greater in subjects receiving an AI when compared to subjects receiving tamoxifen or placebo (Baum et al., 2002; Coombes et al., 2004; Thurlimann et al., 2005; Whelan et al., 2005). The increased rate of musculoskeletal toxicity in subjects receiving AIs represented significant, but relatively small changes, relative to rates in the comparator arm. Due to the immense size of these trials, which individually recruited several thousand study subjects, AIs were considered to be well tolerated and

musculoskeletal toxicities were not expected to impact their clinical use. However, in retrospect, the evaluation of musculoskeletal adverse events was not sufficiently robust or consistent in these trials to detect the increased rate of joint symptoms among AI users. Instead, musculoskeletal toxicity reported in these trials was assessed by a number of different methods, including: case-report forms graded according to the Common Toxicity Criteria of the National Cancer Institute (version 2.0) (Thurlimann et al., 2005), Medical Outcomes Study 36-item Short Form Health Survey and the Menopause Specific Quality of Life Questionnaire (Whelan et al., 2005) or self-reporting by patients (Baum et al., 2002; Coombes et al., 2004). Consequently, it is possible that musculoskeletal toxicities were differentially and inadequately captured by these various methods for a number of reasons. For instance, the Common Toxicity Criteria of the National Cancer Institute (version 2.0) includes a section on musculoskeletal pain and stiffness (grade 0-5), but does not allow for reporting specific site or organ toxicity (National Cancer Institute, 1999). During investigator-initiated evaluation of adverse events, clinicians must attribute the adverse events to the drug intervention. Patients may also underreport toxicities in clinical trials of new cancer therapies. Finally, given the frequency of musculoskeletal pain in postmenopausal women, AI-induced musculoskeletal toxicities may have often been overlooked.

In fact, the overall toxicity burden on breast cancer patients was unrecognized until AIs became widely used in common oncology practice. As shown in the following discussion, after musculoskeletal toxicity was recognized as a major side effect, smaller studies have more carefully collected patient reported musculoskeletal adverse events.

Common symptoms, their severity and frequency

In common clinical practice, the frequency of AIMSS after initiating AI therapy – either new joint pain or worsened pre-existing joint pain – is approximately 50% (Crew et al., 2007; Henry et al., 2007; Moxley, 2010). Of these patients, roughly one-half report new joint pain, and the remaining patients report exacerbations of pre-existing joint discomfort. Additionally, some patients with pre-existing joint pain report the involvement of additional joints after initiating an AI (Moxley, 2010). Irrespective of the method used to evaluate AIMSS, most patients develop joint symptoms within the first 2 to 6 months following treatment initiation (Castel et al., 2013; Henry et al., 2007; Kanematsu et al., 2011; Sestak et al., 2008).

Although there are significant differences in clinical presentation between patients, most patients describe symmetrical pain, with accompanying joint or muscle stiffness that frequently occurs in the morning (Burstein and Winer, 2007; Donnellan et al., 2001; Moxley, 2010). Of the many sites of discomfort reported by patients (includes the hands (fingers and wrists), arms, knees, feet, pelvic and hip bones, and back), the hands, knees and back (lower back and/or shoulders) seem the most affected (Crew et al., 2007; Donnellan et al., 2001). The number of painful joints is variable between patients, with reports ranging from 3 to 20 (Laroche et al., 2007). While the majority of patients describe joint pain, muscle pain of the forearms and arms has been reported, which is inconsistent with a distribution involving strictly the joints (Henry et al., 2007; Laroche et al., 2007). Despite many studies describing the severity of joint pains, there is little information describing the quality of this pain. Descriptions of pain or discomfort during AI therapy include: “aching in joints and muscles” (Moxley, 2010), “soreness” (Khan et al., 2010), “joint pain, achy and stiff joints, muscle pain, morning joint stiffness, tingling, numbness, joint swelling” (in descending frequency) (Henry et al., 2007).

Variability in pain intensity mirrors the overall variability in clinical symptoms. In a study by Henry et al., patients referred to a rheumatologist for AIMSS after at least 6 months of therapy reported a median pain intensity of 51 on a 100 point scale (Henry et al., 2007). However, pain intensity ranged from 0 to 79 in these patients (Henry et al., 2007). In contrast, patients in this trial receiving AIs that were not referred to rheumatology for joint symptoms had a median pain rating of 2.5 with a range of 0 to 80 (Henry et al., 2007). Similarly, Crew et al. reported that 33% of patients reported mild symptoms (patient reported pain rating of 1-4 on a 10-point scale), while 67% of patients experienced moderate to severe symptoms (pain ratings of 5-10 on a 10-point scale) (Crew et al., 2007). Thus, using the thresholds of Crew et al., at least 50% of patients in the studies conducted by Crew et al. and Henry et al. rated their pain as moderate to severe. Patients experiencing AIMSS have significantly increased physical disability, as measured by difficulty performing everyday tasks (e.g. walking, dressing, standing up, grasping small objects) that may be a consequence of increased pain or stiffness (Henry et al., 2007; Morales et al., 2007; Moxley, 2010).

Objective evaluation of joints in patients receiving aromatase inhibitors

Patient-reported complaints of arthralgia and joint stiffness during AI therapy merely describes the symptoms of an underlying pathophysiology, but does not indicate a specific pathological changes. Based on clinical evaluation, patients with AIMSS are diagnosed with a range of conditions, including: tendonitis or tenosynovitis, osteoarthritis, and carpal tunnel syndrome, with multiple rheumatologic conditions diagnosed in a significant fraction of patients (Henry et al., 2007; Morales et al., 2007; Moxley, 2010). Thus, it has been proposed that AI-induced musculoskeletal symptoms may be a result of new or worsened manifestations of common rheumatological conditions of the joints. To describe and identify structural changes that may contribute

to joint symptoms in patients receiving AIs, rheumatologic examination of the hands and wrists has been conducted using magnetic resonance imaging and high-resolution ultrasonography (Dizdar et al., 2009; Henry et al., 2010a; Lintermans et al., 2012; Lintermans et al., 2011; Morales et al., 2008). These are complimentary methods that have been used to describe changes in other rheumatic conditions with associated arthralgia, such as osteoarthritis and rheumatoid arthritis (Braun and Gold, 2012; McGonagle et al., 2001). Magnetic resonance imaging is a sensitive method to visualize bony and soft tissue changes. Specifically, this method can identify areas of bone erosion, formation of soft tissue pannus, changes in tendon and tendon sheath structure, tissue swelling and edema, as well as small cartilage or bone fragments in the joint. Ultrasonography is well suited to visualize tenosynovial and articular cartilage structures. Results from these imaging studies suggest several common changes in breast cancer patients receiving AIs, including: enhancement of the synovium, increase in intra-articular fluid, and tenosynovial changes manifested as swelling of the tendon sheath (Henry et al., 2010a; Morales et al., 2008). There are conflicting reports on abnormalities of the tendon itself during AI therapy. Henry et al. noted that tendon abnormalities were rare, however a second cross-sectional study observed increased tendon thickness in patients receiving AIs versus controls (Dizdar et al., 2009; Henry et al., 2010a). In addition to these cohort studies, tendinopathies have been reported in several case studies (Martens et al., 2007; Papadimitriou et al., 2012). As a whole, these studies show that not all patients develop new or worsening musculoskeletal abnormalities and findings are not uniform between patients, reflecting the heterogeneity of joint and muscle symptoms experienced by patients. If pain during AI therapy is a result of structural changes in the joints then we might expect pain and functional disability to be limited to those body regions most impacted by the diagnosed condition (e.g. pain limited to the wrists and arms in patients with a diagnosis limited to carpal tunnel

syndrome). However, these correlations have not been delineated in the literature. One interesting finding of these studies was the high frequency (25% to 48%) of intra-articular fluid or tenosynovial abnormalities in patients prior to the initiation of AI therapy (Henry et al., 2010a; Morales et al., 2008), which may reflect common underlying rheumatic conditions in postmenopausal breast cancer patients (Moxley, 2010). Therefore, it is important that future studies should appropriately control for the underlying joint structure abnormalities in this patient population and further evaluate patients not treated with AIs to evaluate drug-induced effects.

Importantly, musculoskeletal changes identified in patients receiving AIs do not resemble those that are characteristic of other rheumatologic conditions that are associated with significant arthralgia, such as rheumatoid arthritis and osteoarthritis. Rheumatoid arthritis (RA) involving the hands and wrists is often associated with soft tissue swelling and loss of bone mineralization centered about the joints (Aletaha et al., 2010; Majithia and Geraci, 2007). RA involving the knees often results in progressive cartilage degeneration, leading to areas of joint narrowing, in addition to joint effusions, synovial thickening and inflammation (Aletaha et al., 2010). A prominent characteristic of RA that is also not observed in AIMSS is overtly swollen and warm or hot joints. The non-inflammatory clinical presentation of AIMSS further distinguishes it from a number of inflammatory arthropathies, which are readily detected by physical examination and imaging of the involved joints. Similar to rheumatoid arthritis, osteoarthritis presents with joint space narrowing secondary to localized cartilage loss (Altman et al., 1990; Lanyon et al., 1998). Additionally, progressive osteoarthritis is associated with the formation of osteophytes and the presence of osteochondral or cartilage fragments in the joint due to fragmentation (Lanyon et al., 1998). In fact, a significant number of breast cancer patients are diagnosed with osteoarthritis (71% (12 of 17 of patients) in the study by

Morales et al. and 82% (23 of 28 patients) in the study by Lintermans et al.) or arthritis (36% (36 of 100 patients) in the study by Henry et al.) before initiating AI therapy (Henry et al., 2007; Lintermans et al., 2012; Morales et al., 2008). Consistent with the distinction between AIMSS and inflammatory or autoimmune joint disorders, blood concentrations of biomarkers that indicate an inflammatory or autoimmune response are not elevated during AI exposure (Dizdar et al., 2009; Henry et al., 2007; Henry et al., 2010b). Furthermore, therapeutic approaches that effectively alleviate inflammatory joint disorders, such as nonsteroidal anti-inflammatory drugs (NSAIDS) and acetaminophen, are used for symptom management by a majority of patients (Henry et al., 2007; Sestak et al., 2008). However, these treatments have been described as largely ineffective in alleviating AI-induced musculoskeletal pain (Martens et al., 2007; Morales et al., 2008). Also, in a retrospective cohort study of 29,967 patients' prescription claims for AIs (anastrozole, exemestane, or letrozole), co-prescribing pain modifying medications (among them: NSAIDS, anti-depressants, opioids) along with an AI did not significantly increase persistence on AI therapy (Hashem et al., 2013). Taken as a whole, these observations suggest that AI-induced arthralgias do not arise from musculoskeletal abnormalities associated with other common rheumatic conditions, including those that arise from inflammatory processes or auto-immune reactions.

AI-induced musculoskeletal symptoms reduce compliance

While AIs are effective breast cancer drugs, many recent studies have shown that noncompliance with AI therapy is common (Neugut et al., 2011; Partridge et al., 2008). Of the potential factors influencing patients' inability to continue therapy, intolerable drug-induced musculoskeletal pain is a major contributor (Henry et al., 2012). Indeed, of the one-third of patients prescribed AIs who discontinue treatment prematurely, 60% are attributable to intolerable musculoskeletal pain (Henry et al.,

2012). Thus, approaches to alleviate these side effects are expected to improve tolerability of this class of drugs.

Clinical predictors and factors associated with aromatase inhibitor-induced musculoskeletal symptoms

Demographic and other clinical factors that influence risk of musculoskeletal toxicity

AIs induce musculoskeletal pain in women who have a high baseline risk for musculoskeletal pain due to natural, surgical or chemotherapy-induced menopause (Cecil and Archer, 1925; Loprinzi et al., 1993). The effects of menopause and prior chemotherapy on joint and muscle symptoms, as well as physical, cognitive and behavioral co-morbidities associated with cancer, can obscure our ability to identify which patients are experiencing musculoskeletal pain as a result of AI use, and to specifically identify factors associated with AI-induced musculoskeletal toxicity in the population of breast cancer patients. Therefore, many studies intended to identify clinical factors associated with AIMSS have examined the impact of factors such as prior therapy and baseline pain scores. Additionally, a number of other covariates have been studied, including basic demographic factors (e.g. age and race) and factors with both strong (e.g. body mass index (BMI)) and weak (e.g. age and age from menopause) relationships with estrogen concentrations prior to a patient initiating AI therapy. Results of univariate analysis of six covariates common across five studies are shown in Table 1. Associations in these studies suggest age and BMI are not consistent predictors of AIMSS. Among these variables, prior taxane-based chemotherapy is the factor most consistently associated with the odds of developing AIMSS. In the study by Ingle et al., cases and controls were selected from a large randomized phase III trial and matched based on treatment (exemestane, anastrozole), prior adjuvant chemotherapy (yes, no), age at start of AI treatment (±5 years), celecoxib use (yes, no), and time on study, which

eliminated the ability to analyze prior chemotherapy as a potential AIMSS risk factor (Goss et al., 2013; Ingle et al., 2010b).

The association between prior taxane chemotherapy and risk of AIMSS raises a number of interesting hypotheses. Prior to the onset of neuropathy, paclitaxel use is associated with acute aches and pains, which has been referred to as paclitaxel-induced arthralgias and myalgias (Garrison et al., 2003; Loprinzi et al., 1993). Patients with severe aches and pains within the first week following their first dose of paclitaxel developed more severe peripheral sensory neuropathy symptoms during the entire 12-week course of therapy (Loprinzi et al., 2011). The impact of taxanes on the joints or peripheral nervous system may sensitize these tissues to additional toxicity induced by AIs. Given this hypothesis, patients experiencing severe arthralgia or neuropathy during taxane therapy may be at greater risk for AIMSS. Additionally, there may be a relationship between time from completion of chemotherapy to endocrine therapy initiation and the risk of AIMSS. Alternatively, chemotherapy-induced amenorrhea, which is greatest among patients receiving taxane therapies, may increase the risk of developing AIMSS (Najafi et al., 2011). However, clinical studies have not adequately explored the relationship between chemotherapy and AI therapy to understand the effect on AIMSS risk and the mechanistic implications.

Table 1. Summary of studies reporting an association between clinical predictors and musculoskeletal symptoms during aromatase inhibitor therapy for breast cancer.

	Crew et al. J Clin Oncol 2007 [1]	***Mao et al. Cancer 2009*** [2]	***Ingle et al. J Clin Oncol 2010*** [3]	***Henry et al. J Clin Oncol 2012*** [4]	***Sestak et al. Lancet Oncol 2008*** [5]
Study description	Cross-sectional study of 200 patients with early-stage breast cancer receiving adjuvant ANA, EXE, or LET.[6]	Cross-sectional study of 300 patients with early-stage breast cancer receiving adjuvant ANA, EXE, or LET.	Matched case-control study of 878 patients matched by: AI (ANA or EXE), any prior chemotherapy, age, prior celecoxib use, time on study.	Prospective evaluation of 500 patients with early-stage breast cancer receiving adjuvant ANA, EXE, or LET	Retrospective analysis of ATAC trial.[7] Patients with early-stage breast cancer receiving adjuvant ANA (N=2698) or TAM (N=2735).[6] Analysis did not stratify by therapy.
Primary outcome	Joint pain and joint stiffness	Patient-reports that AIs are causing joint pain	NCI CTCAE v3.0 Grade 3 or 4 MS-AE (yes/no) [8]	Time to discontinuation of AI therapy due to patient-reported MSK symptoms [6]	Any patient reported arthralgia, arthrosis, arthritis, or joint disorder
Endocrine therapy	X [10]	X	X	X	OR=1.25 [9] (ANA=35.2%, TAM=30.3%)
Body mass index (kg/m^2)	Joint pain: <25: 57% 25-30: 34% >30: 54% Joint stiffness: not sig.	X	X	X	<25: OR=1 (31%) 25-30: OR=1.01 (31%) >30: OR=1.32 (37%)
Age (years)	X	<55: OR=1 (65%) 55-65: OR=0.56 (47%) >65: OR=0.31 (33%)	–	HR=0.7 (<55 versus >55)	X
Prior chemotherapy	X	X	–	X	OR=1.34 (Yes=38%, No=31%)
Prior taxane-based chemotherapy	Pain: OR=2.14 (Yes=62%, No=43%) Stiffness: OR=2.73 (Yes=62%, No=37%)	OR=1.94 (Yes=50%, No=34%)	–	HR=1.9-2 (Yes versus No)	–
Prior hormone replacement therapy	–	X		X	OR=1.72 (Yes=41%, No=28%)

1. (Crew et al., 2007)

2. (Mao et al., 2009)

3. (Ingle et al., 2010b)

4. (Henry et al., 2012)

5. (Sestak et al., 2008)

6. ANA – anastrozole, EXE – exemestane, LET – letrozole, TAM – tamoxifen, MSK – musculoskeletal

7. ATAC - Arimidex, Tamoxifen Alone or in Combination (ATAC) study

8. NCI CTCAE v3.0 Grade 3 or 4 MS-AE (yes/no)

9. OR – odds ratio

10. “X” – Association with primary endpoint was not significant at a type I error rate of 5%.

11. “—”– Association with primary endpoint was not analyzed in the study.

Germline genetic variation

Studies determining whether germline genetic variation is associated with AIMSS have utilized both genome-wide and candidate gene approaches. Ingle et al. conducted a genome-wide association study of postmenopausal breast cancer patients with ER+/PR+ cancer (stages I to III) receiving anastrozole or exemestane (Ingle et al., 2010b). Cases were required to either have at least grade 3 musculoskeletal toxicity, according to the NCI-CTCAE v3.0, or go off treatment due to a musculoskeletal adverse event within the first 2 years. This study identified genetic variants in 3′ region of *TCLA1* as having the strongest association with musculoskeletal toxicity. Several additional studies have also utilized case-control designs, however, genetic variation evaluated in these studies was focused on genes in three main pathways: sex steroid synthesis [aromatase (*CYP19A1*), steroid 17-alpha-hydroxylase/17,20 lyase (*CYP17A1*)], estrogen signaling [estrogen receptor 1 (*ESR1*), estrogen receptor 2 (*ESR2*), and progesterone receptor (*PGR*)], and vitamin D metabolism and signaling [7-dehydrocholesterol reductase (*DHCR7*), vitamin D-binding protein (*GC*), vitamin D 25-hydroxylase (*CYP2R1*), 25-hydroxyvitamin D 1-alpha hydroxylase (*CYP27B1*), vitamin D3 receptor (*VDR*), and 1,25-dihydroxyvitamin D 24-hydroxylase (*CYP24A1*)] (Garcia-Giralt et al., 2013; Mao et al., 2011; Wang et al., 2013). An additional study in patients treated with letrozole or exemestane determined whether genetic variation in candidate genes related to estrogen metabolism, estrogen signaling, and AI metabolism were associated with time to treatment discontinuation because of AI-associated toxicity (Henry et al., 2013). This study identified an intronic variant in ESR1 (rs9322336) that was associated with an increased risk of discontinuation of exemestane therapy. The ESR1 variant was not associated with discontinuation in patients receiving letrozole therapy, suggesting a drug-specific effect. Collectively, these studies support association between genetic variants in *TCLA1*, *ESR1*, *CYP19A1*, *CYP27B1*, *CYP17A1* and *VDR* with AIMSS. Taken

together, it is difficult to draw strong conclusions about the influence of genetic variation on AI-induced musculoskeletal toxicity due to differences in the genes and genetic variants studied between these trials. Only genetic variants in *TCLA1*, *ESR1* and *CYP19A1* have been genotyped in more than one study, of which only variation in *ESR1* has shown significant associations in more than one study. As will be discussed, interpretation of results across these studies is also limited by the lack of a standardized definition of AI-induced musculoskeletal toxicity.

Inflammation

The influence of estrogens on the innate and adaptive immune systems has been well documented. Inflammatory cytokines are suppressed by high blood estrogen concentrations, while lower estrogen concentrations can augment inflammatory cytokine production (Islander et al., 2011). Additionally, estrogens modulate the adaptive immune system by inhibiting lymphopoesis and increasing the contribution of T helper type 2 relative to T helper type 1-mediated immune processes (Straub, 2007). The question of whether changes in plasma concentrations of inflammatory cytokines are associated with AIMSS has been evaluated by Henry et al. (Henry et al., 2010b). This study found that before initiation of AI therapy, subjects who would subsequently develop AIMSS had higher baseline serum concentrations of six cytokines and growth factors relative to those subjects that would not develop AIMSS (fibroblast growth factor-basic, interleukin-12 p40, interleukin-1 receptor alpha, macrophage inflammatory protein-1, interleukin-1 beta, and interleukin-17). However, no changes in serum concentrations of 36 factors assayed relative to pre-treatment were observed between cases and controls during AI therapy, suggesting AIMSS is not a consequence of systemic inflammatory response to AIs. Additionally, rheumatologic evaluation of subjects with AIMSS does not support inflammation of affected joints and studies to identify blood biomarkers have shown no

association with biochemical markers of inflammation (e.g. C-reactive protein), muscle injury (e.g. creatinine kinase), or autoimmunity (e.g. rheumatoid factor and anti-nuclear antibody) (Briot et al., 2010; Henry et al., 2007; Henry et al., 2010b).

Reduced bone mineral density

AIs accelerate the loss of bone mineral density of the lumbar spine and hip in post-menopausal breast cancer patients, presumably due to reduced estrogen concentrations. While it has been suggested that AIMSS may be secondary to loss of bone mineral density, to date, no prospective study has directly addressed whether the onset or severity of AIMSS correlates with changes in bone mineral density or biochemical markers of bone turnover (Henry et al., 2008). In several randomized trials, bisphosphonates have effectively prevented or reduced bone loss in women receiving AIs (Brufsky et al., 2007; Gnant et al., 2009; Van Poznak et al., 2010). Therefore, if bone loss leads to AIMSS, bisphosphonates may be effective agents to inhibit or reverse musculoskeletal pain. However, Brufsky et al. showed no difference in the frequency of arthralgia, myalgia, pain in extremities, or back pain, between patients who received zolendronic acid upfront and those who received a delayed treatment (Brufsky et al., 2007). The mean time to initiation of zoledronic acid in the delayed group was 8.8 months (range, 0.03 to 24.15 months), and given that many patients develop symptoms within six months of initiating an AI, a majority of patients would have developed musculoskeletal pain before initiating the bisphosphonate. Furthermore, the rate of arthralgia in the upfront group was similar to that reported in other studies in which patients only received an AI. These data are consistent with an additional study that showed that discontinuation of anastrozole therapy due to arthralgia or arthritis symptoms was not different in postmenopausal patients randomized to receive a bisphosphonate (risedronate) versus placebo (Van Poznak et al., 2010). In another

study, arthralgia adverse events were more frequent in premenopausal breast cancer patients receiving zolendronic acid in addition to anastrozole and goserelin (for ovarian suppression) (150 of 450; 33.3%) than those not receiving zolendronic acid (112 of 453; 24.7%) (Gnant et al., 2009). Collectively, these results do not support the hypothesis that enhanced bone loss represents an important causal factor mediating pain during AI therapy.

Estrogen depletion

As has been hypothesized, AI-associated pain may be initiated by estrogen depletion, as measured by reduction in concentrations of plasma or tissue estrogens (Felson and Cummings, 2005; Henry et al., 2008). Indeed, numerous clinical observations support the association between reduced blood estrogens and musculoskeletal pain: development and intensification of osteoarticular pain is strongly associated with transition into menopause (Berecki-Gisolf et al., 2009; Cecil and Archer, 1925; Dugan et al., 2006; Meriggiola et al., 2012), joint symptoms worsen following discontinuation of hormone therapy (Brunner et al., 2010; Ockene et al., 2005), arthralgia is common during gonadotropin-releasing hormone antagonist treatment (Friedman et al., 1993; Spitz et al., 2012), and myalgias and arthralgias develop following cyclophosphamide-induced ovarian suppression (Loprinzi et al., 1993). Conversely, menopause-associated joint pain and stiffness is relieved by estrogen plus progestin therapy (Chlebowski et al., 2013).

A pair of studies have addressed whether AIMSS is associated with estrogen concentrations during AI therapy. One study reported that serum estradiol concentrations less than 5 pg/mL are associated with a higher incidence of AIMSS (Honda et al., 2011), whereas the second study found no association between serum

concentrations of estradiol or estrone when concentrations were stratified by the analytical lower limit of their detection (1.5 and 1.7 pg/mL respectively) (Mao et al., 2011). Although these studies support seemingly opposite conclusions, several limitations reduce our ability to make strong conclusions based on these findings. First, neither study was sufficiently powered to test this association. Secondly, it is unclear whether the analytical methods utilized to measure serum estrogens were sufficiently sensitive and specific for measuring serum estradiol during AI therapy. Lastly, the estrogen concentration thresholds used have no physiologic basis and no attempt was made in either study to explore a concentration-dependent effect of serum estrogens. Therefore, further clinical studies are needed to fully address this hypothesis.

A retrospective analysis of the Arimidex, Tamoxifen Alone or in Combination (ATAC) study revealed a correlation between symptoms related to endocrine therapy and risk of breast cancer recurrence (Cuzick et al., 2008). Specifically, women experiencing joint pains within the first three months of therapy had significantly reduced risk of recurrent disease. This study was adequately powered to address this question, using 1967 and 1997 women randomized to anastrozole and tamoxifen who were monitored over 9 years. These data support a unifying hypothesis, suggesting the AI-induced estrogen suppression is associated with both aromatase inhibitor efficacy and toxicity. Correlation of drug-induced side-effects with response to treatment has been noted in a few other situations, notably neurotoxicity with increasing exposure to agents such as vincristine or platinum agents, graft-versus-host disease for allogeneic bone-marrow transplantation, and skin rash for antibodies directed at the EGFR or tyrosine-kinase inhibitors. The inferred relationship between AI potency, as measured by estrogen depletion, and outcomes has not been directly tested and the underlying mechanism remains speculative.

Summary

Many clinical studies have been conducted to identify clinical factors and other biomarkers associated with the incidence or severity of AI-induced musculoskeletal symptoms. Factors showing strong association with these side effects could be used in a number of ways, including providing insight into potential mechanisms, guiding interventional strategies, identifying patients at high risk for toxicity, and therapy selection. However, to date, there are no consistent risk factors to predict which patients will develop AI-associated musculoskeletal symptoms. While comparisons among studies are limited by variable trial design and covariates analyzed, a significant limitation is the lack of diagnostic criteria and no accepted definition of what constitutes AI-induced musculoskeletal toxicity. As a result of ambiguity in defining the syndrome, studies have evaluated patients using a variety of quality of life questionnaires and patient self-reporting. Several studies have used rheumatologic questionnaires that are validated for the longitudinal assessment of arthritis, such as the Health Assessment Questionnaire-Disability Index (Henry et al., 2007). However, it has been suggested that AI-induced musculoskeletal pain is not associated with inflammation resembling that found in rheumatoid arthritis, calling into questions the use of instruments designed to measure inflammatory disease (Henry et al., 2007). Additionally, the toxicity may represent a cluster of symptoms, potentially each having a unique mechanistic basis. Thus, better measures of AI-induced musculoskeletal toxicity that are based on a mechanistic understanding of the toxic effects of these drugs are needed.

Many of the the clinical association studies presented here are based on rational assumptions as to the mechanisms (e.g. bone turnover), cells (e.g. immune cells), or organs (e.g. bone) contributing to AI-induced pain. In addition, it has been proposed that changes in pain transmission, specifically reduced inhibitory mechanisms in the CNS,

are altered during AI therapy (Felson and Cummings, 2005). Undoubtably, the nervous system plays a critical role in the perception, transmission, and processing of noxious events in patients with musculoskeleltal pain during AI therapy. As discussed below, altering systemic and tissue estrogen concentrations is known to significantly alter animal models of pain, forming the basis of the hypothesis that estrogen-mediated CNS or PNS changes during AI therapy may result in AI-induced pain (Felson and Cummings, 2005). Additionally, the expression of aromatase in the peripheral nervous system suggests that one effect of AIs may be to alter nociception by directly acting on the peripheral nervous system. On the other hand, AIs may also alter nociception through mechanisms unrelated to their ability to reduce aromatase activity and both potential mechanisms may contribute to pain during AI therapy.

Estrogen deficiency and animal models of pain

Humans with pain may experience dysesthesia, hyperalgesia, or allodynia as a result of altered sensory recognition of a stimulus. In chronic pain states, many human subjects also experience dysesthesia in the absence of an apparent external stimulus. In psychophysical terms, the state of pain is associated with a leftward shift that occurs in the relationship between stimulus intensity (no stimulus in the case of spontaneous pain) and the affected sensations and pain perception. It is likely that animals experience pain-like sensations that may mirror those experienced by humans, however, our inability to communicate with animals restricts our understanding of their perception of a stimulus and relating this experience to what humans might consider painful. Thus, the inability to communicate between animals and humans is the greatest obstacle in generating meaningful animal models of pain. In absence of a clear translation between animal and human recognition of pain, a series of behavior models have been developed that

equate a stimulus or substances known to elicit pain in man and the behavior after introducing the stimulus or substance into animals. While these models are limited in their interpretation, the study of animal behavior in reaction to a stimulus that would be algogenic in humans provides the only indicator of what may be disagreeable to the animal. This cannot be reliably determined using any other types of methods or measures (e.g. electrophysiological parameters).

The ovariectomized (OVX) rat

The *in vivo* effects of reduced estrogen concentrations in animal models of pain are often studied by determining behavioral changes in OVX animals. Two weeks after female rats are ovariectomized, serum estrogen concentrations are significantly depleted (Pfaff, 2002). Mean serum concentrations of estradiol in OVX rats have been estimated to be between 1.83 and 3.9 pg/mL when measured by radioimmunoassay without organic extraction (Kuba et al., 2006; Strom et al., 2008b). These concentrations are near those measured in male rats using radioimmunoassay without organic extraction (3 ± 1 pg/mL) (Toung et al., 1998). Organic extraction prior to analytical measurement of steroids is the gold-standard approach for measuring low steroid concentrations and results in much lower estimated concentrations, presumably due to the elimination of conjugated steroids (Strom et al., 2008a). In a study measuring serum estradiol from male rats that incorporated a diethylether extraction step prior to assaying estradiol by radioimmunoassay, estradiol concentrations were 1.06 ± 0.23 pg/mL (Erben et al., 2000). Furthermore, plasma estradiol concentrations in post-menopausal women and women receiving AI therapy are consistently lower when measured by gas chromatography/tandem mass spectrometry assay than those determined by RIA, presumably due to increased selectivity following chromatography of the steroids (Santen et al., 2007). Thus, serum estradiol concentrations in OVX and male rats are

likely much lower than concentrations reported in many studies using radioimmunoassays.

In the course of several weeks following surgery, ovariectomized female rats and mice develop enhanced sensitivity to mechanical stimulation of the hind paws (Chen et al., 2012; Dina et al., 2001; Ma et al., 2011; Sanoja and Cervero, 2005). These effects are attributed to reduced estrogens following ovariectomy, as estrogen replacement was shown to prevent (Ma et al., 2011; Sanoja and Cervero, 2005) or reverse (Sanoja and Cervero, 2008) OVX-induced mechanical allodynia. As will be discussed, the development of mechanical allodynia in OVX rats has been proposed to be mediated by enhanced sensitivity to endogenous inflammatory mediators in nociceptive sensory neurons (Chen et al., 2012; Ma et al., 2011). In contrast, the effect of estrogen loss modeled by ovariectomy on thermal hypernociception is variable. Some studies have shown that OVX animals respond more rapidly to a noxious thermal stimulus than intact or sham operated animals (Sanoja and Cervero, 2008), others have shown the opposite effect of OVX on thermal hypernociception (Terner et al., 2005), and yet additional studies have demonstrated no effect of ovariectomy or estrogen add-back (Mannino et al., 2007; Sanoja and Cervero, 2005).

The influence of OVX and hormone replacement on hypernociception in response to inflammation has been thoroughly reviewed (Craft, 2007; Fillingim and Ness, 2000). The effect of altering systemic estrogens in inflammatory pain models are complex, and OVX can produce hypernociception or anti-nociception depending on the inflammatory model, the site of inflammation, and the nociceptive behavior measured. One inflammatory mediator whose effects on nociceptive behaviors are altered by estrogens or estrogen depletion is ATP. For example, when compared to sham-operated

controls, overt nociceptive response to intraplantar administration of ATP into the rat hindpaw is augmented in OVX rats (Ma et al., 2011). Augmentation of nociceptive behavior produced by ATP was inhibited by coadministration of an antagonist of $P2X_1$ / $P2X_3$-ATP receptors (2′,3′-O-(2,4,6-trinitrophenyl) adenosine-5′-triphosphate, TNP-ATP), suggesting a change in the activity of these channels. These behavioral changes correlated with increased expression of $P2X_3$ in dorsal root ganglia (DRG) in OVX animals. Conversely, administration of 17β-estradiol (daily subcutaneous injection of 30 μg/kg/day) to OVX rats for five weeks attenuated the enhanced nociceptive response to ATP and reduced $P2X_3$ expression in DRGs (Ma et al., 2011). Interestingly, TNP-ATP administration additionally reversed mechanical sensitivity to von Frey filaments that developed follow ovariectomy, implicating P2X receptor activity in the maintenance of mechanical hypersensitivity following OVX (Ma et al., 2011). Estradiol similarly attenuated overt nociception induced by the $P2X_1$ / $P2X_3$ –selective agonist, α,β-meATP, in female and OVX female rats when the compounds were co-administered in the paw (Lu et al., 2013). This effect was mimicked by co-administration of selective agonists for the estrogen receptors ERα and G protein-coupled estrogen receptor 1 / G protein-coupled receptor 30 (GPER / GPR30), suggesting that the activation of estrogen receptors modulates ATP-evoked behavior when sufficient local concentrations of the steroid are achieved (Lu et al., 2013).

The diverse, and often contradicting, effects of ovariectomy on nociceptive behavior may be explained by the pleiotropic roles of estrogens in the initiation, processing, and response to nociceptive stimuli (Craft, 2007). On the other hand, there may be other contributing factors. Ovariectomy induces hyperphagia that, in turn, results in substantial weight gain and adiposity (Gale and Sclafani, 1977). Adipose tissue can act as an endocrine organ and secretes a number of inflammatory factors (Lyon et al.,

2003). Accelerated bone and cartilage turnover and erosion following OVX in rodents has been used to study mechanisms underlying postmenopausal osteopenia and osteoarthritis (Hoegh-Andersen et al., 2004; Weitzmann and Pacifici, 2006). Upregulation of inflammatory mediators in the joints and in the circulation are expected to alter nociceptive responses to specific stimuli and may augment or oppose the specific actions of reduced estrogen concentrations (Abu-Taha et al., 2009). Thus, interpreting OVX-mediated behavioral changes as a consequence of estrogen depletion in the nervous system is perilous given the additional adaptive and physiological changes that occur in this model.

Although the major source of endogenous estrogen in females is the ovaries, it is well established that males and females synthesize estrogens in other tissues including the adipose, spinal cord, DRGs, and select brain regions. For instance, estradiol content in the rat brain varies widely between brain regions, and while region-specific content does not show a clear correlation with blood estradiol concentrations, regions with relatively high levels of aromatase activity correspond to high estradiol content (Konkle and McCarthy, 2011a). Therefore, the amount of estrogen in aromatase-expressing tissues may be asynchronous with blood estrogen concentrations. For example, aromatase activity in adipose tissue is unchanged following ovariectomy in rats (Zhao et al., 2004). However, OVX rats gain considerable amounts of adipose tissue, suggesting non-gonadal aromatase activity contributes little to blood estrogen concentrations in rats (Gale and Sclafani, 1977). In aromatase-expressing tissues, mechanisms may exist to rapidly modulate the bioavailability of estrogen in a space-, concentration-, and time-dependent manner, details that could not be well controlled with estrogens derived from the circulation. Based on these observations, the use of OVX animals to model the effect of tissue estrogen depletion on pain may be most appropriate for tissues with estrogens

supplied primarily by the blood. Tissues expressing aromatase, with the ability to synthesize local estrogens on demand may be less influenced by ovariectomy. Despite this, estrogen exposure is expected to be reduced in most tissues in OVX animals and changes in nociceptive behaviors in OVX rats may be helpful in guiding studies of AI effects on nociception, particularly those influenced by aromatase inhibition.

Aromatase inhibitor treatment

Despite the clinical significance of AI-induced arthralgia, few studies have attempted to determine the effects of AIs in animal models of nociception. Naïve and ovariectomized female rats treated systemically with letrozole exhibited augmented hypernociceptive behaviors following intraplantar administration of formalin (Moradi-Azani et al., 2011). More specifically, letrozole augmented the second phase of formalin-induced behavior, which is mediated by an inflammatory response at the site of formalin administration and altered integration of peripheral afferent activity by second order neurons in the spinal cord dorsal horn (Tjolsen et al., 1992). The effect of letrozole to augment nociceptive behavior is consistent with previous reports suggesting that OVX rats have augmented formalin-induced nociception, which is attenuated by systemic estrogen replacement (Ceccarelli et al., 2003; Fischer et al., 2008; Kuba et al., 2006; Mannino et al., 2007). The ability of AIs to alter inflammatory nociceptive behavior in OVX rats suggests that estrogen synthesis in non-ovarian tissues may play an additional role in mediating the integrated nociceptive response to formalin. Aromatase knockout mice also display increased grooming during interphase and phase II following formalin injections in the lip, suggesting an ability of AIs to augment the response to formalin is mediated by altered aromatase activity (Multon et al., 2005). In comparison, studies in the male Japanese quail showed systemic and intrathecal administration of the AI, vorozole, either increased or had no effect on withdrawal latency following immersion of

the birds' feet in hot water, depending on the birds' hormonal status (Evrard and Balthazart, 2004a, b). Collectively, these studies suggest that AIs alter behavior responses to nociceptive stimuli, although there may be differences depending on the stimulus, route of administration and the model organism. However, the effects of AIs in these models have not been sufficiently studied to draw strong conclusions as to their potential effects and mechanisms.

It is clear from studies using OVX rats and estrogen replacement that nociceptive behaviors to a variety of stimuli are modulated by altering systemic and local concentrations of estrogens. Studies using isolated sensory neurons have also shown that estrogen can alter several features that contribute to their function, suggesting that their effects *in vivo* may be attributed, in part, to their actions at the level of the nociceptor. For instance, a microarray analysis of trigeminal ganglia from OVX rats identified 21 genes whose expression was significantly altered by systemic estradiol treatment (Diogenes et al., 2006). As will be discussed below, in sensory neuron cultures, estradiol exposure has been shown to alter the expression of neurotransmitters, as well as, as the expression and activity of several ion channels. These molecular changes could be expressed as altered neuronal function *in vivo*. Since AIs induce musculoskeletal pain in humans, and preliminary studies in animals suggest AIs also alter nociceptive behaviors, these drugs may directly or indirectly alter the response of the peripheral nervous system to a variety of stimuli. As will be discussed, the recent observation of aromatase expression in DRG neurons suggests that local estrogen synthesis may regulate the function of estrogen-sensitive sensory neurons. Moreover, one mechanism by which AIs may alter sensory neuron function may be secondary to aromatase inhibition in these cells.

Sensory neurons

General anatomy and physiology

Sensory neurons are neurons that detect stimuli external to the organism and encode the stimulus in the form of action potentials. Sensory neurons are therefore distinct from neurons of the central nervous system (CNS), which receive stimuli from other neurons and from glia. The cell bodies, or soma, of primary sensory neurons are clustered in DRGs, ganglia that lie laterally along the spinal column. Primary sensory neurons are morphologically pseudo-unipolar, in that the axon is bifurcated; one branch projects to form synapses on second-order sensory neurons of the spinal cord and the other branch innervates peripheral tissue. When sensory fibers resident in peripheral tissues are subjected to a sufficient external stimulus, they transmit the stimulus in the form of action potentials toward the CNS. Due to a vast heterogeneity in stimuli that are encoded by these specialized cells, they collectively relay a continuum of information to the CNS, contributing to proprioception (awareness of body position), kinesthesia (awareness of body movement), discriminative touch, vibration, itch, temperature gradations (cool to cold and warm to hot), and mechanical gradations. The summation of these sensory transmissions to the CNS allows the brain to “perceive” the organism’s environment.

A body of work has related the excitation of a subset of ‘noci-receptive’ sensory fibers, termed ‘nociceptors’, and the perception of pain, which are of principally important to this body of work (Sherrington, 1906). Nociceptors are specialized primary afferent sensory neurons that are functionally defined by their distinct stimulation thresholds. Under physiological conditions, nociceptors generate action potentials in response to stimulus intensities just below that which would generate tissue damage. Conversely,

under resting conditions, nociceptors respond weakly or not at all to innocuous stimuli. When nociceptors are subjected to an injury within their receptive field, they may be physically damaged or exposed to inflammatory mediators released at the site of injury. Under these conditions, they often develop a lowered threshold for generating action potentials and display an enhanced response to suprathreshold stimuli. Therefore, the implied physiologic function of nociceptors is two-fold: to notify the CNS when stimuli approach intensities that may result in damage to the organism and to discern and adapt to an ongoing injury. In parallel with these changes in sensory neuron function, the individual may perceive pain at the site of injury (*primary hyperalgesia*) or pain in the surrounding skin or tissue (*secondary hyperalgesia*).

Nociceptors can detect and react to several stimulus modalities, including: temperature (thermoreceptors), mechanical force (mechanoreceptors), and many endogenous and exogenous chemicals (chemoreceptors). As described by Bessou and Perl using cats as a model, unmyelinated cutaneous sensory neurons elicit action potentials in response to one or more of these stimuli delivered over a range of intensities, yielding a response pattern that can be grouped into several categories (Bessou and Perl, 1969; Perl, 1996b). Among C-fibers, the most common nociceptors are ‘polymodal’ (30 per cent of neurons); these cells are excited by strong mechanical stimulation (needle pricks and von Frey hairs), by noxious heat, and by irritant chemicals (a drop of 0.1N hydrochloric acid applied to the skin). Another fourteen percent of the C-fibers are activated by strong mechanical stimulation, but are unresponsive to noxious heat (60°C) and cooling the skin to abnormal temperature (10°C), and thus could be considered as selective mechanoreceptors. The remaining neurons surveyed could be described by neuronal discharge in response to gentle mechanical stimuli (von Frey hairs of 0.01 to 0.045 grams) and cooling, small innocuous temperature changes, or no

response to skin stimulation. Thus, approximately 44% of the slowly conducting C-fibers innervating the skin are excited by noxious stimuli and are therefore, by definition, nociceptors. A similar survey of lightly myelinated sensory neurons innervating the cat hind limb (classified as Aδ-fibers by conduction velocities from 6 to 51 meters per second), suggested this class of sensory neurons is unresponsive to noxious heat (> 50°C) and cooling to 20°C or acid applied to the skin (Burgess and Perl, 1967). Rather, they found that 14% of Aδ-fibers responded to one or more forms of noxious mechanical stimulation, while the remaining neurons were excited by innocuous mechanical forces or completely insensitive to all stimulus modalities (Burgess and Perl, 1967). Cutaneous nociceptors in other species, including the rat and mouse, have been identified with similar properties, although the relative proportion of receptor types within C- and Aδ-fibers are dependent on the species and innervated tissue (Koltzenburg et al., 1997; Leem et al., 1993). These classifications are not comprehensive and several excellent articles describe the functional classification of nociceptive fibers, including further subdivision based on additional stimuli, under physiological, pathological, and inflammatory conditions (Dubin and Patapoutian, 2010; Kumazawa et al., 1996). Importantly, a feature of many polymodal C-fibers and myelinated mechanoreceptors is enhancement of responsiveness after exposure to an initial noxious stimulus or inflammatory mediators (Bessou and Perl, 1969; Perl, 1996a). This adaptable property, termed ‘sensitization’, is manifest by an increase of discharge for a given stimulus and a lowering of the threshold to evoke neuronal discharge.

Molecular classification

Estrogen receptors

The physiological effects of estrogens are mediated by a family of intracellular ligand binding proteins called the estrogen receptors (ERs) that orchestrate both

transcriptional and ′non-genomic′ functions secondary to ligand binding. Due to their lipophilicity, unconjugated estrogens (e.g. predicted logP of estradiol is 3.75) diffuse freely through lipid bilayers to bind ERs. When estrogens bind the classical ERs (ERα and/or ERβ), these receptor complex(es) translocate to the cell nucleus and bind DNA at estrogen response elements to either induce or repress gene expression (Lin et al., 2007). The binding and activity of ER-interacting proteins confer distinct ER functionality, and therefore, the pleiotropic and tissue-specific actions of estrogens result from the differential expression and interaction between the ERs and their coactivators and corepressors (Moggs and Orphanides, 2001). In L6 and S1 DRG of adult female rats, roughly 40% of small and medium diameter neurons are immunoreactive for ERα or ERβ, and only 5% of neurons display immunoreactivity to both ERs (Papka and Storey-Workley, 2002). However, the expression level or distribution of ERs in DRG neurons may be dependent on the ganglion level (Taleghany et al., 1999).

In addition to the classic ERs, the seven-transmembrane spanning G-protein-coupled estrogen receptor GPR30 is also expressed in DRG neurons (Takanami et al., 2010). GPR30 is a Gαs-coupled receptor that was identified based on the ability of estrogens to activate adenylyl cyclase in cells that lack ERα and ERβ (Filardo and Thomas, 2005). Although estradiol is an agonist at GRP30, the receptor has pharmacology distinct from ERα and ERβ and can be activated by partial and pure antagonists of ERα and ERβ (Aronica et al., 1994). GPR30 is expressed in small (< 30 μm), medium (≥ 30, ≤ 40 μm), and large (> 40 μm) diameter neurons in the lumbar DRG, with roughly 40% of small diameter neurons and 20% of larger diameter neurons displaying immunoreactivity (Takanami et al., 2010).

Transient receptor potential cation channel subfamily V member 1 (TRPV1)

Cell surface receptors expressed in peripheral nerve terminals conduct stimuli impinging upon the receptive field(s) of sensory neurons. For a given stimulus, activation of one or more of a diversity of protein families, including ion channels, G-protein coupled receptors, and tyrosine kinase receptors initiate nociceptor excitation (Lumpkin and Caterina, 2007). Among these many receptors, the temperature-activated, transient receptor potential (TRP) family of cation channels mediate thermosensation. While sensory neurons are activated by a wide range of temperatures, individual TRP channels conduct cations in response to a limited range of temperatures. For instance, TRPM8 is activated by cooling from normal skin temperatures (approximately 30°C) to temperatures below 30°C (Peier et al., 2002). Conversely, temperatures of 43°C and 52°C activate TRPV1 and TRPV2, respectively (Caterina et al., 1999; Tominaga et al., 1998). Like many TRP channels, TRPV1 is polymodally activated: additional stimuli include non-selective physiologic molecules (such as low pH or protons and eicosanoids) and selective xenobiotic agonists (such as capsaicin and resiniferatoxin). Experiments with mice lacking several transmembrane regions of TRPV1 (TRPV1 KO) support the role of this ion channel in encoding noxious heat and as a vanilloid receptor. When compared to wild-type mice, TRPV1 KO mice exhibit marked thermal hypoalgesia when placed on a hot plate at temperatures ≥ 52.5°C and have reduced flinching and licking responses to intradermally administered TRPV1 agonists (Caterina et al., 2000). In sensory neurons of the rat DRG, TRPV1 is predominantly expressed in small diameter sensory neurons (< 35 μm) that also express neuropeptides: approximately 35% of TRPV1-expressing neurons also express substance P and 50% co-express calcitonin gene-related peptide (CGRP) (Price and Flores, 2007).

The activity of TRPV1 and nociceptive behaviors generated by TRPV1 agonists is both enhanced and diminished by estrogens through several mechanisms. For example, exposing DRG neurons to estradiol for 24 hours inhibits capsaicin-stimulated TRPV1 currents (Xu et al., 2008). In neuronal cultures from trigeminal ganglia, estradiol upregulates the prolactin receptor, which confers the ability of prolactin to sensitize capsaicin-stimulated TRPV1 currents (Diogenes et al., 2006). *In vivo*, intraplantar co-injection of estradiol with capsaicin potentiates capsaicin-induced nocifensive response in male rats (Lu et al., 2009). Using an alternative behavioral model to study activation of TRPV1-expressing nociceptors, ten days of systemic estradiol administration (20 μg/d) did not alter nocifensive behavior elicited by capsaicin applied to the eyes. However, estradiol treatment did augment the effect of prolactin to augment this behavior (Diogenes et al., 2006). These studies suggest that the response of sensory neurons to TRPV1 activation may be sensitive to changes in estrogen concentrations during AI treatment.

Calcitonin gene-related peptide (CGRP)

CGRPα is a 37 amino acid peptide that is produced by alternative splicing of the calcitonin messenger RNA, transcribed from *Calca* (Amara et al., 1982; Rosenfeld et al., 1992). Another gene (*Calcb*) encodes another CGRP isoform, CGRPβ, which differs from CGRPα by one amino acid (Amara et al., 1985). In DRG neurons, CGRPα is the predominant isoform due to higher expression of *Calca* than *Calcb* (Schutz et al., 2004). CGRP and substance P immunoreactivity in sensory neurons has been used to demarcate the “peptidergic” class of nociceptors, though the expression of these peptides is not limited to nociceptive neurons (Lawson et al., 2002). The neuropeptides CGRP and substance P are upregulated by estradiol. Estradiol increases mRNA and content of CGRP and substance P in a concentration and time-dependent manner *in*

vitro and *in vivo* (Gangula et al., 2000; Mowa et al., 2003a; Mowa et al., 2003b). Estrogens may upregulate the expression of these neuropeptides by ER-initiated transcription of the target genes or upregulation of the NGF receptors, p75NGFR and trkA, that mediate NGF-induced expression of both neuropeptides (Sohrabji et al., 1994).

CGRP is implicated in the underlying pathology of several painful joint disorders, including temporomandibular joint disorder and rheumatoid arthritis. In rats, CGRP-immunoreactive DRG neurons innervate many tissues of the lower hind limbs, including glabrous skin, the knee joint, as well as gastrocnemius and tibialis anterior muscles (Fernihough et al., 2005; McCoy et al., 2013; O'Brien et al., 1989). CGRP expression is particularly prominent in sensory neurons innervating the rat knee, where approximately 70% of joint afferent soma display CGRP immunoreactivity (Fernihough et al., 2005; O'Brien et al., 1989). Interestingly, experimentally-induced inflammation of the rat knee (by intra-articular injection of iodoacetate or complete Freund's adjuvant) results in increased expression of CGRP and TRPV1 in DRG neurons (Fernihough et al., 2005; Staton et al., 2007) and enhanced capsaicin-stimulated CGRP release in spinal cord dorsal horn slices (Nanayama et al., 1989). However, this phenomenon is not limited to inflammation originating in the articular space, as subcutaneous inflammation elicits a similar enhancement of basal or capsaicin-stimulated release of the neuropeptide (Fehrenbacher et al., 2003; Garry and Hargreaves, 1992; Vasko, 1995). Microinjection of the CGRP receptor antagonist CGRP(8-37) close to dorsal horn neurons with joint input inhibits inflammation-evoked hyperexcitability, as well as responses to noxious pressure onto the knee (Bullock et al., 2014; Kumazawa, 1996). These data suggest CGRP expressing neurons play a role in the expression of pain behaviors, including mechanical sensitivity, secondary to inflammation that is in part due to the release of CGRP by the central terminals of primary afferent nociceptors. Additionally, CGRP may contribute to

neurogenic inflammation in the joint by increasing blood flow, recruiting immune cells, and activating resident sensory neuron fibers. Given the ability of estradiol to regulate CGRP and its role in experimental joint pain models, CGRP expressing neurons may contribute to AI-induced pain. However the expression of CGRP or release of CGRP from sensory neurons has not been investigated in animals or cells treated with AIs.

Purinergic receptors

All living cells utilize adenosine 5′-triphosphate (ATP) for numerous cellular processes and intracellular concentrations are estimated between 1 and 10 mM, while concentrations in synaptic vesicles in neurons can achieve 100 mM (Beis and Newsholme, 1975; Burnstock, 2007). Early observations of pain and hyperalgesia induced by ATP applied to blister bases and injected intracutaneously suggested ATP activates or sensitizes peripheral sensory neuron fibers (Bleehen and Keele, 1977; Coutts et al., 1981). The potential release of large amounts of ATP into the extracellular space following tissue damage has prompted speculation that ATP is an important chemical mediator of pain during inflammation. Experimental evidence for this phenomenon has been shown in sensory neuron cultures, where damage to neighboring cells or focal application of cell lysates resulted in excitation of DRG neurons and generated inward currents that were inhibited by pre-treatment with purinergic receptors antagonists (Cook and McCleskey, 2002). Subsequent findings that dissociated sensory neurons are depolarized and generate action potentials in response to ATP suggest that the ability of ATP to act as an algogen is a result of direct actions on the neurons (Jahr and Jessell, 1983).

Once released, ATP is subject to rapid degradation by membrane-bound and soluble nucleotideases, generating adenosine 5′-diphosphate, adenosine 5′-

monophosphate, and adenosine, all of which have receptor-mediated activities (Burnstock, 2007). The effects of these compounds on cells are mediated by the purinergic receptor superfamily that preferentially bind purine nucleosides (e.g. adenosine; P1 receptors) and purine nucleotides (e.g. ATP; P2 receptors). In turn, this superfamily of receptors can be subdivided into those that are G-protein coupled receptors (P1 and P2Y receptors) and those that are of the ligand-gated ion channel-type (P2X receptors) (Burnstock, 2007; North, 2002).

P2X receptors are ligand-gated, nonselective cation channels that mediate transmembrane transport of Ca^{2+}, Na^{+} and K^{+} (Evans et al., 1996). In humans, rats, and mice, there are seven genes encoding P2X receptor subunits ($P2X_1$ to $P2X_7$), of which six are expressed in primary sensory neurons (subunits 1 through 6) (North, 2002). When individually expressed in various expression systems, all P2X subunits form functional homodimers. Additionally, functional heterodimers are also formed when two P2X subunits are expressed together, forming an array of P2X channels in cells expressing a few P2X genes. The selective expression of $P2X_3$ homodimers and $P2X_{2/3}$ heterodimers in nociceptors has attracted much attention on the role of these channels in pain (Collo et al., 1996; Lewis et al., 1995; Vulchanova et al., 1997; Xiang et al., 1998). While $P2X_3$ expression is largely believed to be a marker for non-peptidergic sensory neurons, approximately 20% of $P2X_3$-immunoreactive neurons also express CGRP (Bradbury et al., 1998). The presence of $P2X_3$ and $P2X_1$ channels can be pharmacologically identified using α,β-meATP, a $P2X_1/P2X_3$ - selective ATP analog that is resistant to enzymatic degradation (Khakh et al., 2001). ATP and α,β-meATP exposure generates inward cation currents and a transient burst of action potentials, whose duration mirrors the inactivation of the P2X channels (Molliver et al., 2002).

Eight mammalian P2Y receptors have been cloned ($P2Y_{1,2,4,6,11,12,13,14}$) that are differentially activated by endogenous purine nucleotides ligands (ATP and ADP) and also by pyrimidine nucleotides (UTP and UDP) (Donnelly-Roberts et al., 2008). In DRG neurons from adult rats, P2Y1, P2Y2, P2Y4, and P2Y6 mRNA have been detected (Sanada et al., 2002). ATP and UTP-mediated activation of $P2Y_2$ receptors has been shown to induce a slow-onset and sustained excitation and sensitize capsaicin-stimulated CGRP release in DRG neuron cultures (Huang et al., 2003; Molliver et al., 2002).

In addition to the ability of ATP to induce pain in humans, activation of G-protein-coupled P2Y and ionotropic P2X nucleotide receptors contributes to inflammatory and neuropathic pain behaviors in rodents and may be an important mediator of enhanced mechanosensory transduction in these models (Chen et al., 2005; Cockayne et al., 2000; McGaraughty et al., 2003; Souslova et al., 2000; Tsuda et al., 1999; Xu and Huang, 2002). For example, mice lacking the P2X3 gene have significantly decreased flinching behavior in response to 5% formalin (Cockayne et al., 2000; Souslova et al., 2000). Pharmacological activation of purinergic receptors by ATP or α,β-meATP in the dermis rapidly induces nocifensive behavioral responses and reduces hindpaw withdrawal thresholds to von Frey hair stimulation, which is also induced by intrathecal administration of either agent (Bland-Ward and Humphrey, 1997; Nakagawa et al., 2007; Tsuda et al., 2000). As discussed, nociceptive behavior produced by ATP or α,β-meATP injections is significantly augmented in OVX rats and attenuated by systemic administration of estradiol and co-administration of estradiol. In cultures of dissociated rat DRG neurons, estradiol and the estrogen receptor agonists PPT (ERα-selective) and G-1 (GPR30-selective) attenuate α,β-meATP-induced currents, suggesting the hypernociceptive behaviors to purinergic receptor activation in OVX rats may be

attributed to changes at the level of the sensory neuron (Lu et al., 2013). In addition, estradiol has also been shown to inhibit increases in intracellular Ca^{2+} following stimulation with ATP in DRG cultures from rats and mice (Chaban et al., 2003; Chaban and Micevych, 2005). Since activation of P2X and P2Y receptors increases intracellular Ca^{2+}, estradiol may inhibit either pathway. Given the importance of intracellular Ca^{2+} to the release of neurotransmitters, changes in estradiol exposure in sensory neurons may alter neurotransmitter release following ATP exposure.

Aromatase

While it is clear that estrogens have diverse roles in modulation of pain or nociception, the potential contribution of local estradiol synthesis has been relatively unexplored. The capacity for *de novo* synthesis of estrogens and other steroids in the vertebrate nervous system is well established. In situ hybridization studies have localized *CYP19* (aromatase) mRNA to the preoptic area, hypothalamus, amygdala, and hippocampus (Wagner and Morrell, 1996, 1997). In these brain regions, aromatase immunoreactivity is located in neuronal cell bodies, presynaptic boutons and postsynaptic neurons and in glia (Hojo et al., 2004; Naftolin et al., 1996; Peterson et al., 2005; Schlinger et al., 1994). It has been shown that testosterone that diffuses into the preoptic area of the male neonatal rat is locally aromatized to estradiol. Exposure to estradiol during this developmental period confers the ability of adult sex-specific hormones to activate male-specific reproductive behaviors (McCarthy, 2008; Naftolin et al., 1975). The significant effects of aromatase in the preoptic area are believed to be mediated by estradiol-induced changes in the expression of numerous genes and the ability of estradiol to alter the number and pattern of dendritic spines, resulting in a sex-specific neuronal organization (McCarthy, 2008). Thus, tissue-specific aromatase activity

can alter neuronal behavior as a result of altered molecular phenotypes and the formation of altered synaptic patterning.

In the songbird, aromatase activity in the caudomedial nidopallium (NCM), the bird auditory cortex, is rapidly upregulated during 30 minutes of social interaction, mimicked by audio playback of bird songs (Remage-Healey et al., 2008). Intracerebral microinjections of an aromatase inhibitor (1,4,6-androstatrien-3,17-dione) in the NCM suppressed auditory-stimulated neuronal firing rates of NCM neurons, whereas estradiol microinjections increased the mean firing rate, providing evidence that estradiol formed locally in the NCM modulates the processing of sensory information (Tremere et al., 2009). These observations demonstrate that brain-derived estrogens influence integrated behaviors by eliciting organizational effects during development that manifest in adult behaviors and can alter the processing of sensory information.

As compared to the central nervous system, little is known about the expression, activity, and potential role of aromatase in the peripheral nervous system. As discussed, Evrard and Balthazart have demonstrated that intrathecal delivery of an AI alters nociceptive behaviors in the Japanese quail (Evrard and Balthazart, 2004a, b). In the spinal cord of these birds, aromatase immunoreactivity has been localized to the superficial dorsal horn, in proximity to substance P immunoreactive terminals (Evrard et al., 2000). Thus, as suggested by Evrard and colleagues, aromatase activity may influence or be influenced by sensory transduction from the peripheral nervous system (Evrard et al., 2000; Evrard et al., 2003). In contrast, aromatase activity was not detected in rat spinal cord homogenates in two separate studies. It is unclear whether experimental differences contribute to these differences or whether these results indicate significant species differences in the localization and contribution of aromatase activity in

the spinal cord (MacLusky et al., 1987; MacLusky et al., 1994). However, aromatase immunoreactivity and synthesis of ^{3}H-estradiol from the steroid precursor ^{3}H-pregnenolone was shown in lumbosacral DRGs from rats (Schaeffer et al., 2010). The capacity of a neural center to synthesize steroids requires the expression and activity of key steroidogenic enzymes and the presence of the requisite steroid precursors. It is expected that aromatase substrates could be effectively delivered to aromatase expressed in DRG cells by the circulatory system given the high density of blood capillaries in ganglion tissue (Jimenez-Andrade et al., 2008). Alternatively, aromatase substrates may be formed by metabolism, as testosterone and androstanediol are known to be formed from progesterone within the DRG (Schaeffer et al., 2010). Furthermore, if locally produced steroids impart biological activity in an autocrine or paracrine fashion, in turn regulating a neurobiological process, formation of the terminal steroid product should occur within the involved neural circuit, in the proximity of steroid receptors. Expression of aromatase and estrogen receptors in DRG neurons raises the interesting possibility that, in addition to exposure to blood supplied estrogens, estrogen synthesis within sensory neurons may alter their physiology via intracrine or paracrine signaling (Schaeffer et al., 2010).

Sensory neuron cultures from the dorsal root ganglia

Psychophysical studies have demonstrated that a number of endogenous and exogenous substances applied within the receptive field of sensory neuron fibers can induce pain or sensitize the response to numerous stimuli. One approach to studying the underlying mechanisms has been to use behavioral animal models, which allow further manipulations than those which would be acceptable in human studies. However, responses measured in humans and animal models are the summation of an integrated response of a substance acting on multiple potential cellular targets. Therefore, using *in*

vivo models, it is difficult to interpret whether the measured response results from direct action of a substance on neurons, and further, differentiate between peripheral and central mechanisms.

One approach to study the role of peripheral sensory neurons is to utilize isolated sensory neuron preparations. These cellular models have been used by many investigators to study basic properties of sensory neurons, including the composition and pharmacology of ion channels and other receptors that control the generation of action potentials and neurotransmitter release. These preparations have also been extensively used to study the action of xenobiotics known to cause pain in humans on sensory neurons. In this context, an advantage of the isolated sensory neuron model is the ability to precisely control drug exposure (concentration x time) in the cell preparation. While drug exposure can be manipulated *in vivo* by altering the dose, route of administration, or frequency of administration, the effects of these changes are often only understood in the context of drug concentrations in the blood while dynamic effects in tissues, such as the DRG are not examined. Therefore, concentration – response relationships can be more easily determined using isolated cells. The use of sensory neuron cultures to study the effects of AIs also removes circulating sources of endogenous sex steroids or other potential inflammatory mediators that may be altered following administration of AIs to animals or humans and which could otherwise cloud interpretation of the data. Thus, this *in-vitro* model is useful to study whether AIs directly alter the function of sensory neurons.

Neuronal cell bodies (soma) from dissociated DRGs express many of the same receptors and signaling molecules that are expressed in the central terminals, peripheral terminals, and axons of nociceptors (Basbaum et al., 2009). As a result, sensory neuron

cultures reproduce the broad diversity of neuron types and physiological properties observed in less reductionist models (e.g. skin nerve preparations) and *in vivo*. Since many neurotransmitters are released from both central terminals as well as receptive endings, investigating the release of neurotransmitters from sensory neuron cultures can be used as an indicator of overall neuronal function. As is the case with any *in vitro* preparation that seeks to be relevant to *in vivo* physiology, these preparations also have some limitations. The use of dissociated DRG cells clearly disrupts sensory neuronal interactions with other neurons and non-neuronal components that may play important roles *in vivo*. For instance, spinal transmission from first order to second order sensory neurons is a regulated process, recruiting facilitory and inhibitory modulation by interneurons, glia, and descending pathways. Thus, the physiological relevance of changes in neuronal excitability or neurotransmitter release from neuronal cultures must be viewed in the context of loss of these interactions and carefully interpreted. Furthermore, DRG cultures are often supplemented with growth factors that play pivotal roles in the maintenance of neuronal phenotypes and excitability. For example, NGF regulates the expression of many ion channels (for example, TRPV1: (Winter et al., 1988); TRPM8, a cold-sensitive channel: (Babes et al., 2004); and ASIC3, an acid-sensing ion channel: (Mamet et al., 2002)) and neuropeptides (Lindsay et al., 1989). Also, neurotrophic factors have been shown to directly sensitize nociceptors *in vitro* (Shu and Mendell, 1999). Thus, supplementing culture medium with neurotrophic factors, in combination with other factors, such as serum, may alter the detection of many stimulus modalities and the subsequent response.

Summary and Research Aims

Although AI-induced pain is thought to be a consequence of aromatase inhibition and estrogen deprivation, alleviating symptoms with estrogenic treatments cannot be ethically tested in the clinical setting. Thus, alternative methods are needed to establish the pathophysiology and mechanisms linking AI treatment to musculoskeletal pain. Given that AIs are used to treat breast cancer in postmenopausal women, the question remains whether AI-induced pain syndromes are secondary to a reduction in the already low concentrations of circulating estrogens, or caused by other potential mechanisms, including inhibition of the local production of estrogens. Additionally, the specific tissue(s) or cell type(s) relevant to pain during AI therapy are unknown, although changes in bone (Muslimani et al., 2009), tendon (Morales et al., 2007), nerve (Felson and Cummings, 2005), and the immune system (Laroche et al., 2007) have been proposed. However, the expression of aromatase and estrogen receptors in DRGs and the spinal cord raises the interesting possibility that aromatase activity in pain-transduction pathways may modulate the processing of afferent sensory information via autocrine or paracrine signaling.

My central hypothesis is that aromatase inhibitors sensitize nociceptors resulting in hypersensitivity during AI treatment. Studies outlined in this dissertation test this hypothesis through the following specific aims:

Specific aim 1. To develop an animal model of AI-induced hypernociception.

Specific aim 2. To determine if AIs sensitize sensory neurons.

MATERIALS AND METHODS

Animals

Experiments were performed using adult male and female Sprague Dawley rats (150-200 grams; Harlan Laboratories, Indianapolis, IN), housed two to three per cage under a 12-hour dark-light cycle (facility was illuminated from 7:00 A.M. to 7:00 P.M.). Ovariectomies were performed by the supplier. Briefly per Harlan's procedures, the female rat was anesthetized and the dorsal mid-lumber area was shaved and disinfected with iodine and alcohol. A 2-3 cm dorsal midline skin incision was made midway between the caudal edge of the ribcage and the tail base. To gain access to the ovaries, incisions of 5.5-10 cm were made into the muscle wall on both sides of the animal, approximately one-third of the distance between the spinal cord and the ventral midline. The ovaries and oviducts were externalized and removed with single cuts through the oviducts proximal to the ovary. Remaining tissue was replaced into the peritoneal cavity and a sterile wound clip was applied to close the skin incisions. Animals were closely examined for incision repair and infection for 72 hours post-surgery and wound clips were removed 10 days post-surgery, as recommended by the supplier. Male rats were housed for at least one week, while ovariectomized rats were housed for at least two weeks, before beginning experiments. Food and water were available *ad libitum*. All experiments were performed in accordance with the ethical guidelines for investigations of experimental pain in conscious animals and the guidelines of the Indiana University School of Medicine Institutional Animal Care and Use Committee (Zimmermann, 1983).

Chemicals and other materials

Letrozole and exemestane were obtained from United States Pharmacopeia (Rockville, MD). Prostaglandin E_2 (PGE_2) was obtained from Cayman Chemical (Ann Arbor, MI). Adenosine 5′-triphosphate disodium salt (ATP), alpha, beta-methyleneadenosine 5'-triphosphate lithium salt (α,β-meATP), 2-hydroxypropyl-β-cyclodextrin (HPβCD), capsaicin, desmethyldiazepam (DMD), 1-methyl-2-pyrrolidinone (MPL), methanol (MeOH), Phe-Ala, bacitracin, L-Ascorbic acid, collagenase type IA, poly-D-lysine, laminin, 5-fluoro-2′-deoxyuridine, uridine, tyrosine phosphatase inhibitor cocktail #2, serine/threonine phosphatase inhibitor cocktail #3, 0.01M phosphate buffered saline (PBS, pH 7.4), methanol, β-mercaptoethanol, RNAseZAP, and phenylmethanesulfonyl fluoride were obtained from Sigma Chemical Company (St. Louis, MO). CGRP (rat) was obtained from Tocris (1161; Bristol, United Kingdom) and [Tyr^{27}]-$CGRP_{27-37}$ peptide (canine, mouse, rat) for iodination was obtained from BACHEM (H-5504; Torrance, CA). HEPES buffer (25mM HEPES, 135mM NaCl, 3.5 mM KCl, 3.3 mM $CaCl_2$, 1.1 mM $MgCl_2$, 3.7 mM D-glucose, and 0.1% (w/v) bovine serum albumin (pH 7.4)) was prepared with chemicals from Sigma Chemical Company. Protease inhibitor cocktail III and radioimmunoprecipitation assay buffer (RIPA) were obtained from EMD Millipore (Billerica, MA). Nerve growth factor (NGF) was obtained from Harlan (Indianapolis, IN). Cell culture plates were obtained from BD Biosciences (San Jose, CA) or Thermo Scientific (Waltham, MA). All other cell culture supplies were obtained from Life Technologies (Carlsbad, CA). iScript cDNA synthesis kit, Bio-Rad Protein Assay Dye Reagent, a Coomassie® Brilliant Blue G-250 based-dye, Bovine plasma gamma globulin, and anti-mouse horseradish peroxidase-conjugated (HRP) secondary antibody were purchased from Bio-Rad (170-6516; Hercules, CA).

Western blots were run using the NuPAGE® sodium dodecyl sulphate – polyacrylamide gel electrophoresis gel system using a Mini-Cell electrophoresis chamber: NuPAGE® pre-cast Bis-Tris gels, 2-(N-morpholino) ethanesulfonic acid SDS running buffer (20x), antioxidant, transfer buffer (20X), sample reducing agent containing 500mM dithiothreitol (10X), lithium dodecyl sulfate sample buffer (4X), SeeBlue Plus2 Prestained Standard, Invitrolon polyvinylidene difluoride (PVDF) membranes, and filter paper were obtained from Invitrogen (Carlsbad, CA). The mouse anti-human aromatase monoclonal antibody was obtained from Serotec (MCA2077S; Oxford, UK) and its selectivity has been previously characterized (Turner et al., 2002). The mouse anti-actin monoclonal antibody that reacts with all six known vertebrate isoforms of actin and two cytoplasmic actins (β, γ) was obtained from Thermo Scientific (MS-1295-P1ABX) and the polyclonal rabbit anti-human hypoxanthine phosphoribosyltransferase 1 (HPRT) antibody was obtained from Santa Cruz (sc-20975; Dallas, TX). The goat anti-rabbit HRP-conjugated secondary antibody was purchased from Jackson ImmunoResearch Laboratories (111-035-046; West Grove, PA). SuperSignal® West Femto Maximum Sensitivity Substrate was obtained from Thermo Scientific and Western Lightning® Plus-ECL Substrate was obtained from Perkin Elmer (Santa Clara, CA). USB PrepEase RNA Spin Kit for RNA isolation was obtained from the USB Corporation (Cleveland, OH). Materials and reagents for quantitative real-time polymerase chain reaction (RT-PCR) were obtained from Applied Biosystems (Foster City, CA): TaqMan® Universal PCR master mix, MicroAmp® 96-well plates, MicroAmp® optical adhesive film, as well as, TaqMan® probe and primer sets for relative quantification of CYP19a1 (Rn00567222_m1), Esr1 (Rn01430445_m1), Esr2 (Rn00562610_m1), Gper (Rn00592091_s1), and GAPDH (4352338E). The rabbit anti-rat CGRP antiserum was a gift from Dr. Michael Iadorola and its selectivity has been previously characterized

(Vasko et al., 1994). ddiH_2O was produced by a EMD Millipore Milli-Q water purification system (Billerica, MA).

Drug administration

In behavioral experiments, on the day of drug injection, letrozole and exemestane powders were dissolved in a 2.5 to 30 percent solution of HPβCD in sterile normal saline. AIs were administered as single or multiple intraperitoneal (i.p.) injections (1 to 30 mg/kg) using a 26G needle. In all experiments, percent solutions and/or volumes of vehicle and saline injections administered to control animals were the same as those administered to animals in the experimental group. ATP was prepared in ice-cold sterile PBS and kept on ice until injection. Prior to injection, ATP and PBS vehicle solutions were drawn into a syringe and warmed to room temperature. Injections in the paw were administered intradermally in the mid-plantar footpad using a 31G needle (50 µL injection volume). With the exception of experiments determining the effect of acute AI exposure, if systemic drug injections and behavioral evaluation occurred on the same day, behavior was measured prior to drug administration.

Behavioral testing

Experiments were performed between 7 am and 3 pm during the animals' light cycle. After a minimum of one week in the animal care facility, animals were acclimated to the testing environment on multiple days for one week preceding any behavioral measurement or drug administration. Prior to each measurement session, animals were acclimated in the testing apparatus for approximately 30 minutes or until grooming or

exploratory behavioral ceased. In all experiments, the observer was blinded to treatment and data analysis was completed at the conclusion of the experiment.

For repeated measures experiments evaluating sensitivity to mechanical and thermal stimuli, baseline responses were obtained by exposing animals to stimuli two to three times on separate days prior to drug administration. The measurement immediately prior to the first drug injection, however, was used as the baseline response. In preliminary experiments with OVX rats, I observed variability in baseline withdrawal thresholds to von Frey filaments. In order to minimize the potential confounding effect of baseline response on drug-induced changes in these longitudinal experiments, male and OVX rats with baseline paw withdrawal thresholds greater than 15 grams, or less than 4 grams, were excluded from the study. To normalize baseline response between treatment groups, animals were rank ordered according to baseline paw withdrawal thresholds and block randomized into treatment groups.

To ascertain mechanical sensitivity (von Frey filament test), rats were placed in an elevated cage with a wire mesh bottom that allowed for stimulation of hind paws. Paw withdrawal response to mechanical stimulation was evaluated with calibrated Semmes and Weinstein monofilaments, using a modification of the “up-down method” (0.4 - 26 grams, the lower and upper limit of the test; Stoelting, Wood Dale, IL) (Chaplan et al., 1994). Filaments were applied to the mid-plantar surface of each hind paw. Trials were started with the four gram filament. A trial consisted of three applications of a filament for approximately five seconds, with at least five seconds separating successive stimulation. A positive response was defined as sharp paw withdrawal when the stimulus was applied, or paw withdrawal immediately upon removal of the filament. The paw withdrawal threshold (PWT) was the stimulus/filament evoking a consistent paw

withdrawal response. PWT was measured for both hind paws and averaged to generate final withdrawal threshold at the specified time point.

To assess thermal sensitivity (Hargreaves test), rats were placed in a ventilated acrylic cage atop a flat glass surface. Paw withdrawal latency (PWL) to noxious radiant heat was assessed using an infra-red heat source (Ugo Basile, Italy) applied to the mid-plantar surface of each hind paw (Hargreaves et al., 1988). Upon initiating the thermal stimulus, an electronic timer was activated. A paw withdrawal (flinching or lifting the paw) was detected by a photocell, which switched off the infra-red source and timer, yielding the PWL. The heat source intensity was chosen to yield baseline paw withdrawal latencies of 10 seconds in the rats. A cut-off of 30 seconds was used to avoid tissue damage to the paw. At least 30 seconds separated successive trials in the same animal. PWL from each hind paw was measured three times and all six measurements were averaged to generate the final latency at the specified time point.

Overt nociceptive behavior in response to ATP was made by observing unrestrained animals on a glass surface covered by an inverted and ventilated four liter plastic beaker. Mirrors were positioned below and behind the beaker to assist behavioral assessment, regardless of animal orientation. Once acclimated to the testing environment, animals were removed, lightly restrained, and administered an intradermal injection in the left hind paw. Animals were immediately returned to the testing apparatus and behavior was observed. As a measure of overt, spontaneous nocifensive behavior, flinching or shaking of the injected paw or hindquarters was recorded (McGaraughty et al., 2003; Wheeler-Aceto and Cowan, 1991). Each observed behavior was recorded as one flinch and behavioral responses were tallied in one minute intervals for 10 or 15 minutes following the injection.

Harvest of rat spinal cord and DRG neurons

Sensory neuron cultures were prepared using a modification of our previously published protocol (Burkey et al., 2004). Briefly, rats were sacrificed by rendering them unconscious by exposure to CO_2 and then decapitating them with a guillotine. The dorsal skin was disinfected with 70% ethanol prior to cutting away fur and skin from the spinal column using scissors sterilized in ethanol. The spinal column was isolated with a transverse cut across the spinal column near the pelvic girdle, followed by dissection along parasagittal and coronal incisions along the long axis of the spinal column.

For experiments utilizing the spinal cord, a sterilized 10 mL syringe fitted with a blunt end needle was inserted into the caudal end of the vertebral canal. Using sufficient pressure, the spinal cord was ejected from the spinal column into ice-cold Hank's balanced salt solution (171 mM NaCl, 6.7 mM KCl, 1.6 mM $NaHPO_4$, 0.46 mM KH_2PO_4, and 6.1 mM D-glucose; pH 7.4). This procedure often required a small amount of the cranial spinal column to be removed because the cranial vertebral canal orifice was too constricted to eject the cord.

To isolate spinal ganglia, residual fur and blood were removed by quickly rinsing the column in running hot tap water and the tissue was subsequently placed in a 50 mL conical tube filled with ice-cold Hank's solution. Excess muscle was trimmed away before the vertebral column was bisected by making cuts through vertebrae along the rostral-caudal axis on the dorsal and ventral sides, yielding two halves of the vertebral column with the spinal cord and spinal ganglia exposed. The bisected column was returned to ice-cold Hank's solution. Dorsal root ganglia of adult male rats were dissected into ice-cold Hank's solution and their axons were trimmed. For experiments

quantifying mRNA, detecting protein immunoreactivity, or quantifying drug concentrations from DRGs, excess Hank's solution was removed and the intact ganglion were either frozen in liquid nitrogen or further processed in lysis buffers, as discussed later. Wet tissue weight of ganglia used for quantifying drug concentrations was recorded. Additional experiments utilized cultured cells from dissociated DRGs that were generated using the following procedure.

Cell culture of rat DRG neurons

Cell culture plates and dishes were prepared prior to DRG harvest; culture surfaces were first coated with poly-D-Lysine overnight at 37°C (3% CO_2) and then coated with laminin overnight at 37°C (3% CO_2). Ganglia were digested in collagenase for one hour at 37°C (3% CO_2) and single-cell suspensions were produced by mechanical agitation using a sterile fire polished Pasteur pipette. Approximately 30,000 cells per well were plated into 12-well Falcon culture plates (3.8 cm^2 surface area; approximately 7900 cells per cm^2), whereas 60,000 cells were plated into 6-well Falcon culture plates (35 mm well diameter) or individual 35 mm culture dishes (8.8 cm^2 surface area; approximately 6800 cells per cm^2). Cells were grown in 3% CO_2 in F12 media or phenol red-free DMEM/F12 media supplemented with 3 mM glutamine, 50 units/mL penicillin, 50 µg/mL streptomycin, 30 µM 5-fluoro-2′-deoxyuridine, 75 µM uridine, and 10% (v/v) heat-inactivated horse serum. Unless specified otherwise, media was supplemented with 30 ng/mL NGF prior to its additional to cells. Cultures were typically grown in F12 media for 12 days and DMEM/F12 media for 9 days, with media changed the day after harvest and every other day until an experiment. For experiments testing the effect of drug exposure on cells in culture, water insoluble drugs (e.g. letrozole and PGE_2) were initially dissolved in 1-methyl-2-pyrrolidinone and then diluted to appropriate

concentrations in culture media. In these experiments, biological controls were treated with the solvent(s) at the same dilution.

Isolation and storage of other rat tissues

Isolation of DRGs and spinal cord was carried out as described above. Rat tissues isolated to quantify mRNA, protein, or drug concentrations were harvested using sterilized surgical tools using the following general procedure. Following sacrifice of the animal, trunk blood was captured in a 15 mL plastic conical tube by inverting the animal. To isolate serum, blood samples were placed in ice for 15 to 30 minutes to allow sufficient coagulation, followed by centrifugation at 2500 rpm (approximately 1400 g). Plantar foot pads were dissected using a sterile 6mm biopsy punch (Miltex, York, PA). Other solid tissues were isolated within minutes of the animal's sacrifice, immersed in Hank's solution, and trimmed of adipose and connective tissue using a scalpel. After excess Hank's solution was removed and tissue wet weight was recorded, the tissues were placed in 1.5 mL Eppendorf tubes or plastic conical tubes and snap frozen in liquid nitrogen. Tissues to be used for RNA quantification were stored in RNAse-free tubes. All tissues were stored at -80°C.

Measuring CGRP by radioimmunoassay

Immunoreactive calcitonin gene-related peptide (iCGRP) release from sensory neurons was measured as previously described (Vasko et al., 1994). CGRP released into HEPES buffer from sensory neurons in culture and perfused spinal cord slices was quantified using a standard curve of 0 – 250 fmol CGRP, prepared in duplicate in HEPES buffer. Standards were prepared in an equivalent volume to the unknowns being

measured in a given experiment. To each unknown and standard, 25 µL of a 1:13 dilution of rabbit anti-rat CGRP antiserum stock (final titer = 1:910,000) were added. Antiserum was not added to two additional blank standards that contained no CGRP (NSB, non-specific binding). Following a 12 – 18 hour incubation at 4°C, a volume of ^{125}I-[0Tyr]-CGRP$_{27-37}$ containing 2000 – 2500 CPMs (typically 25 µL of freshly iodinated peptide) was added to all samples. The same volume of ^{125}I-[0Tyr]-CGRP$_{27-37}$ was added to two additional tubes to represent total counts of the radiolabeled peptide (totals). The samples were incubated at 4°C for 12 – 18 hours and 0.5 mL of an activated charcoal suspension (0.1 M NaH2PO4, 50 mM NaCl, 0.1% BSA, and 1% Norite charcoal (pH 7.4)) was added to all tubes except the ′totals′ containing only the radioactive peptide. Samples were equilibrated for 10 minutes to allow unbound peptide to be bound by the charcoal and then centrifuged at 3000 x g for 20 minutes (4°C) to pellet the charcoal. Supernatants were decanted to a new tube and radioactivity in the samples was measured using a Wallac Automatic Gamma Counter (model 2470) (Perkin Elmer, Waltham, Massachusetts). A calibration curve was constructed by four-parameter log-logistic curve fitting of the signal (partial binding or $y = (CPM_{standard} - CPM_{NSB}) / (CPM_{totals} - CPM_{NSB})$) versus $\log_{10}$-transformed amount of standards (x) (Perkin Elmer Workout software, v2.5). The amount of iCGRP in experimental samples was estimated by interpolation of the fitted line.

Release of iCGRP from sensory neurons in culture

iCGRP release was measured from sensory neurons grown in culture for 7 to 12 days, as previously described (Vasko et al., 1994). Release of iCGRP was measured from sequential 10-minute incubations of neuronal cultures in 400 µL HEPES buffer maintained at 37°C. Basal iCGRP release was determined by incubating cells in HEPES

buffer alone. Subsequently, cells were exposed to drugs diluted in HEPES to determine their effect on basal release. The effect of drugs on evoked release was determined by re-exposing cells to drugs in the presence of 10 or 30 nM capsaicin or 30 mM KCl (substituted for equimolar sodium chloride). Lastly, cells were re-exposed to HEPES buffer alone to demonstrate basal release could be re-established. Buffer (300 µL) was collected following each incubation and transferred to plastic 5 mL tubes. Finally, to measure remaining iCGRP content, cells were lysed in 0.1 N HCl. Cell lysates were serially diluted in HEPES buffer (typically a 24x dilution) and 300 µL were assayed along with the collected fractions for iCGRP using radioimmunoassay, as described. In all experiments, three wells of cells from at least 3 independent harvests were exposed to each experimental condition. Water insoluble compounds (e.g. capsaicin, letrozole, and PGE_2) were initially dissolved in MPL, and then diluted to appropriate concentrations in HEPES buffer. ATP and α,β-meATP were initially dissolved in $CaCl_2$-free and $MgCl_2$-free 0.01 M phosphate buffered saline (PBS, pH 7.4), and then diluted in HEPES buffer. Biological controls were treated with the solvent(s) at the same dilution. Previous studies in Dr. Vasko's lab have established that iCGRP content, nor basal or stimulated release of iCGRP, are affected by MPL at dilutions used in these experiments.

Release of iCGRP from spinal cord tissue

Spinal cord slices were prepared as previously described (Chen et al., 1996). After rats were anesthetized and sacrificed using CO_2 asphyxiation and decapitation, a 1 cm segment of the lumbar enlargement was dissected and chopped transversely and parasagitally into 0.3 x 0.3 mm sections. Tissue from each animal was placed into an individual cylindrical perfusion chamber and is reported as one experimental sample. Slices were perfused at a flow rate of 0.5 mL/min with HEPES buffer (pH 7.4)

supplemented with 200 μM ascorbic acid, 100 μM Phe-Ala, 20 μM bacitracin, and 10 μM phenylmethanesulfonyl fluoride, aerated with 95% O_2–5% CO_2, and maintained at 37°C. After perfusing slices for 20 minutes to equilibrate the tissue, perfusate was collected in 3 minute intervals throughout the experiment (1.5 mL/fraction) using an automatic fraction collector. Baseline release was established by perfusing tissue with HEPES for 18 minutes (6 fractions), with the last 3 fractions considered as 'basal' release. Subsequently, potassium-stimulated release was determined by perfusing tissue for an additional 9 minutes (3 fractions) with HEPES buffer containing 30 mM KCl (substituted for equimolar NaCl). Lastly, slices were perfused with HEPES buffer for 21 minutes (7 fractions) to re-establish basal release. In experiments determining the effect of acute PGE_2 exposure, slices were perfused with HEPES buffer containing vehicle (1:2000 dilution MPL) or 30 μM PGE_2 for 9 minutes (3 fractions) prior to, and throughout stimulation with 30 mM KCl. Following tissue perfusion, spinal cord tissue was collected and homogenized in 2 mL of 0.1 N HCl. Homogenate was centrifuged at 3,000 rpm for 20 minutes at 4°C. The supernatant was serially diluted with HEPES buffer and assayed for iCGRP along with perfusate fractions by radioimmunoassay. The total iCGRP content in each tissue slice was calculated as the content measured in all perfusate fractions plus the tissue homogenate.

Western blotting for aromatase immunoreactivity

Total protein isolation from sensory neuron cultures and rat tissues

Sensory neurons in culture were washed, then scraped in ice-cold PBS, supplemented with 1 mM EDTA, 1 mM EGTA, 1X protease inhibitor cocktail and 1X tyrosine and serine/threonine phosphatase inhibitor cocktails. Cells were pelleted at 18,500 g for 4 minutes at 4°C. The supernatant was discarded and the pellet was re-

suspended in RIPA buffer supplemented with protease and phosphatase inhibitors. DRG, spinal cord, plantar foot pads, and ovaries were dissected into ice-cold Hank's solution and DRG axons were trimmed. After removing residual Hank's solution with a glass pipette, the tissues were snap-frozen in liquid nitrogen and stored at -80°C. Tissues were re-suspended in 1X RIPA buffer supplemented with protease and phosphatase inhibitors. Fibrous tissues (ovaries and skin) were first mechanically homogenized on ice with a Janke and Kunkel Ultra-Turrax rotor-stator homogenizer fitted with a 8 mm turret (three times 5-seconds) (IKA, Breisgau, Germany). Tissues were disrupted using ultrasonicatic homogenization with a Fisher Scientific Sonic Dismembrator 550 (Waltham, MA) fitted with microtip probe (three 5-second pulses at 30 percent intensity). Samples were centrifuged at 18,500 g for 4 minutes (4°C) and the resulting supernatant was transferred to a new tube. Total protein concentrations of the resulting lysates were measured with the Bio-Rad Protein Assay using Bovine plasma gamma globulin standards (50 – 500 µg/mL).

Western blot

Each protein sample was diluted in 10 µL of NuPAGE lithium dodecyl sulfate sample buffer, 4 µL of NuPAGE reducing agent, and ddiH_2O to a final volume of 40 µL. Samples were heated at 70°C for 10 minutes and then loaded in a NuPAGE Novex Bis-Tris gel (4-12%) immersed in 2-(N-morpholino) ethanesulfonic acid SDS buffer (diluted in ddiH_2O to 1X, containing NuPAGE antioxidant diluted to 1X), along with 10 µL of a pre-stained protein standard. Proteins were separated for 1.5 hours at 200V and then transferred at 15V to a PVDF membrane overnight at 4°C in NuPAGE Transfer Buffer (diluted to 1X in ddiH_2O, containing 10% MeOH and NuPAGE antioxidant diluted to 1X). The membrane was subsequently blocked for two hours in 5% milk (w/v) diluted in Tris-buffered saline containing 0.1% Tween 20 (v/v) (TBST). Aromatase immunoreactivity in

DRGs and ovaries was detected by incubating the membrane in mouse anti-aromatase antibody overnight at 4°C (1:250 dilution in blocking buffer). Following three washes in TBST, the membrane was incubated with a HRP-conjugated anti-mouse secondary antibody (1:2,000 to 1:20,000 dilutions in blocking buffer were utilized) for two hours at 4°C. Membrane was washed and incubated in Western Lightning® Plus-ECL substrate.

Detecting aromatase expression in sensory neuron cultures required a modified protocol that utilized an ultra-sensitive chemiluminescent substrate system (SuperSignal® West Femto Maximum Sensitivity Substrate) that enables detection of low femtogram amounts of antigen bound by horseradish peroxidase (HRP)-conjugated antibodies. Due to the intense chemiluminescence generated using this substrate, manufacturer's suggestions were used to minimize background chemiluminescence while probing for aromatase immunoreactivity. Specifically, following incubations in a more dilute mouse anti-aromatase antibody (1:1,000 dilution in blocking buffer), the membrane was vigorously washed in a large volume of TBST (10 mL) for 10 minutes on a rotary shaker. Membranes were then incubated with the secondary anti-mouse antibody, diluted in TBST (0.1% tween) and pre-filtered through a 0.45um Steri-flip filter (Millipore) ((1:100,000 final dilution) for 1 hour at room temperature. Membranes were then vigorously washed in TBST, replaced 5 times over 10 minutes, using a rotary shaker, followed by incubation in the SuperSignal® West Femto Maximum Sensitivity Substrate.

Actin and HPRT immunoreactivity were determined by incubating membranes with a mouse anti-actin antibody (1:10,000 in 5% milk) or a rabbit anti-HPRT antibody (1:500 in 5% milk) overnight at 4°C. Following three washes in TBST, the membranes were incubated with a HRP-conjugated anti-mouse secondary antibody (1:20,000 in 5%

milk in TBST) or HRP-conjugated anti-rabbit secondary antibody (1:5000 in 5% milk in TBST) for two hours at 4°C. The membranes were washed three times in TBST and incubated in the Western Lightning® Plus-ECL substrate.

Protein immunoreactivity on the immunoblots was visualized by chemiluminescence. Membranes were overlaid with X-ray film in a film cassette in a darkroom. Following exposure, the film was processed in an X-ray film developer.

Gene expression analysis using real-time PCR

Total RNA isolation from sensory neuron cultures

Each sample corresponds to RNA isolated from DRG neurons cultured from a single male Sprague Dawley rat. DRGs were cultured in 35 mm dishes or 6-well plates at a density of 60,000 cells/well. Cultures were maintained in F12 media with the addition of 30ng/mL NGF for 12 days. Cells were lysed for RNA extraction using the following steps: media was aspirated, cells were washed 2X with PBS, and cells were disrupted in 300uL of RA1 buffer (USB PrepEase RNA Spin Kit) and 3 µL β-mercaptoethanol by aspirating and pipetting the cells five times with a pipetteman. Lysis solution from wells with similar treatments were pooled in a 1.5mL eppendorf tube and stored at -80°C.

Total RNA isolation from ovaries and dorsal root ganglia

Ovary tissue was thawed in 300 µL of RA1 buffer + 3 µL β-mercaptoethanol and samples were re-frozen for 15 minutes at -80°C. Samples were then thawed and disrupted with a rotor stator homogenizer (three time 5-seconds). To reduce RNA degradation, the rotor was treated with RNAseZAP, rinsed 2X with ddiH_2O, spun in a

tube of ddiH_2O, and patted dry with a Kim Wipe before, between, and after samples. Samples were placed on ice and sonicated (30% intensity) for 10 sec, three times.

Dissected DRGs were transferred to 300 µL of RA1 and 3 µL of β-mercaptoethanol in a 1.5mL RNAse-free tissue homogenization tube (Kimble Chase, Vineland, NJ). DRGs were immediately transferred to -80°C freezer and stored for at least 1 hour prior to homogenization. DRGs were thawed, pelleted and the RA1 buffer was transferred to an RNAse-free 1.5mL eppendorf tube. DRGs were then homogenized in the small volume of remaining lysis buffer using the 1.5mL tube using the corresponding pestle (Kimble Chase, Vineland, NJ). Cell lysate was transferred to the same 1.5 mL tube and an additional 200 µL of RA1 buffer was homogenized to collect any residual RNA from tube and pestle.

RNA was isolated using the USB PrepEase RNA Spin Kit per manufacturer's instructions and eluted in 50 µL of nuclease-free water. Total RNA content was measured using a Nanodrop 1000 UV-Vis Spectrophotometer (Thermo Scientific). RNA was immediately stored at -80°C or used to synthesize complimentary deoxyribonucleic acid (cDNA).

cDNA synthesis and RT-PCR

Isolated total RNA was converted to cDNA via a reverse transcriptase (RT) reaction using random hexamer primers (iScript cDNA synthesis kit). cDNA synthesis from each sample was performed in duplicate 40 µL reactions (consisting of: 500 ng total RNA, buffer containing primers and salts, RT enzyme, and nuclease-free water) and incubated at 25°C for 5 minutes, 42°C for 30 minutes, then at 85°C for 5 minutes, and 4°C until the reaction tubes were recovered. Duplicate RT reactions were pooled to

generate 1000 ng in 80 µL total volume, yielding a final cDNA concentration of 12.5 ng/µL, assuming complete reaction efficiency.

RT-PCR amplification of each cDNA was performed in triplicate in 20 µL reactions containing: 8 µL cDNA (100 ng), 10 µL master mix, 1 µL primer mix, and 1 µL nuclease-free water. Quantification of target and reference (endogenous control) genes in each cDNA was performed in separate wells (single-plex reactions). Reactions were prepared in 96-well reaction plates and RT-PCR was performed using an Applied Biosystems StepOnePlus system.

Measuring letrozole concentrations in serum and tissue

A quantitative assay to measure letrozole concentrations in rat serum and tissue was utilized based on a validated assay to measure letrozole in human plasma (Desta et al., 2011). The assay utilizes high pressure liquid chromatography (HPLC) with fluorescence detection for letrozole (excitation: 230 nm; emission: 295 nm) and UV-VIS detection of the internal standard DMD (234 nm; 0.1 absorbance units full scale (AUFS)). HPLC analysis was carried out on a Waters System (Milford, MA) consisting of a Waters 717 plus autosampler, Waters 600S pump and controller, Waters 486 absorbance detector, and a Hewlett Packard 1046A fluorescence detector (Palo Alto, CA), controlled by Waters Empower software. Analytes were separated on a Zorbax SB-C18 column (3.5 µm particle size, 150 × 4.6 mm; Agilent, Santa Clara, CA), a Nova-Pak C18 guard column (Waters, Milford, MA) (4-µm particle size) using isocratic elution at flow rate of 1 mL/min. Under the above conditions, letrozole eluted at approximately 17 minutes and DMD eluted at 27 minutes. Previously validated using human plasma

samples, the assay has a limit of quantification of 7 ng/mL, with interday and intraday coefficients of variation of <6.5% and <10%, respectively (Desta et al., 2011).

Tissues isolated for HPLC analysis were thawed on ice and mechanically homogenized in 1000 to 5000 µL PBS with a Janke and Kunkel Ultra-Turrax rotor-stator homogenizer fitted with a 8 mm turret (two times 5-seconds). Tissue homogenate (100 µL of DRG homogenate or 300 µL brain homogenate) was transferred to 1.5 mL Eppendorf tubes and frozen at -20°C until assayed. Frozen serum or tissue homogenate was thawed on ice and vortex-mixed before use. Serum (100 µL), brain homogenate (300 µL) or DRG homogenate (100 µL) produced from letrozole or vehicle-treated rats was spiked with 25 µL MeOH and 50 µL of 1 µg/mL DMD (internal standard) dissolved in methanol. Standard curves were generated by spiking equivalent volumes of serum or tissue isolated from naïve animals with 25 µL of letrozole (0 to 100 µg/mL) and 50 µL of 1 µg/mL DMD. The samples were vortex-mixed for 15 seconds and centrifuged at 18,500 g for two minutes. The resulting supernatant was transferred to a glass culture tube and extracted with 0.5 mL of 1M NaOH/1M glycine buffer (pH 11.3) and 6 mL of ethyl acetate. Samples were vigorously vortex-mixed and centrifuged at 3600 rpm for 15 minutes. The organic phase was removed, transferred to a clean glass culture tube, and evaporated in a SpeedVac Concentrator (Thermo Scientific; Waltham, MA) for approximately two hours to dryness. The residue was reconstituted in 150 µL of mobile phase (35% acetonitrile, 65% 10 mM KH_2PO_4 titrated to pH 6.5 with 5M KOH) and transferred to an injection vial containing a 200 µL polyethylene insert and 50 µL was injected onto the analytical column. For a single analytical run, technical duplicates of experimental samples and calibration standards were prepared, extracted together and assayed in sequence via HPLC. Method evaluation using rat tissues was performed using tissue obtained from naïve rats.

Area under the curve (AUC) for letrozole and DMD peaks were automatically integrated by the Empower software and manually confirmed and adjusted if necessary. For each sample, the ratio of the letrozole peak area to the internal standard peak area (AUC_{LET} / AUC_{DMD}) was calculated and averaged over the technical replicates. A calibration curve was constructed by weighted least-squares linear regression of the AUC ratios (y) versus known concentrations of the standards (x) in each analytical run, with a weighting factor of $1/x^2$. Letrozole concentrations in experimental samples were estimated by interpolation of the least-squares line.

Data analysis

Data analysis software

Data manipulation and analysis was performed using GraphPad Prism versions 5.04 and 6.01 (GraphPad Software Inc., La Jolla, CA), Excel 2010 (Microsoft, Redmond, WA) and R v2.7.1 (R Foundation for Statistical Computing, Vienna, Austria). Analysis and visualization of raw RT-PCR data was performed using StepOne Software v2.2 (Applied Biosystems). Protein sequence alignments were performed using ClustalW implemented in CLC Sequence Viewer v6.9 (CLC bio, Cambridge, MA).

Behavioral studies

Repeated measures studies evaluating treatment effects on PWT and PWL were analyzed using two-way analysis of variance with repeated measures (two-way RM-ANOVA), followed by post hoc two-sample t-tests. One-way RM-ANOVA was used to evaluate whether PWT and PWL change during behavioral testing. PWT data are reported in grams (mean ± S.E.M.). Due to logarithmic intervals in pressure exerted by sequential filaments, log10-transformed thresholds were used for data analysis. PWL

data are reported as the observed latency in seconds (mean ± S.E.M.) and analysis was performed using this metric. To compare treatment effects on PWT and PWL between studies, we normalized baseline responses by calculating percent change from baseline for each rat. In experiments evaluating overt nociceptive behavior, numbers of flinches observed in one-minute intervals are reported as mean ± S.E.M. flinches and compared between treatment groups using the Mann-Whitney U test. Cumulative ATP-induced nociceptive behavior is reported as median (25th percentile, 75th percentile) and was compared between treatment groups using the Mann-Whitney U test. Boxplots depict overt nociceptive behavior as five-number summaries with horizontal lines representing (from top to bottom): 75th percentile + (1.5 x interquartile range) (upper whisker), 75th percentile, median, 25th percentile, 25th percentile - (1.5 x interquartile range) (lower whisker).

Release of iCGRP from sensory neurons in culture

Release of iCGRP is presented as the mean ± S.E.M. of the amount of peptide released in ten minute incubations as percent of the total peptide content in each well. Treatment effects on basal and evoked iCGRP release were evaluated using t-tests, while treatment effects on total content of iCGRP was determined using one-way analysis of variance. Statistical significance for each comparison was assessed using a Type I error rate of 5%.

Release of iCGRP from spinal cord slices

iCGRP released in spinal cord perfusate is expressed as the mean ± S.E.M. of peptide measured per minute in each fraction, divided by the total iCGRP content for that spinal cord sample (percent of total content per minute). Treatment effects were compared by determining the fractional release of peptide (percent of total content per

minute) during the three basal and three stimulated fractions. The difference between iCGRP released during exposure to high potassium (stimulated) and iCGRP released during drug or vehicle exposure prior to high potassium stimulation (basal) is termed evoked release. Treatment effects on basal, stimulated, and evoked iCGRP release were evaluated using t-tests. Total iCGRP content measured in spinal cord slices is normalized to the wet weight of tissue placed in perfusion chambers (fmol/mg) and presented as mean ± S.E.M. Treatment effects on total iCGRP content were evaluated using two-sample t-tests. Statistical significance for each comparison was assessed using a Type I error rate of 5%.

RT-PCR

The threshold cycle (C_T) for each RT-PCR reaction was determined by StepOne Software. For each RT-PCR reaction, the amount of target cDNA was normalized the endogenous reference by calculating ΔC_T (ΔC_T = C_T target – C_T reference) (Livak and Schmittgen, 2001). The standard deviation of ΔC_T was calculated from the standard deviations of the target and reference genes as follows: $SD_{\Delta C_T} = \sqrt[2]{\left(SD_{C_{T,target}}\right)^2 + \left(SD_{C_{T,reference}}\right)^2}$ (Livak and Schmittgen, 2001).

RESULTS

Effect of aromatase inhibitor administration on experimental pain models in rats

Letrozole induces mechanical hypersensitivity in ovariectomized female rats

I first examined whether AIs alter basal and evoked responses in OVX rats by measuring changes in PWT and PWL following treatment with a single dose of 1 mg/kg or 5 mg/kg letrozole (Figure 3A); these doses that have been shown previously to effectively inhibit aromatase in rats (Schieweck et al., 1993). Administration of 1 mg/kg letrozole (n = 11) significantly reduced the response threshold to a mechanical stimulus compared to vehicle-treated controls (100 mg/kg HPβCD; n = 9) (two-way RM-ANOVA, $P < 0.05$; Figure 3B). Post-hoc analysis demonstrated a significant reduction in PWTs in animals treated with 1 mg/kg letrozole at 5, 10, and 30 days following drug administration compared to vehicle-treated rats. Baseline PWT was not different between treatment groups. In a similar manner, a single injection of 5 mg/kg letrozole (n = 5) produced mechanical hypersensitivity after 3 days compared to vehicle treatment (750 mg/kg HPβCD; n = 5), and this effect was maintained for 30 days after drug administration (Figure 3C). Baseline PWT was not different between treatment groups. Comparing baseline-normalized PWT between letrozole doses did not reveal a significant effect of dose, suggesting PWT was maximally reduced by 1 mg/kg letrozole.

In contrast to letrozole-induced mechanical hypersensitivity, response latency to noxious thermal stimulation was not altered at any time points examined after administration of 1 mg/kg or 5 mg/kg letrozole (Figure 3D and Figure 3E). Additionally, no significant changes in PWL in vehicle treated animals were observed during 30 days of evaluation.

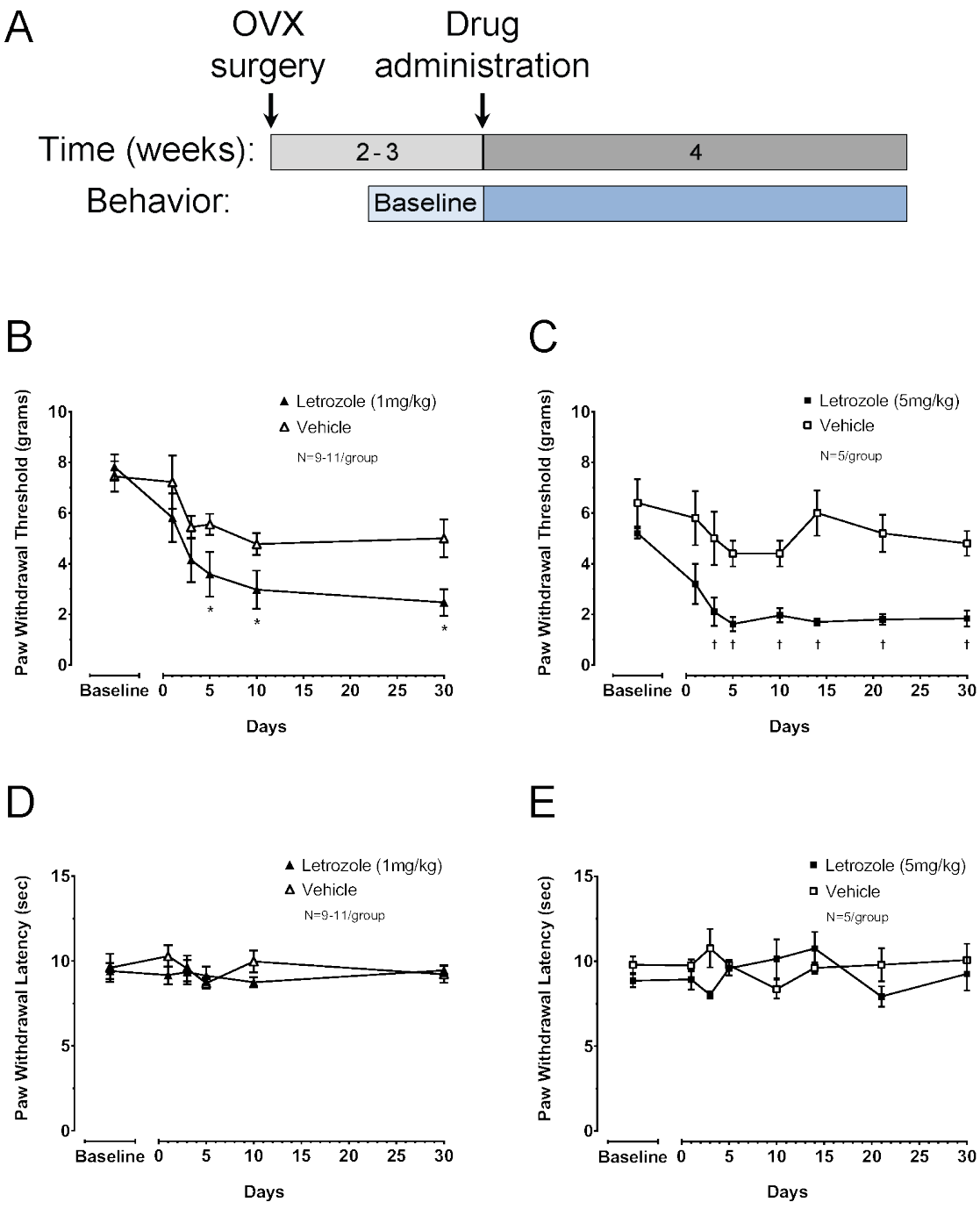

Figure 3. A single dose of letrozole induces sustained mechanical, but not thermal hypernociception in OVX rats.
A: Depiction of the experimental design. Each point represents the mean ± S.E.M. of (B, C) paw withdrawal threshold (PWT) in grams or (D, E) paw withdrawal latency (PWL) in seconds. Letrozole (1 mg/kg: B, D or 5 mg/kg: C, E) or vehicle was administered in a single dose on day 0. An asterisk represents significant differences in PWT following treatment with 1 mg/kg letrozole versus vehicle, whereas a cross represents significant differences in PWT following treatment with 5mg/kg letrozole versus vehicle using two-way RM-ANOVA followed by post-hoc two-sample t-tests.

Analysis of all vehicle-treated animals evaluating time and vehicle dose showed PWTs were significantly reduced over the course of the experiment (two-way RM-ANOVA, $P < 0.05$). Consequently, we determined whether this reduction was caused by injection of vehicle or secondary to OVX by measuring PWT in OVX rats treated with a single injection of 750 mg/kg HPβCD ($n = 5$) or saline ($n = 5$) (Figure 4A). PWTs were significantly reduced over 30 days in all rats independent of vehicle or saline injection, suggesting enhanced mechanical sensitivity following ovariectomy is not directly attributable to vehicle administration (Figure 4B). A post-hoc analysis of the combined animals showed PWTs were significantly reduced from baseline during the experiment and mechanical hypersensitivity developed after 5 days of evaluation (RM-ANOVA followed by post-hot t-tests, $P < 0.05$; data not shown).

While letrozole significantly reduces PWTs in OVX rats, ovariectomy results in a steady decline in PWTs for at least 30 days following recovery from surgery (Figure 3B**,** Figure 3C, Figure 4B). While letrozole treatment reduces PWTs during this time, it is unclear whether this effect is a result of augmenting the development of OVX-induced hypersensitivity or whether letrozole treatment might further reduce PWTs of OVX rats once they reached their minimum. To address whether PWTs in OVX rats reach a steady state beyond 30 days of evaluation, PWTs were measured in untreated rats for 52 days (approximately 7 weeks) following ovariectomy (Figure 5A). In this experiment, rats with baseline PWTs considered to be outliers (> 15 g or < 4 g) were not excluded during the initial 7 week evaluation period. As shown in Figure 5B, PWTs declined following ovariectomy and were significantly lower by 23 days after behavioral testing was initiated (Figure 5B). PWTs had reached a minimum by this timepoint, as changes in the average PWT were not observed beyond 23 days (Figure 5B). Administration of 5 mg/kg letrozole ($n = 8$) did not alter response thresholds to a mechanical stimulus

compared to vehicle-treated controls, suggesting that AI-induced mechanical hypersensitivity cannot be reliably detected in OVX rats once their PWTs have stabilized (750 mg/kg HPβCD; n = 7) (two-way RM-ANOVA, $P > 0.05$; Figure 5C).

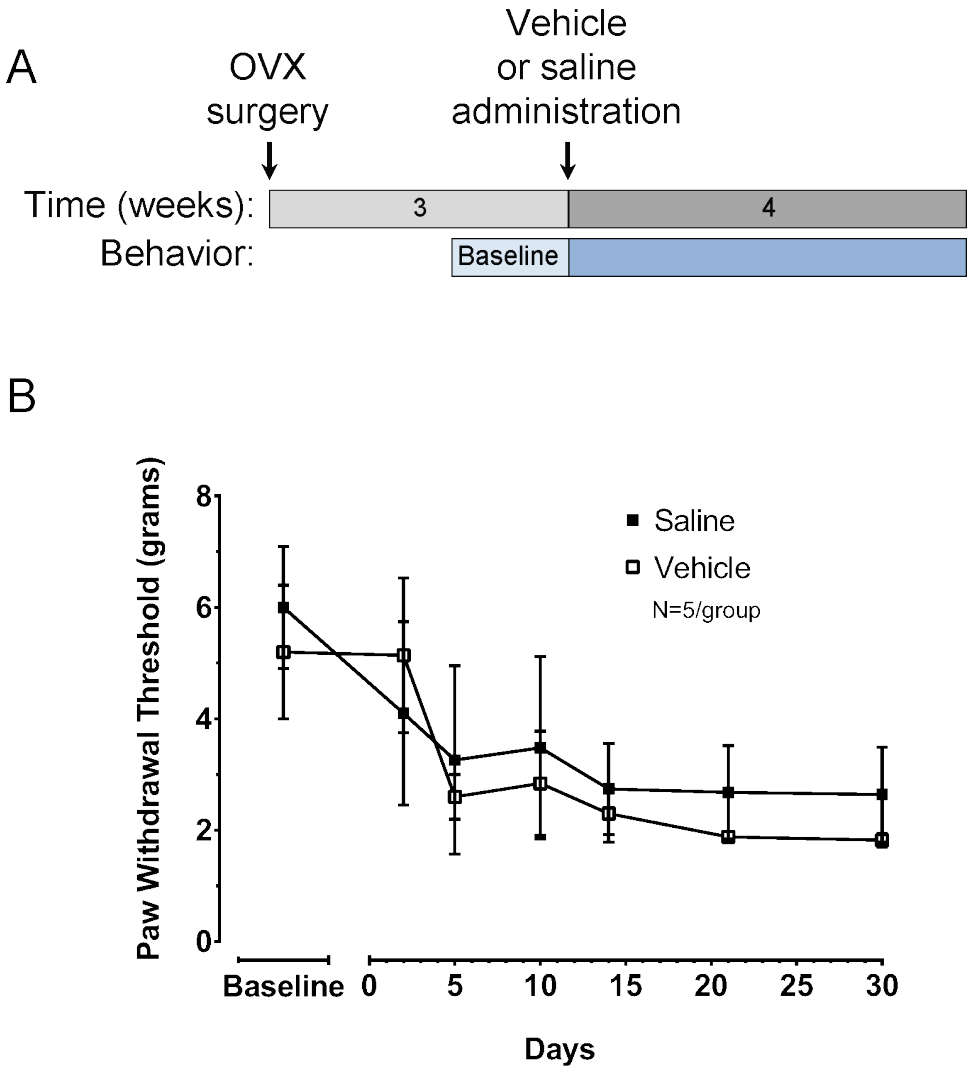

Figure 4. Vehicle administration does not alter mechanical hypersensitivity in OVX rats.
A: Depiction of the experimental design. **B:** Each point represents the mean ± S.E.M. of paw withdrawal threshold (PWT) in grams. Vehicle or saline was administered in a single dose on day 0.

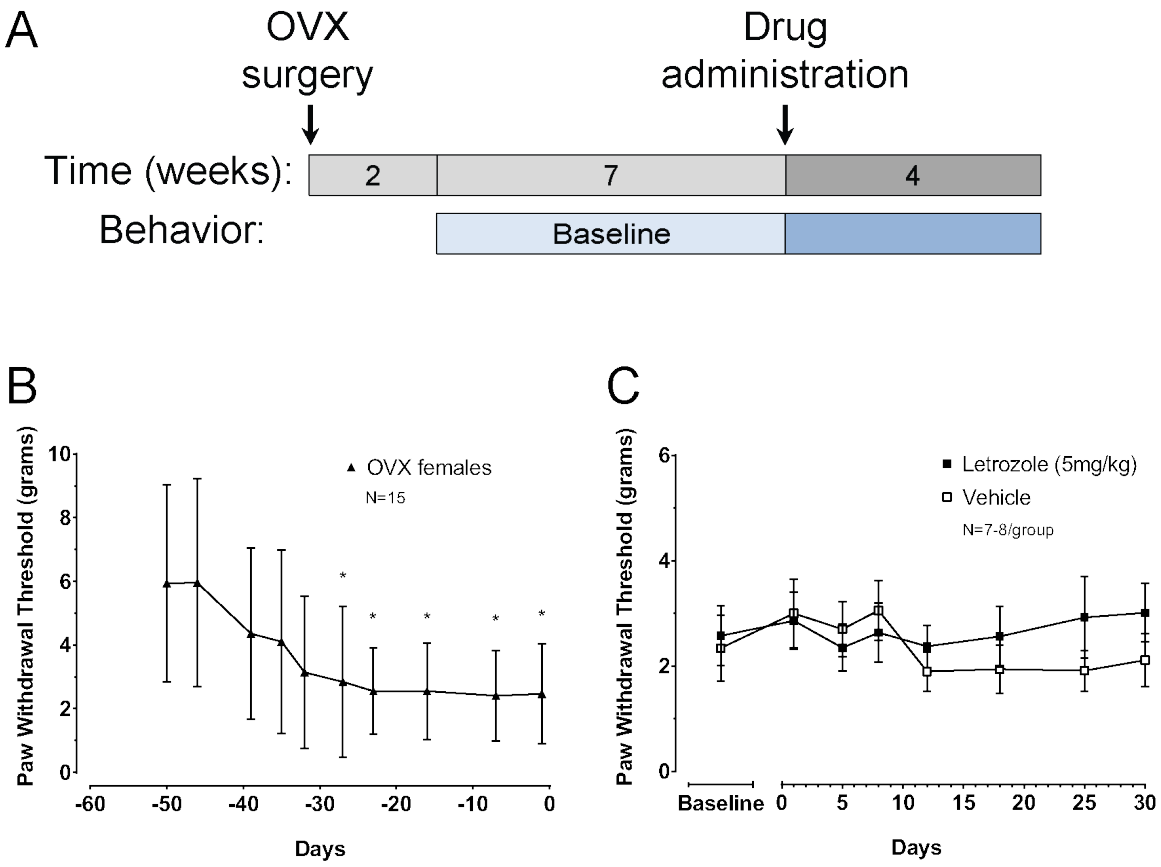

Figure 5. A single dose of letrozole does not alter mechanical hypersensitivity after long-term ovariectomy.
A: Depiction of the experimental design. **B and C:** Each point represents the mean ± S.E.M. of paw withdrawal threshold (PWT) in grams. **B:** PWT of female rats was measured for approximately 7 weeks following ovariectomy. Rats were then randomized to letrozole (5 mg/kg) or vehicle treatment. An asterisk represents significant differences in PWT from baseline using RM-ANOVA followed by post-hoc paired t-tests. **C:** PWT measurements immediately prior to drug injections (day -1 in (B)), was used as the baseline response. Letrozole (5 mg/kg) or vehicle was administered in a single dose on day 0.

Letrozole induces mechanical hypersensitivity in male rats

The effect of letrozole to reduce PWTs in OVX rats suggests the observed behavioral change may not attributed to changes in circulating estrogens. If letrozole-induced mechanical hypersensitivity is secondary to a reduction in tissue estrogen concentrations, we should observed the effects in other animals with very low circulating estrogen concentrations. For this reason, we determined whether AIs also augment nociception in males. To test this, male rats were treated with 5mg/kg letrozole (n = 8) or vehicle (750 mg/kg HPβCD; n = 8) daily for 15 days and PWT and PWL were measured (Figure 6A). We chose to use chronic dosing in males since previous pharmacokinetic estimates of cyclodextrin-complexed letrozole in male and female rats suggest male rats have approximately 5-fold greater clearance of the drug following intravenous delivery (Wempe et al., 2007). When evaluating the main treatment effect, daily dosing with 5 mg/kg letrozole significantly reduced the PWT compared to vehicle treated controls (two-way RM-ANOVA, $P < 0.05$; Figure 6B). Post-hoc analysis showed letrozole-treated animals had reduced PWTs five days after initiating drug administration and at days 10 and 15 during treatment (n = 8; Figure 6B). For example, at 5 days of treatment PWT was 5.3 ± 0.5 g in vehicle-treated rats and 1.6 ± 0.4 g in letrozole-treated animals. In contrast to reduced PWTs observed in vehicle-treated OVX females, PWT in vehicle-treated male rats did not significantly change during the treatment period (one-way RM-ANOVA). After discontinuing drug administration, animals remained hypersensitive to mechanical stimulation for at least 72 hours. However, no significant difference in PWT between treatment groups was detected 7 days after stopping treatment (experiment day 21), suggesting the effect of letrozole was reversible (Figure 6B). As we observed in OVX rats, treating male rats with letrozole did not significantly alter the PWL when compared to vehicle treated rats (two-way RM-ANOVA; Figure 6B).

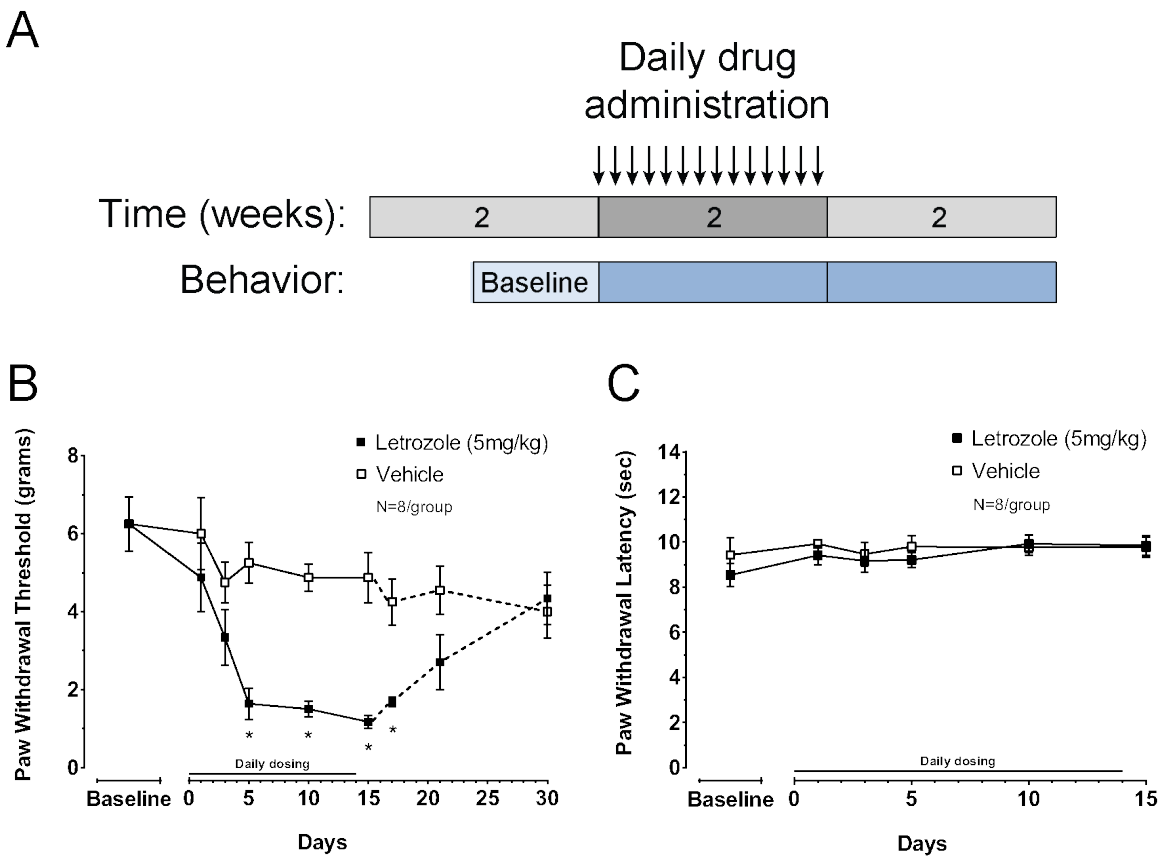

Figure 6. Daily dosing of 5 mg/kg letrozole induces mechanical, but not thermal hypernociception in male rats.
A: Depiction of the experimental design. **B and C:** Each point represents the mean ± S.E.M. of (B) paw withdrawal threshold (PWT) in grams or (C) paw withdrawal latency (PWL) in seconds. Letrozole or vehicle was administered daily on days 0 through 14 (15 total doses) during which behavior was measured (solid lines). PWT continued to be measured following drug discontinuation (dashed lines in (B)). An asterisk represents significant differences in PWT between treatment groups using two-way RM-ANOVA followed by post hot two-sample t-tests.

Intraplantar ATP administration induces dose-dependent flinching of the injected paw

Intradermal injection of purinergic receptor agonists induces dose-dependent overt nociceptive behavior in rats, as measured by hind paw lifting and licking activity [Bland-Ward Br J Pharmacol 1997]. Interestingly, estrogens have been shown to alter overt nociceptive responses to ATP [Ma Purinergic Signal 2011]. By depleting estradiol from blood and tissues, aromatase inhibitors may also be altering excitability of sensory neurons through similar mechanisms. To address this intriguing possibility, I first determined whether the findings of Ma et al. 2011 could be replicated. Specifically, I asked whether ovariectomy increases overt nociception following intraplantar injection of ATP. To evaluate the dose-dependency of ATP-induced overt nociception as measured by flinching, and effect of ovariectomy, OVX and intact female rats were administered 100, 1,000 or 10,000 nmol ATP in an intradermal injection in the mid-plantar left hind paw. Following the injection, flinching of the injected paw was observed and counted during 1 minute intervals for 15 minutes.

In response to intradermal administration of 100 nmol ATP, rats exhibited a small amount of flinching behavior that subsided by 10 minutes following the injections (Figure 7A). Of the 7 animals administered 100 nmol ATP, the distribution of the total number of flinches was as follows: 0 (1 OVX, 1 intact), 1 (1 OVX), 2-3 (1 OVX, 1 intact), >3 (1 OVX, 1 intact) (Figure 7D). These data suggested there was a small and variable effect on nociceptive responses to ATP at this dose. In comparison, intradermal administration of 10,000 nmol ATP rapidly elicited a large number of flinches within the first minute following injection of the algogen. All animals injected responded with flinching behavior throughout the observation period that did not appear to diminish by 15 minutes (Figure

7C). The two OVX rats tested responded with 75 and 81 cumulative flinches, whereas the intact females responded with 50 and 75 flinches (Figure 7D). Due to the large amount of nociceptive behavior induced by 10,000 nmol ATP, no more animals were evaluated at this dose. Due to limited observations in OVX and intact females at the 100 and 10,000 nmol doses, cumulative nociceptive responses were not formally compared between these groups.

Intradermal administration of 1000 nmol ATP rapidly elicited flinching behavior within the first minute following injection in 13 of 16 animals (Figure 7B). The 3 rats that did not immediately response to this dose were intact female rats. In 12 of the 16 rats, the flinching rate (flinches per minute) of the injected paw was maximal during the first two minutes following ATP injection. In OVX and intact female rats, flinching behavior declined during the observation period and subsided by 10 minutes (Figure 7B). Compared to intact females, OVX rats exhibited significantly more flinches 1 and 8 minutes after ATP injection (Figure 7B). Furthermore, OVX rats exhibited greater cumulative nociceptive response to 1000 nmol ATP than intact females (Figure 7D).

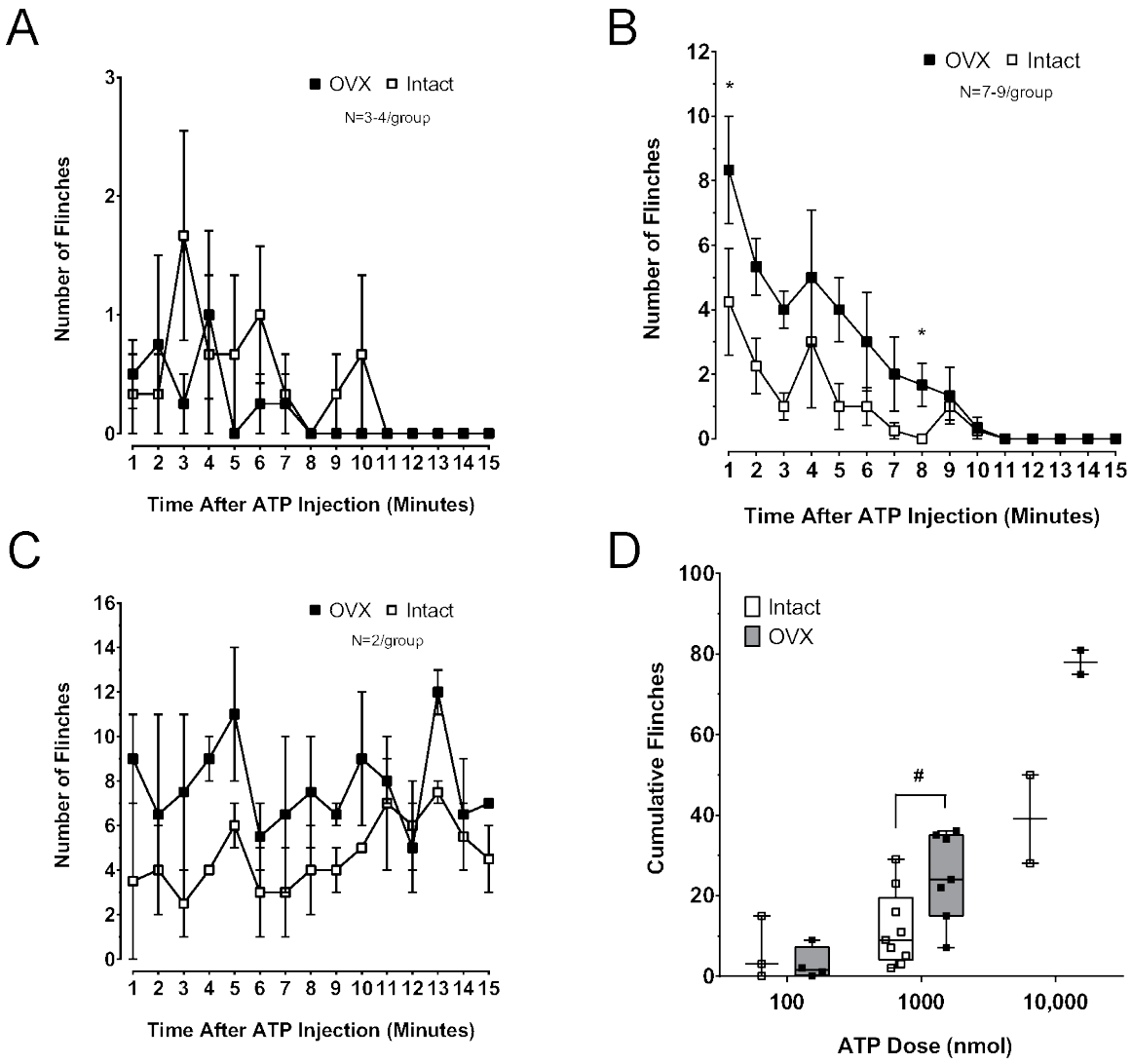

Figure 7. ATP-evoked flinching is augmented in OVX rats.
A, B and C: Each point represents the mean ± S.E.M. of flinches observed in one minute intervals after injection of 100 (A), 1,000 (B) or 10,000 nmol ATP (C) in OVX and intact female rats. An asterisk represents significant differences in the number of flinches observed in one-minute intervals between these groups using Mann-Whitney U tests. **D:** Cumulative hind paw flinches observed for ten minutes following ATP injections are presented as box plots for each ATP dose, with cumulative responses for each animal shown. The pound symbol indicates significantly different ATP-induced cumulative flinches between the groups using Mann-Whitney U tests.

Aromatase inhibitors augment ATP-induced overt nociception

Effects of chronic dosing of AIs on ATP-induced flinching

To determine if AIs alter nociceptive behavior produced by intraplantar ATP injection, male rats were administered AIs or vehicle (HPβCD) daily for five days (i.p.), a time when letrozole-treated rats in our previous experiments had significantly lowered PWTs. The day following the last injection, we measured flinching in response to 1000 nmol ATP injected in the rat hind paw (Figure 8A). In vehicle (750 mg/kg HPβCD; n = 13) and letrozole-treated (5 mg/kg; n = 10) rats, flinching of the injected paw was observed within one minute following ATP injection (Figure 8B). The flinching rate (flinches per minute) in 19 of 23 rats was maximal during the first two minutes following ATP injection and declined rapidly during the observation period. In letrozole treated rats, significantly more flinches were observed 2, 4, 7, 8, and 10 minutes after ATP injection when compared to vehicle injected animals (Figure 8B). The letrozole treatment significantly augmented the cumulative ATP-induced flinches observed for 10 min after intraplantar injection of the nucleotide (Figure 8C). In a series of control experiments, male rats administered saline (n = 8) versus vehicle (750 mg/kg HPβCD; n = 13) daily for five days did not have different flinching behavior after injection of 1000 nmol ATP: The median (25th percentile, 75th percentile) of cumulative flinches measured for 10 minutes after ATP injection was 17 (9, 24) in saline treated animals versus 14 (6.5, 22) in vehicle treated animals (Figure 8C). In addition, flinching behavior in response to intraplantar PBS, the vehicle for intraplantar injections, was measured in male rats following administration of saline (n = 5), vehicle (750 mg/kg HPβCD; n = 5), or 5 mg/kg letrozole (n = 5) for five days. Cumulative flinching behavior measured for 10 min after PBS injection was not significantly different between these treatment groups (saline: 1 (0, 4.5), vehicle: 1 (0, 3), and 5 mg/kg letrozole: 2 (0, 3)) (Figure 8C).

In an analogous series of experiments, I evaluated whether a mechanism-based inhibitor of aromatase, exemestane could enhance ATP-induced nocifensive behavior (Giudici et al., 1988). Male rats were administered vehicle (1000 mg/kg HPβCD; n = 9) or 30 mg/kg exemestane (n = 7) daily for five days (i.p.). This dose was chosen because it likely produces substantial aromatase inhibition in rats [Giudici J Steroid Biochem. 1988, Zaccheo Cancer Chemother Pharmacol. 1989] Twenty-four hours following the last injection, nociceptive behavior in response to an intraplantar injection of 1000 nmol ATP was measured (Figure 8A). The maximal flinching rate of all rats occurred within the first minute of observation and diminished during the 10-minute observation period. Flinching behavior in exemestane-treated rats (n=7) was greater than in those receiving vehicle (n=9) at 8, 9 and 10 minutes following ATP injection (Figure 8D). Cumulative flinching over the 10 min after intraplantar injection of 1000 nmol ATP was significantly greater in exemestane-treated rats when compared to vehicle treated animals (Figure 8E).

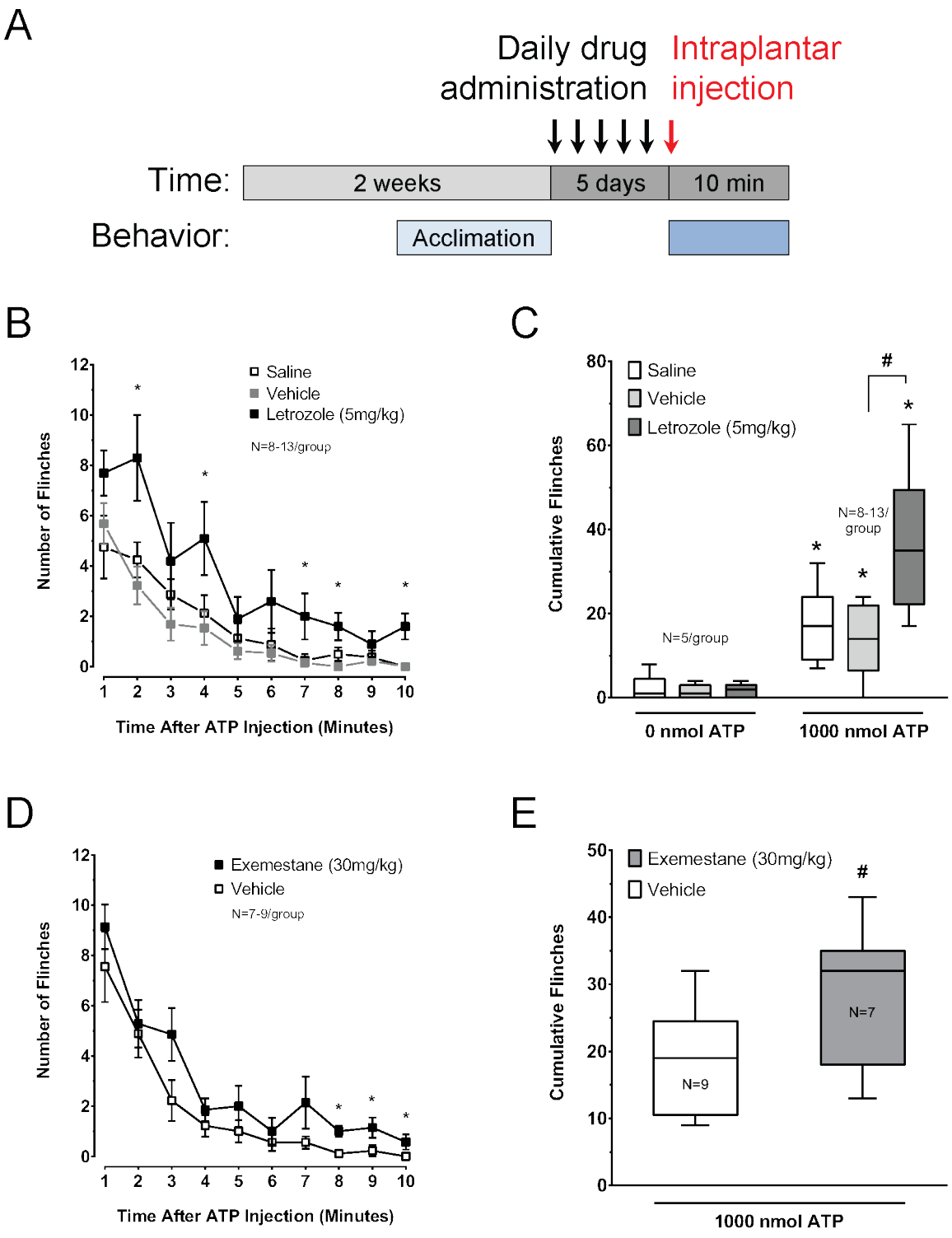
A
Daily drug administration
Intraplantar injection
Time:
2 weeks
5 days
10 min
Behavior:
Acclimation
B
Saline
Vehicle
Letrozole (5mg/kg)
N=8-13/group
Number of Flinches
Time After ATP Injection (Minutes)
C
Saline
Vehicle
Letrozole (5mg/kg)
N=5/group
N=8-13/ group
Cumulative Flinches
0 nmol ATP
1000 nmol ATP
D
Exemestane (30mg/kg)
Vehicle
N=7-9/group
Number of Flinches
Time After ATP Injection (Minutes)
E
Exemestane (30mg/kg)
Vehicle
N=9
N=7
Cumulative Flinches
1000 nmol ATP

Figure 8. ATP-induced nocifensive behavior in male rats is augmented following five days of treatment with aromatase inhibitors.
A: Depiction of the experimental design. **B and D:** Each point represents the mean ± S.E.M. of flinches observed in one minute intervals after injection of 1000 nmol ATP in rats treated for five days with letrozole, exemestane, vehicle, or saline as indicated. An asterisk represents significant differences in the number of flinches observed in one-minute intervals between rats treated with AIs versus vehicle using Mann-Whitney U tests. **C and E:** Cumulative hind paw flinches observed for ten minutes following ATP injections are presented as box plots for each treatment group. Star symbols indicate significantly different cumulative flinches following intraplantar injections of 1000 nmol ATP versus PBS (0 nmol ATP), comparing rats administered the same systemic treatment (saline, vehicle, or letrozole; Mann-Whitney U tests). The pound symbol indicates significantly different ATP-induced cumulative flinches in vehicle-treated controls versus (C) letrozole and (E) exemestane-treated rats using the Mann-Whitney U test.

A single dose of 5 mg/kg letrozole augments ATP-induced flinching

My results demonstrate that the nociceptive response to intraplantar ATP in male rats is enhanced with repeated administration of aromatase inhibitors. I also examined the effect of a single dose of letrozole on ATP-induced flinching behavior. Male rats were treated with a single i.p. dose of vehicle (750 mg/kg HPβCD; n = 7) or 5 mg/kg letrozole (n = 6) and 3 hours following drug administration, flinching behavior in response to intraplantar injection of 1000 nmol ATP was observed for 10 minutes (Figure 9A). Flinching evoked by intraplantar ATP was significantly greater in letrozole-treated rats at 1, 2, and 3 minutes after injection of the nucleotide (Figure 9B). Unlike the chronic dosing with letrozole, the ATP-induced flinching behavior returned to the level of those seen in the vehicle by 4 min. A single dose of letrozole significantly augmented the cumulative number of ATP-induced flinches over 10 min compared to animals treated systemically with the vehicle (Figure 9C).

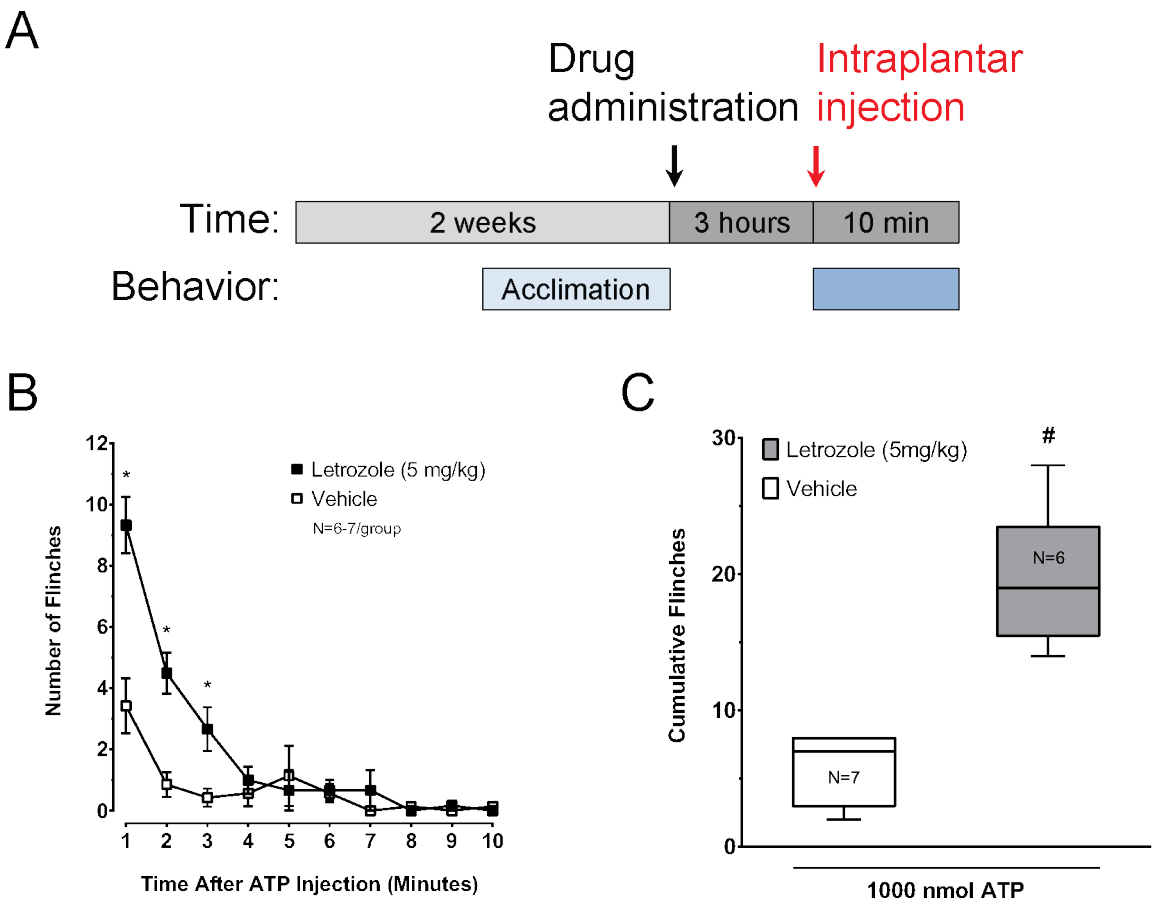

Figure 9. ATP-induced nocifensive behavior in male rats is augmented by a single dose of 5 mg/kg letrozole.
A: Depiction of the experimental design. **B:** Each point represents the mean ± S.E.M. of flinches observed in one minute intervals after injection of 1000 nmol ATP, which was administered three hours after letrozole or vehicle treatment. An asterisk represents significant differences in the number of flinches observed in one-minute intervals between treatment groups using Mann-Whitney U tests. **C:** Cumulative hind paw flinches observed for ten minutes following ATP injections are presented as box plots for each treatment group. The pound symbol indicates significantly different ATP-induced cumulative flinches in rats treated with vehicle versus letrozole using the Mann-Whitney U test.

Extracting and quantifying letrozole in rat tissues

Any effect of letrozole to alter nociceptive responses in male and female rats may be a consequence of altered aromatase activity in tissues mediating pain transduction or perception, but whether letrozole distributes to cells comprising the peripheral and central nervous systems has not been described. Pharmacokinetic studies conducted by CIBA Geigy using ^{14}C-labeled letrozole showed higher radioactivity in tissues (e.g. adrenals - 7.1 µg/g and liver – 2.2 µg/g) compared with plasma (0.6 µg/mL) five minutes after intravenous administration of 1 mg/kg to female rats (U.S. Food and Drug Administration, 1996). A separate study of letrozole pharmacokinetics in female Sprague Dawley rats showed initial plasma concentrations following intravenous administration of 1 mg/kg were approximately 1 µg/mL (Tao et al., 2006). Tao et al. dissolved letrozole in hydroxypropyl-β-cyclodextrin, the same formulation I used for *in vivo* studies. Any influence of the vehicle on letrozole disposition would be represented in pharmacokinetics determined by Tao et al. An assay to measure letrozole concentrations in blood and tissues following a single dose of 1 mg/kg would optimally measure concentrations in this range. To determine whether letrozole could be quantified from rat serum and tissue (brain and DRGs) using a method validated in human plasma, standard curves were generated by spiking known concentrations of the drug into samples obtained from naïve male rats. Linearity of the extracted standard curves was compared with direct injection of these letrozole standards. Standards for direct injection were generated by evaporating solvent from 25 µL of letrozole (0 to 100 µg/mL) and 50 µL of 1 µg/mL DMD added to Eppendorf tubes and reconstituting the compounds in 150 µL mobile phase.

Figure 10 demonstrates representative chromatograms of letrozole and DMD following direct injection and extraction of the compounds from rat tissues. Direct

injection of 208 ng letrozole (25 µg/mL standard) and 17 ng DMD on column resulted in two peaks in the chromatogram, with letrozole eluting at 17.5 minutes and DMD eluting at 27.5 minutes (Figure 10A). Note that while letrozole was also detected by absorbance (as seen at 17.5 minutes in the absorbance spectra in Figure 10A), however this method utilized fluorescence detection for letrozole quantification due to better signal-to-noise properties. Peaks corresponding to these compounds were also observed at the same retention times following extraction of the same amounts of letrozole and DMD from rat serum and DRGs (Figure 10B). Letrozole fluorescence from the 0.05 µg/mL standard (0.42 ng on column) was distinguishable from noise following direct injection and extraction from serum, however letrozole was less reliably detected at this concentration extracted from brain. The lowest standard extracted from DRGs was 0.1 µg/mL (0.83 ng on column), which gave a strong signal. Coefficients of variation (CV%) of AUC_{LET} / AUC_{DMD} less than 15% were obtained from direct injection and extraction from serum, brain, and DRGs from the 0.05, 0.05, 0.25, and 0.1 µg/mL standards, respectively, suggesting these may be lowest effective concentrations for future quantification. Peak integration ratios of letrozole to the internal standard (AUC_{LET} / AUC_{DMD}) resulting from direct injections and extraction from tissues increased linearly with increasing amounts of letrozole (Figure 11). Letrozole and DMD extraction efficiencies from serum, calculated as the percent of peak area observed in extracted tissue relative to direct injection at a given concentration, averaged 64% and 61% over the concentration range, resulting in a similar slope. Letrozole and DMD extraction efficiencies were higher in DRGs, averaging 94% and 80%, also resulting in a similar slope. However, DMD was not as efficiently extracted from brain (average = 32%), resulting in larger AUC_{LET} / AUC_{DMD} ratios and a greater slope (Figure 11). R^2 values of 0.99 obtained from least-squares linear regression suggest highly linear relationship between letrozole concentrations and detector response.

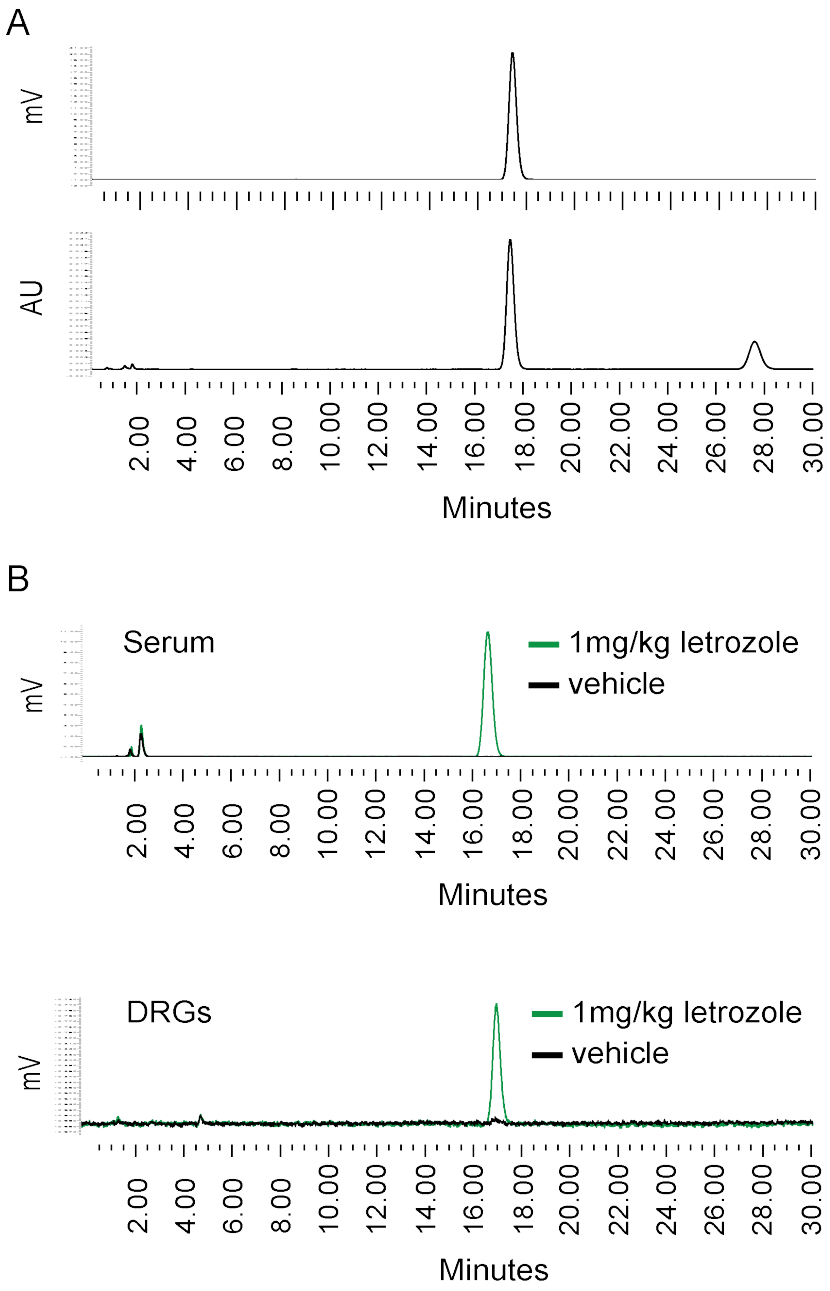

Figure 10. Chromatograms of letrozole and internal standard following direct injection and extraction from rat tissues.
Typical chromatograms of letrozole and the assay internal standard (desmethyldiazepam; DMD) following HPLC separation and fluorescence detection for letrozole (excitation: 230 nm; emission: 295 nm) and UV-VIS detection of DMD (234 nm; 0.1 AUFS). **A:** Fluorescence (mV) and UV-VIS (AUFS) detector response after direct injection of letrozole (25 µg/mL standard – 208 ng on column) and DMD (1 µg/mL standard – 17 ng on column). **B:** Comparing fluorescence chromatograms for letrozole quantification from serum and DRGs harvested from two OVX rats three hours following intraperitoneal administration of either 1 mg / kg letrozole or vehicle (HPβCD).

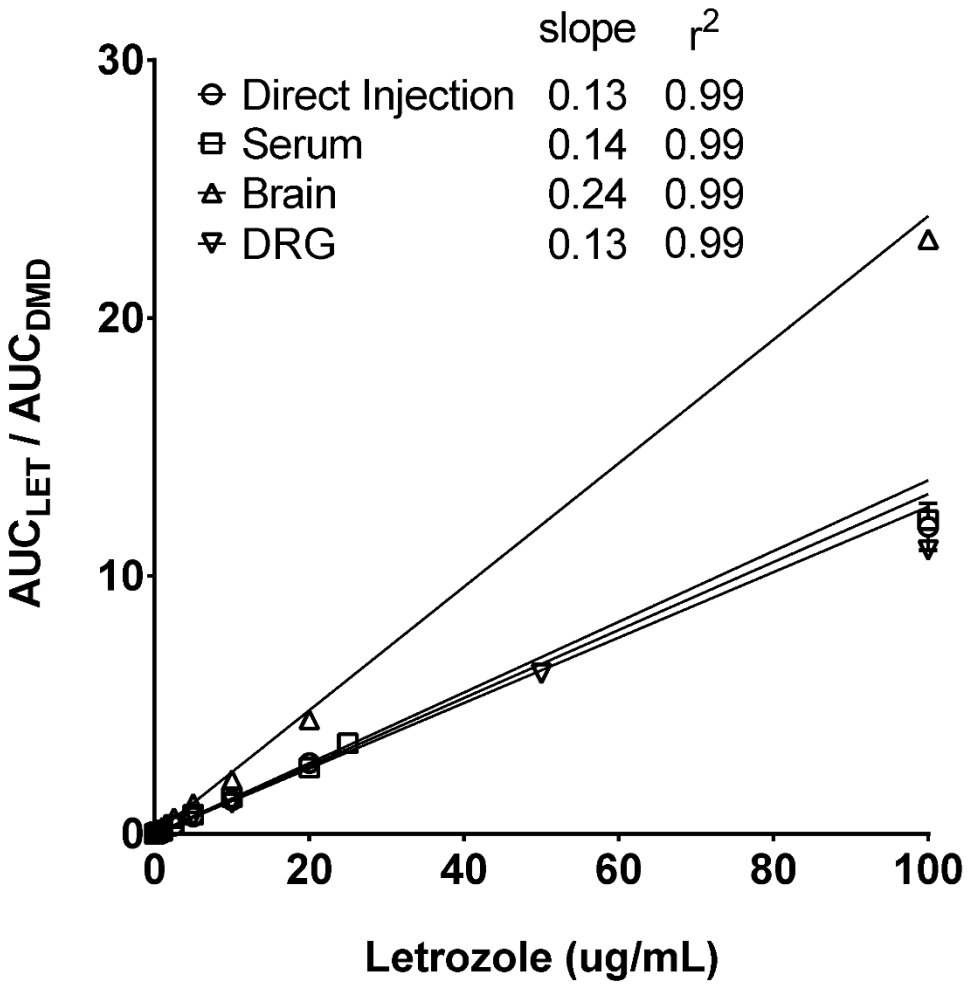

Figure 11. Comparison of calibration curves for letrozole by direct injection and extraction from rat tissues.
The relationship between peak integration ratios of letrozole to the internal standard (AUC_{LET} / AUC_{DMD}) determined by HPLC analysis is compared to letrozole concentrations achieved by spiking increased amounts of letrozole in HPLC buffer (direct injection), serum, and tissue homogenates. Each point represents the mean ± standard deviation of triplicate measurements.

Letrozole concentrations in the serum, brain and dorsal root ganglia following intraperitoneal administration to ovariectomized and intact female rats

To determine letrozole concentrations achieved in the brain and DRGs of rats following i.p. administration of the drug, intact and OVX rats were administered either 1 mg/kg letrozole (N = 4 per group) or vehicle (N = 2 per group). Using a dense sampling strategy within 5 hours of an oral dose of 0.5 mg/kg letrozole, Tao et al. observed that maximum plasma concentrations of the drug (Cmax) were achieved 1.5 hours after dosing. Thus, serum, brain, and DRGs were isolated at 0.5 hours or 3 hours following drug administration. To understand the terminal elimination characteristics of the drug from the circulation, another group of OVX rats (N = 9) were administered 1 mg/kg letrozole and serum was isolated 3, 4, and 21 days following drug administration.

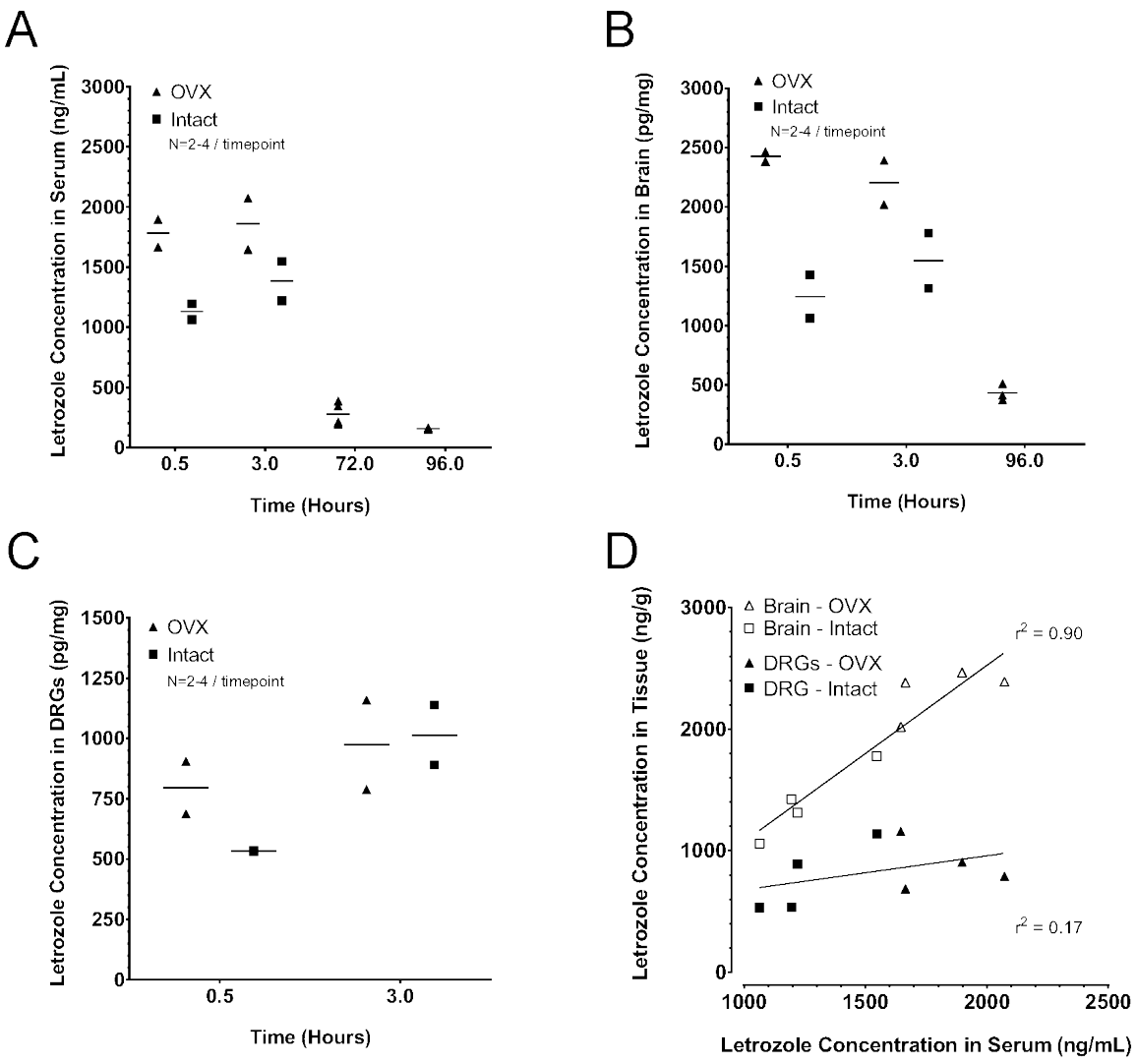

Figure 12. Letrozole concentrations in serum, brain, and DRGs following drug administration to OVX and intact female rats.
Following administration of 1 mg/kg letrozole to OVX and intact female rats, animals were sacrificed 0.5, 3, 72, or 96 hours post-dose and tissue samples were collected. **A, B, and C:** Letrozole concentrations measured in serum (A), brain homogenate (B) and DRG homogenate (C) samples from each animal are shown, along with the median concentration at each time point. **D:** Correlation between serum and tissue concentrations of letrozole. Coefficients of determination (r^2) were calculated using letrozole concentrations measured in serum and tissue from OVX and intact female rats.

Letrozole was observed in serum within 30 minutes of i.p. administration, suggesting rapid absorption of the drug into the bloodstream from the intraperitoneal cavity. When compared to intact females, serum concentrations achieved at 30 minutes and 3 hours in OVX females appeared higher, although the mean difference could not be reliably determined given the small number of samples in each group (Figure 12a). In both groups, concentrations at 30 minutes and 3 hours were comparable, which is consistent with Cmax occurring between these two time points or potentially little change in serum concentrations during this time. While sparse sampling time points were not sufficient for precise characterization of serum elimination, concentrations measured 3 and 4 days (72 and 96 hours) following letrozole administration are consistent with slow clearance of the drug (Figure 12a). At 21 days following administration of letrozole to OVX rats, letrozole was undetectable in the serum. Using serum letrozole concentrations from only the OVX rats, the elimination half-life was estimated to be 26 hours, based on the slope obtained from a least-squares linear regression of natural log transformed concentrations versus time.

Letrozole concentrations measured in the brain and DRGs of intact and OVX females followed a similar concentration-time profile as serum concentrations, however brain concentrations were higher than serum concentrations (Figure 12b,c). Assuming the density of brain and DRGs in rodents is approximately 1 g/mL (Leithner et al., 2010), the ratio of median brain concentrations to median serum concentrations measured at 0.5 and 3 hours was 1.4 and 1.2 in OVX rats and 1.1 at both time points in intact rats. This ratio rose to 2.6 in OVX rats 96 hours after letrozole administration. Thus, letrozole concentrations achieved in the brain exceed serum concentrations throughout its duration in the body following an i.p. dose. Additionally, there was a strong correlation between serum and brain concentrations of letrozole, suggesting rapid equilibrium is

reached between these tissues and the brain's capacity to bind the drug is not saturated at these concentrations (Figure 12d). In contrast, the ratio of median DRG concentrations to median serum concentrations measured at 0.5 and 3 hours was 0.4 and 0.5 in OVX rats and 0.5 and 0.7 in intact rats. The correlation between letrozole concentrations in the serum and DRGs was weak, suggesting that the binding capacity of DRG tissue has been reached at the observed concentrations (Figure 12d). These data suggest differential distribution of the AI to these tissues.

CYP19A1 mRNA transcripts and aromatase protein are expressed in DRG neurons in culture

Validating conditions for the relative quantification of target and control genes using Applied Biosystems TaqMan® gene expression assays

Utilizing the comparative C_T method (also known as the $\Delta\Delta C_T$ method) for quantifying the relative expression of two genes in a biological sample requires two method validation steps. The first validation step is to empirically determine the range of input mass RNA in the reverse transcription (RT) reaction that results in a linear amplification of target and reference genes during RT-PCR, also known as the dynamic range of RT. If there are no factors altering the efficiency of the RT reaction for both mRNA targets, a plot of $\log_{10}$(input RNA amount) versus ΔC_T ($C_{T,target} - C_{T,reference}$) has a slope of approximately zero. Non-linear relationships may occur with large amounts of input RNA due to interference of agents used in RNA purification and inhibitory compounds native to biological samples. To determine the dynamic range of RT, I generated RNA dilution curves by varying amounts of input RNA in the RT reaction. Total RNA pools were generated by extracting and pooling equal amounts of RNA from tissues isolated from three rats: rat ovaries obtained from intact female rats, freshly

dissected DRGs isolated from male rats, and DRG cells from male rats maintained in culture for 12 days (supplemented with 30 ng/mL NGF). Equal amounts (ng) of RNA from samples comprising each pool were combined and diluted to a final concentration of 100 ng/µL. Serial dilutions of 100, 50, 25, 12.5 and 6.25 ng/µL were prepared and 10 µL of each dilution was used as input in a 20 µL RT reaction. Final cDNA pools were made by adding 70 µL of nuclease-free water (11.1, 5.55, 2.78, 1.39, and 0.694 ng/µL) and RT- PCR of *CYP19A1* and *GAPDH* (reference gene) was performed using 9 µL of each cDNA pool in 20 µL reactions (in triplicate). Figure 13 demonstrates there is little variation in ΔC_T ($C_{T,CYP19A1} - C_{T,GAPDH}$) with increasing amounts of total RNA input into the RT reaction. These results suggest the reverse transcription and PCR amplification of the two mRNA transcript targets are not differentially affected by impurities present in up to 100 ng RNA and support using this amount of total RNA for RT-PCR analysis.

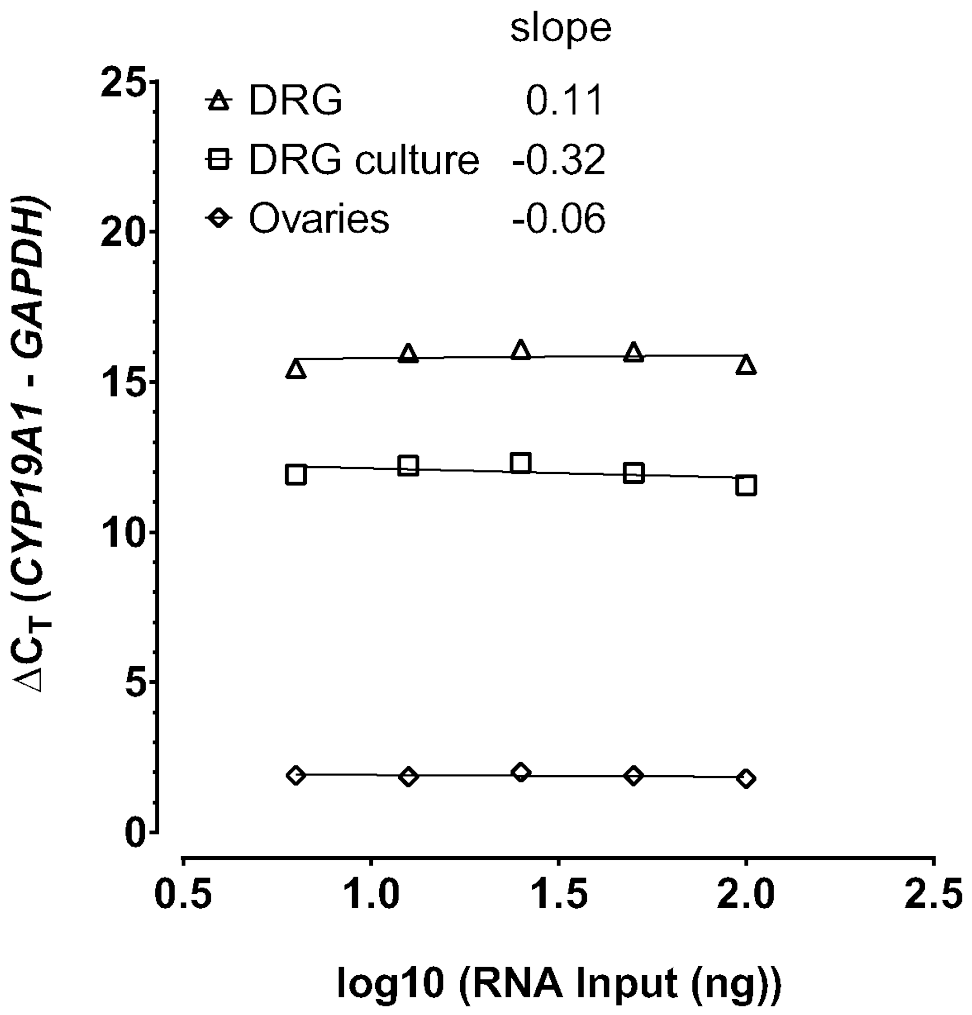

Figure 13. Determining the dynamic range of reverse transcription.
Total RNA isolated from DRGs, DRGs in culture, and ovaries were serially diluted, converted to cDNA, and used in real-time PCR of *CYP19A1* and *GAPDH*. ΔC_T ($C_{T,CYP19A1}$ - $C_{T,GAPDH}$) was calculated at each RNA dilution using the mean C_T from triplicate reactions. For each tissue, the slope was determined using linear least-squares regression analysis.

For the comparative C_T method of relative quantitation to be valid, the amplification efficiency of the target and reference genes must be approximately equal. For this experiment, the expression level of the target and reference genes (C_T) is determined from serially diluted cDNA, ideally over 5 logs (i.e. 100 ng to 10 pg). If the efficiencies of the two PCR reactions are equal, a plot of $\log_{10}$(input RNA amount) versus ΔC_T has a slope of approximately zero. As shown in Figure 13, *CYP19A1* C_T values in DRGs (33.85 ± 0.30; mean ± S.D.) and DRG cultures (30.36 ± 0.15) measured with 100 ng of input cDNA suggest low expression levels in these tissues. Therefore, RT-PCR of *CYP19A1* and *GAPDH* were performed using 100 to 1 ng of cDNA prepared by serial dilution. Using mRNA isolated from freshly dissected DRGs isolated from male rats, differences in amplification efficiency between the two targets were noted at cDNA input less than 30 ng, as indicated by a deviation in ΔC_T ($C_{T,CYP19A1} – C_{T,GAPDH}$). *CYP19A1* was undetectable in 1 ng of cDNA template from DRGs (as indicated by the lack of ΔC_T data at 1 ng in Figure 14a), suggesting the lower limit of detection of *CYP19A1* mRNA had been reached. However, amplification of *GAPDH* in DRGs was highly efficient across this range of input cDNA, with calculated efficiencies of 82 – 86% (efficiency = $10^{(-1/slope)} – 1$) (Figure 14c). Similarly, differences in amplification efficiency between the two targets were also observed using less than 30 ng of cDNA produced from DRGs maintained in culture for 12 days (supplemented with 30 ng/mL NGF) (Figure 14b). Amplification of *GAPDH* in DRGs maintained in cultures was highly efficient across this range of input cDNA (Figure 14d. Given the low expression of CYP19A1 relative to GAPDH in these tissues, these results suggest the highest amount of input RNA should be used in any experiments utilizing the $\Delta\Delta C_T$ method to estimate fold-differences in *CYP19A1* mRNA expression between samples. Furthermore, accurate quantification of

reduced *CYP19A1* mRNA expression may be not be feasible in these tissues without prior targeted amplification.

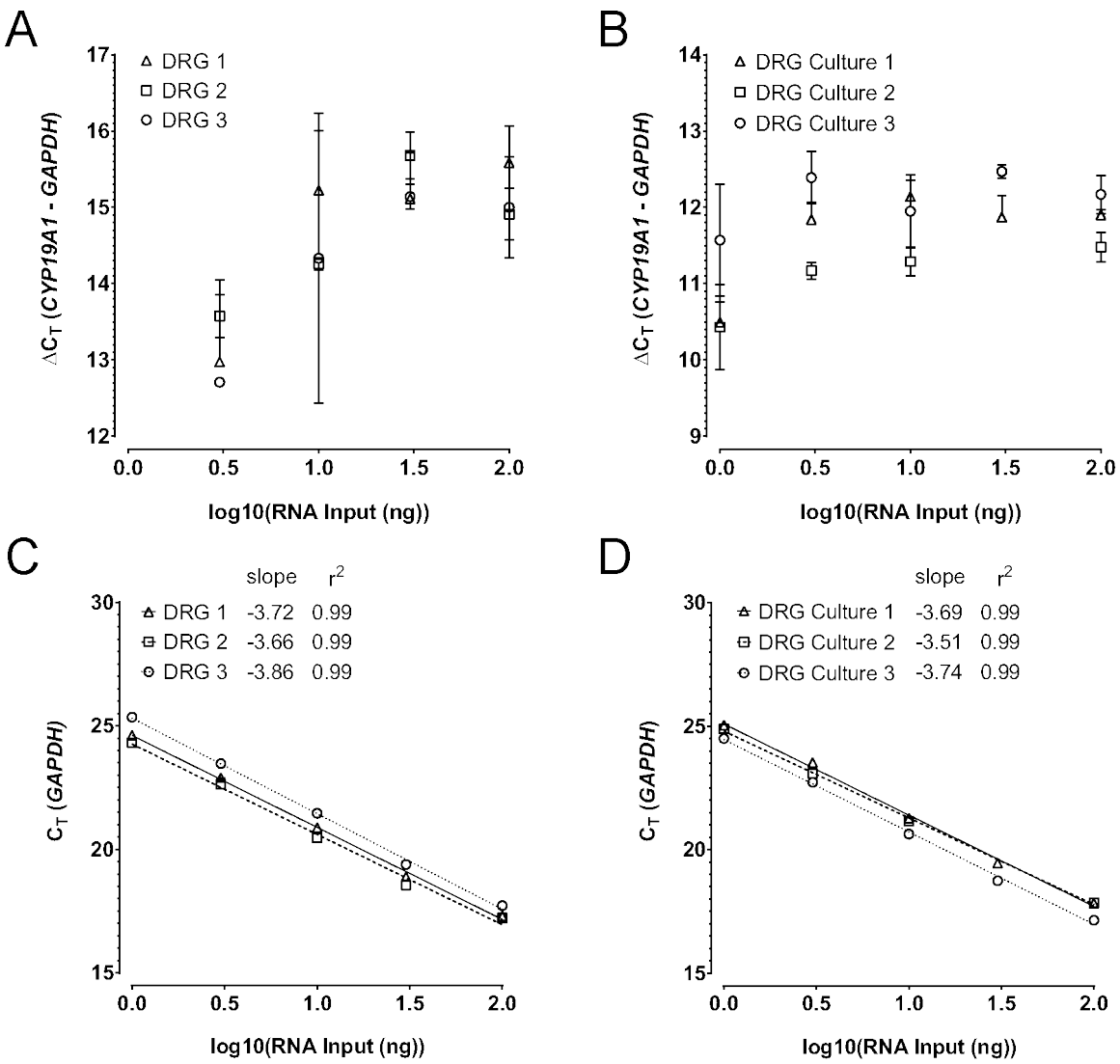

Figure 14. Determining the efficiency of real-time PCR amplification of *CYP19A1* and *GAPDH*.
Serial dilutions of cDNA synthesized from DRGs and DRGs in culture was used in real-time PCR of *CYP19A1* and *GAPDH*. **A and B:** Each point represents the mean ± S.D. of ΔC_T ($C_{T,CYP19A1}$ - $C_{T,GAPDH}$) calculated from triplicate reactions at each cDNA dilution. **C and D:** Each point represents the mean C_T for *GAPDH* at each cDNA dilution. For each sample, the slope and r^2 was determined using linear least-squares regression analysis.

Aromatase expression in dorsal root ganglia persists in sensory neuron cultures

To address whether sensitization of primary sensory neurons by AIs may contribute to AI-induced hypernociception, I determined if aromatase is expressed in DRGs or the spinal cord and whether aromatase expression is maintained in sensory neuron cultures. Specifically, aromatase immunoreactivity and beta-actin immunoreactivity was determined in total protein lysates from pooled cranial, thoracic, lumbar, and sacral DRGs isolated from independent male rats (75 µg total protein), independent cultures of male rat DRGs maintained in F12 media (supplemented with 30 ng/mL NGF and 10% horse serum) for 12 days (63 to 75 µg total protein), and ovaries isolated from two different female rats (25 µg total protein). Aromatase immunoreactivity and beta-actin immunoreactivity was additionally determined in total protein lysates from spinal cords isolated during DRG harvests from the male rats in the combined experiment (150 µg total protein), plantar foot pads isolated with sterile 6mm biopsy punch (150 µg total protein), and independent ovary samples (25 µg total protein).

Proteins lysates were separated in NuPAGE Bis-Tris (4-12%) gels and proteins were transferred to a PVDF membrane overnight at 4°C. After blocking the membrane in 5% milk, aromatase immunoreactivity was determined by incubating the membranes in mouse anti-aromatase antibody overnight at 4°C (1:250 dilution in blocking buffer). The membrane was washed and then incubated with a HRP-conjugated anti-mouse secondary antibody (1:5,000 in blocking buffer) for one hour at room temperature. After washing the membrane again, immunoreactivity detected using Western Lightning® Plus-ECL substrate.

An immunoreactive band at approximately 55kDa, corresponding to the expected molecular weight of aromatase was evident in DRG lysates from all male rats (Figure 15A). In contrast, no immunoreactive bands were observed in lysates from sensory neuron cultures, suggesting aromatase expression in cells composing the DRG is downregulated when dissociated and grown in culture (Figure 15a). As a positive control, immunoreactive bands of similar molecular weights were detected in total protein lysates from independent rat ovaries, however the molecular weight of aromatase in the second ovarian sample appeared slightly larger (Figure 15A, lane 9). The difference did not appear to be due to differences in the gel between these lanes, as actin immunoreactive bands were identical between samples. Despite the relatively large amount of tissue lysates used in the experiment, aromatase immunoreactivity was not observed in lumbar spinal cord lysate or plantar skin of the foot pad under these conditions (Figure 15B).

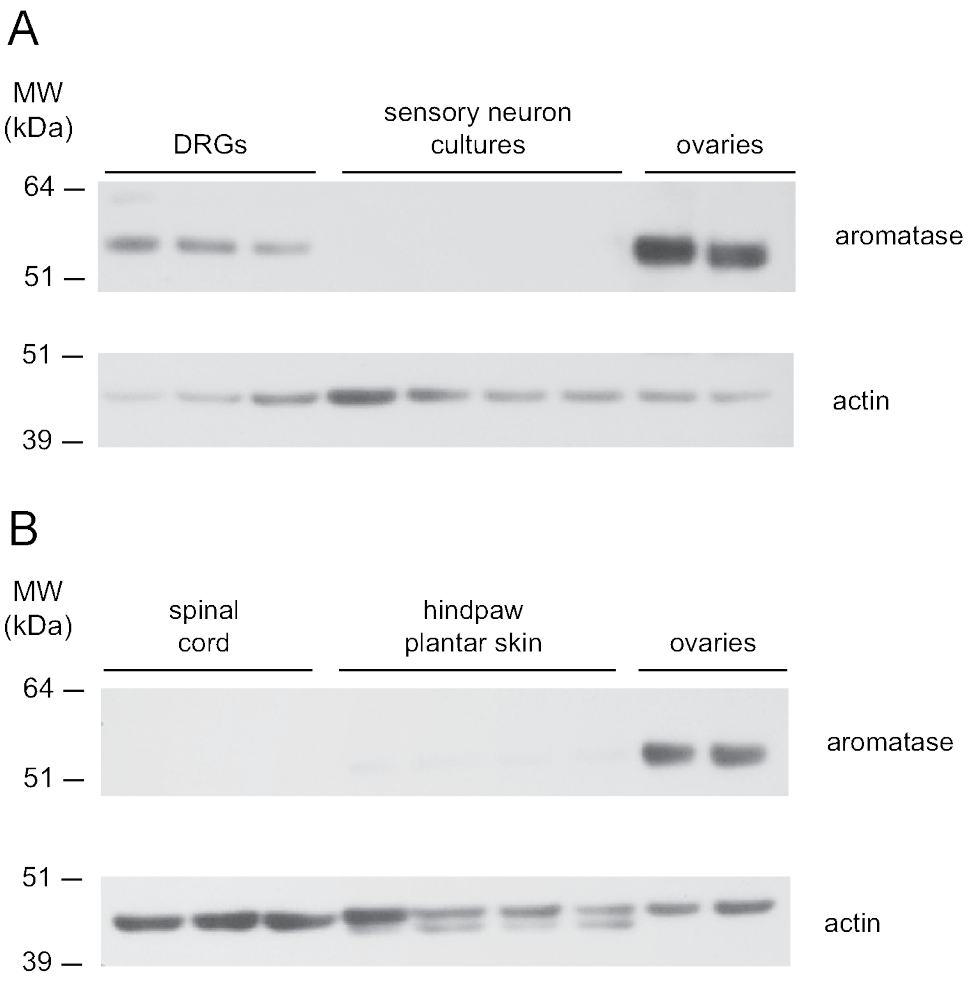

Figure 15. Aromatase is differentially expressed in DRGs, spinal cord, glabrous hind paw skin and ovaries from male and female rats.
A: Immunoblot of total protein isolated from DRGs of three male rats, sensory neuron cultures from three male rats maintained for 12 days, and rat ovaries (100 µg of total protein was loaded for DRG and sensory culture lysates, whereas 50 µg of total protein was loaded for ovary lysate). **B:** Immunoblot of total protein isolated from spinal cords and glabrous hind paw skin lysates from three male rats and ovary lysates used in (A). 150 µg of total protein was loaded from spinal cord and hindpaw skin lysates, whereas 50 µg of total protein was loaded for ovary lysates. Membranes were probed with anti-aromatase and anti-actin antibodies.

The lack of observable aromatase immunoreactivity in sensory neuron cultures may be due to very low expression levels of the enzyme. To enable the detection of potentially low levels of aromatase protein in sensory neuron cultures, aromatase immunoreactivity was determined using the western procedure optimized for an ultra-sensitive chemiluminescent substrate. Aromatase immunoreactivity was again compared between lysates of pooled DRGs (cranial, thoracic, lumbar and sacral) isolated from independent male rats (100 µg total protein), independent cultures of male rat DRGs (100 µg total protein), and ovaries isolated from two different female rats (50 µg total protein). Using the enhanced ECL solution, aromatase was detected in all tissue lysates (Figure 16), suggesting low levels of aromatase expression in DRG neurons in culture. Furthermore, aromatase immunoreactivity was observed in all three cultures at similar expression levels. This expression pattern resembled consistent aromatase expression among DRG lysates from different rats (Figure 15A and Figure 16). Interestingly, aromatase immunoreactive bands in the sensory neuron cultures appeared at slightly higher molecular weight than in the whole DRG lysates. These differences in aromatase molecular weight were also observed in the two ovarian lysates, suggesting the higher molecular weight isoform is expressed after placing cells of the DRGs in culture. Furthermore, these two isoforms may be expressed in a single tissue, such as the ovaries.

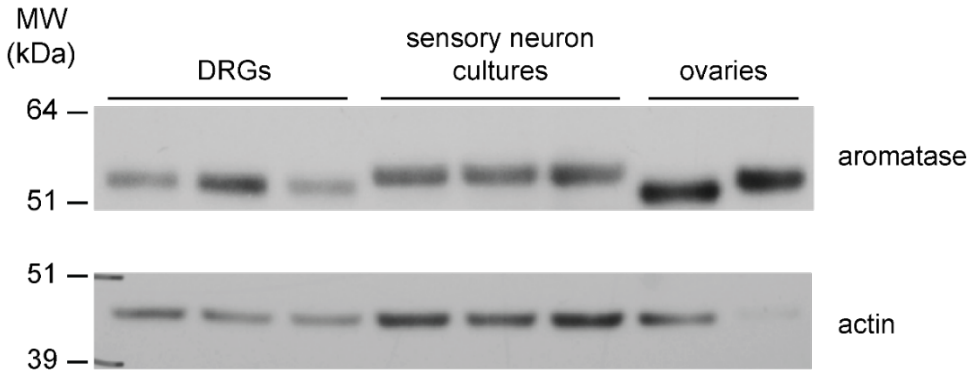

Figure 16. Aromatase expression in DRGs persists in dissociated DRG cultures. Immunoblot of total protein isolated from DRGs of male rats, sensory neuron cultures from male rats maintained for 9 days, and rat ovaries (100 µg of total protein was loaded for DRG and sensory culture lysates, whereas 50 µg of total protein was loaded for ovary lysate). Sensory neurons in culture were isolated from cranial, thoracic, lumbar, and sacral DRGs; acutely isolated DRGs were also taken from these ganglia. Protein samples were isolated from independent rats or DRG cultures. Membrane was probed with anti-aromatase and anti-actin antibodies.

To determine whether aromatase expression is maintained throughout the time DRG cells are in culture, aromatase immunoreactivity was compared between acutely dissociated DRG cells and DRG cells maintained in culture for 1, 4, 7, and 12 days. DRGs from two male rats were harvested, triturated, and re-suspended in F12 media supplemented with 10% horse serum and 30ng/mL NGF. Cells were plated in five 35 mm culture dishes at a density of 60,000 cells per well, with cells from each rat cultured independently. Following 1, 4, 7 and 12 days in culture, cells from one culture dish from each animal were collected and processed as described in the methods, and stored at -80°C. Using the modified western blot procedure for detecting aromatase immunoreactivity in sensory neuron cultures, immunoreactive bands corresponding to the molecular weight of aromatase were observed in 50 µg of total protein lysate from all samples (Figure 17A). This suggests that aromatase expression is maintained at low levels in culture and its expression level is relatively consistent throughout. Normalizing aromatase immunoreactivity to that of two internal controls, actin and HPRT, suggested some variability in aromatase expression between cultures. Sources of variability may be technical variability between cultures or inter-animal variability in expression of the proteins examined. Normalized aromatase expression in sensory neuron culture one decreased with length in culture, while normalized expression in the second culture suggested an increase over time (Figure 17B).

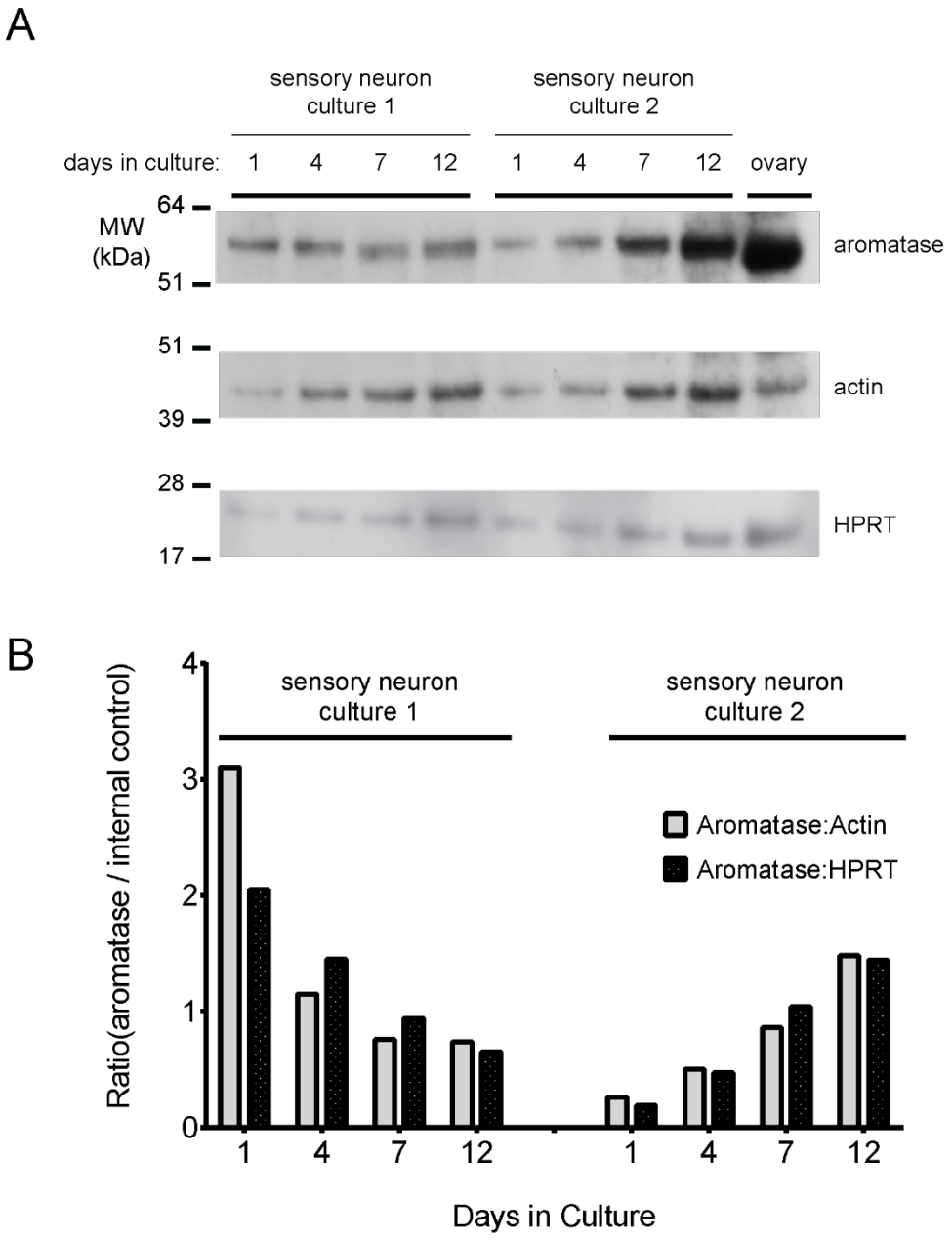

Figure 17. Aromatase is expressed throughout the duration of DRG cultures. **A:** Immunoblot of total protein isolated from independent sensory neuron cultures derived from male rats and ovary lysates (50 and 25µg total protein loaded for culture and ovary lysates, respectively). Total protein was isolated from neuronal cultures after 1, 4, 7, or 12 days in culture. Membrane was probed with anti-aromatase, anti-actin, and anti-HPRT antibodies. **B:** Data represent the density ratios of aromatase and actin or HPRT immunoreactive bands observed in (A), quantified by densitometry analysis.

The presence of aromatase in the immunoreactivity in lysates from DRGs isolated from all levels of the spinal column does not demonstrate whether aromatase is selectively expressed in one or more of these structures. Therefore, to determine whether aromatase is expressed in DRGs containing sensory neurons that innervate the rat hind limbs, aromatase immunoreactivity was determined in lumbar 4, 5, and 6 (L4-6) DRGs. Furthermore, to determine whether aromatase is also expressed in DRGs from OVX females, total protein lysates of L4-6 DRGs (isolated bilaterally) isolated from three male rats and three OVX female rats (100 µg total protein) were separated in a polyacrylamide gel, along with ovaries isolated from two different female rats (25 µg total protein). Following overnight transfer to a PVDF membrane (at 4°C), the membrane was blocked and aromatase immunoreactivity was determined by incubating the membranes in mouse anti-aromatase antibody overnight at 4°C (1:250 dilution in blocking buffer). The membrane was washed and then incubated with a HRP-conjugated anti-mouse secondary antibody (1:5,000 in blocking buffer) for one hour at room temperature. After washing the membrane again, immunoreactivity detected using Western Lightning® Plus-ECL substrate. As seen in Figure 18, immunoreactive bands were observed in L4-6 DRGs isolated from both male and female rats. When normalized to actin, aromatase immunoreactivity was several fold higher in OVX females when compared to males. Immunoreactive bands appearing in the male DRGs appeared to be of slightly higher molecular weight than those appearing in DRGs from OVX females, suggesting there may be several aromatase isoforms.

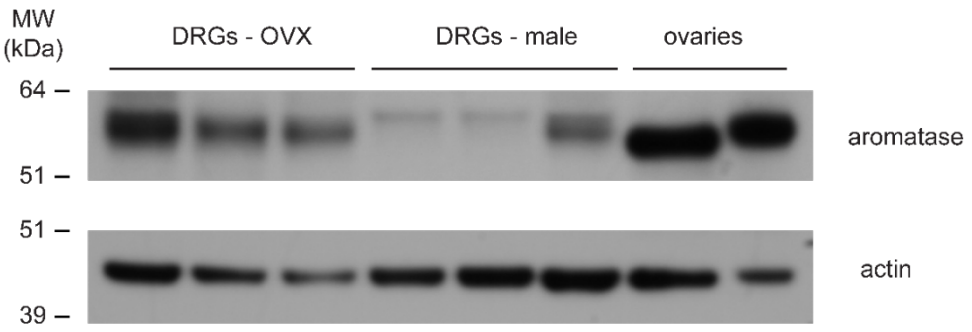

Figure 18. Aromatase is expressed in L4-6 DRGs from OVX female and male rats.
Immunoblot of total protein isolated from L4-6 DRGs from three OVX female rats and three male rats, in addition to ovary lysates (100 and 50 µg total protein was loaded for DRG and ovary lysates, respectively). Membrane was probed with anti-aromatase and anti-actin antibodies.

Effect of the aromatase inhibitor letrozole on release of the calcitonin gene-related peptide from sensory neurons in culture

In sensory neuron cultures from OVX rats, capsaicin-stimulated iCGRP release is not sensitized by long-term letrozole exposure (10 pM to 1 μM)

One mechanism that could mediate AI-induced hypersensitivity is the ability of the drugs to augment transmitter release from small diameter sensory neurons that conduct noxious information. Consequently, I conducted a series of studies examining whether acute or long-term exposure to letrozole would increase the basal or stimulated release of CGRP from sensory neurons in culture. For my initial studies, cells were stimulated with the TRPV1 agonist, capsaicin. In rat DRG cultures, capsaicin activates an inward current carried predominately by sodium and calcium ions and stimulates the release of CGRP in a concentration-dependent manner (Dymshitz and Vasko, 1994; Hingtgen and Vasko, 1994). Given the pattern of TRPV1 in rat DRGs and DRG cultures, CGRP released from DRG cultures following capsaicin exposure originates from the approximately 50% of TRPV1-expressing small diameter sensory neurons that also express CGRP (Price and Flores, 2007).

Neuronal cultures were prepared from DRGs isolated from OVX female rats and maintained in F12 media for 12 days, supplemented with 30 ng/mL NGF. To determine whether letrozole might sensitize sensory neurons to capsaicin stimulation in a concentration-dependent manner, cells were treated with letrozole (10 pM to 1 μM) or vehicle (1:10,000 dilution of MPL) daily for the last five days in culture and then release experiments were performed. The cultures were washed in HEPES buffer for 10 minutes and then re-exposed to the drug or vehicle for 10 minutes prior to and throughout exposure to 30 nM capsaicin. Basal release of iCGRP was not altered by letrozole

concentrations up to 1 μM (Figure 19A). Although exposing sensory neuron cultures to 30 nM capsaicin resulted in over 15-fold increase in peptide release over release in HEPES buffer alone (Figure 19A, vehicle control), treatment with letrozole did not alter stimulated iCGRP release (Figure 19A). The content of iCGRP in sensory neuron cultures exposed to letrozole for five days was not significantly different from vehicle-treated cultures (Figure 19B).

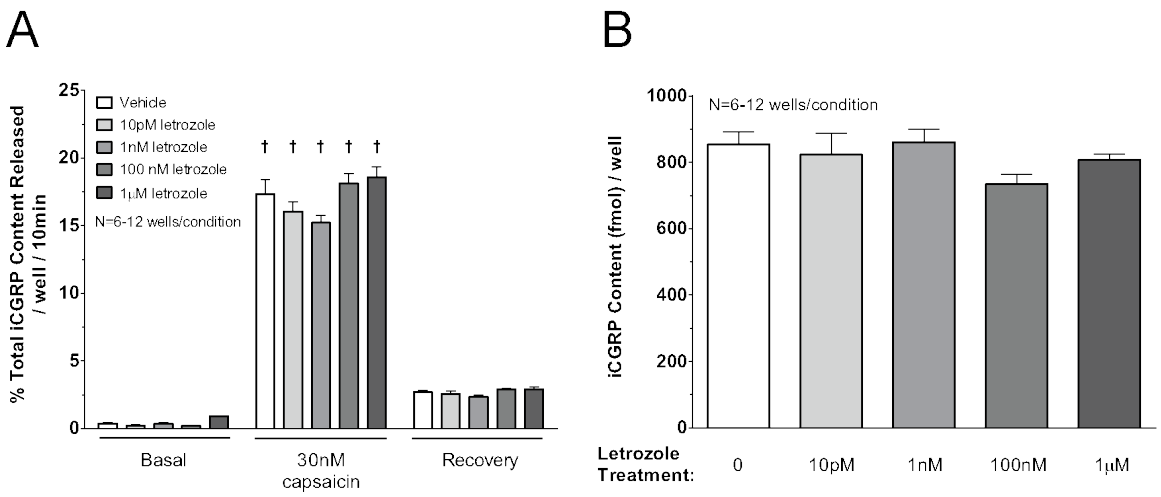

Figure 19. Release of iCGRP is not altered in sensory neurons from OVX rats after five days of letrozole exposure.
A: The ordinate represent the mean ± S.E.M. release of iCGRP as percent of total content per well. Cells were treated with vehicle, 10 pM, 1nM, 100nM or 1 μM letrozole for five days prior to measuring iCGRP release then were exposed to vehicle or the same concentration of letrozole in the absence (Basal) or presence of 30 nM capsaicin. Within each treatment group, a cross indicates a significant difference in capsaicin-stimulated release from basal release. **B:** Total iCGRP content measured from each treatment group.

10μM letrozole sensitizes capsaicin-stimulated iCGRP release from sensory neuron cultures isolated from OVX rats, but not cultures from intact female or male rats

When administered letrozole, OVX female rats and male rats developed mechanical hypersensitivity to stimulation with von Frey filaments. While basal or capsaicin-stimulated iCGRP release from DRG cultures from OVX rats was not altered by letrozole concentrations up to 1 μM, the average letrozole concentration achieved in DRG neurons following a single dose of 1 mg/kg to OVX females was approximately 1000 pg/mL (3.5 μM) (Figure 12). Drug concentrations were measured at 0.5 and 3 hours following drug administration and it is therefore unclear whether the observed concentrations approximate the maximum concentrations achieved in this tissue. In fact, following letrozole administration to female rats, the time at which maximum concentrations are achieved in the brain have been shown to lag behind maximum concentrations measured in plasma (Liu et al., 2000).

Neuronal cultures were prepared from DRGs isolated from OVX, intact female, and male rats and maintained in F12 media for 12 days, supplemented with 30 ng/mL NGF. Basal and capsaicin-stimulated iCGRP release was compared between cultures prepared from ovariectomized versus intact female rats to determine whether there are differences in sensitivity to either stimulus following ovariectomy. To mimic the effect of higher tissue letrozole concentrations, neuronal cultures were treated with 10 μM letrozole or vehicle (1:10,000 dilution of MPL) daily for five days and then release experiments were performed. The effect of acute letrozole exposure was determined using cells treated for five days with vehicle (1:10,000 dilution of MPL). The cultures were washed and then treated with vehicle (1:10,000 dilution of MPL) or 10 μM letrozole for 10 min to prior to and throughout exposure to 30 nM capsaicin.

In cultures derived from male, female, and OVX female rats, basal release of iCGRP was not altered following acute (10 min) or long-term (5 days) exposure to 10 μM letrozole (Table 2). There were no differences in basal peptide release among the different culture types, irrespective of treatment. Exposing sensory neuron cultures to 30 nM capsaicin resulted in a significant increase in iCGRP release from baseline in all culture types (difference of 6.1% to 9.4% from baseline; Table 2). In cultures from OVX rats exposed to letrozole, capsaicin-stimulated iCGRP release (as percent of total iCGRP) was significantly increased by 2.6 percentage points (vehicle: 9.9% ± 0.0%, 10 μM letrozole: 12.5% ± 0.0%; Table 2). Five days of letrozole exposure similarly increased iCGRP release in response to capsaicin, with an absolute difference of 1.6% relative to cells exposed to vehicle for five days (Table 2). Capsaicin-stimulated iCGRP release was also enhanced by acute letrozole treatment in cultures from male rats, with an absolute difference of 0.8% from vehicle-treated cells (Table 2). In contrast to OVX cultures, long-term exposure to letrozole did not enhance capsaicin-stimulated peptide release in male cultures.

A secondary analysis of capsaicin-stimulated release between the culture types treated with vehicle showed capsaicin-stimulated release was significantly higher in OVX cultures compared to cultures derived from intact female and male rats (one-way ANOVA followed by two-sample t-tests; Table 2). Total iCGRP content in vehicle-treated cultures from intact females were significantly higher than OVX and male cultures (one-way ANOVA followed by two-sample t-tests; Table 2), which may account for differences when data are presented as percent of total content. However, capsaicin-stimulated release from OVX cultures was significantly higher when femtomoles of iCGRP released were compared (mean ± S.E.M: OVX: 193 fmol ± 7, Intact: 169 fmol ± 7, Male: 142 fmol ± 6). Capsaicin-stimulated iCGRP release was also higher in OVX cultures than intact

female or male cultures treated with letrozole (acute or long-term) (Table 2). Additionally, total iCGRP content was significantly higher in cultures from intact female rats compared to the other culture types irrespective of vehicle or letrozole treatment (Table 2).

Table 2. Comparing the effect of letrozole on basal and capsaicin-stimulated release of iCGRP from rat sensory neuron cultures isolated from male, OVX female, and intact female rats.

	5 days pre-treatment:	Vehicle	Vehicle	10 μM letrozole
	Acute treatment:	Vehicle	10 μM letrozole	10 μM letrozole
Basal iCGRP release	OVX female	0.5 ± 0.0	0.6 ± 0.1	0.6 ± 0.1
	Intact female	0.3 ± 0.0	0.4 ± 0.0	0.4 ± 0.0
	Male	0.3 ± 0.1	0.3 ± 0.1	0.3 ± 0.1
iCGRP release stimulated by 30 nM capsaicin	OVX female	9.9 ± 0.0 †	12.5 ± 0.0 †,*	11.5 ± 0.0 †,*
	Intact female	6.4 ± 0.2 †	6.8 ± 0.4 †	6.9 ± 0.2 †
	Male	6.8 ± 0.2 †	7.6 ± 0.3 †,*	7.4 ± 0.6 †
Total iCGRP content (fmol)	OVX female	1979 ± 79	1895 ± 95	1999 ± 95
	Intact female	2667 ± 163	2479 ± 191	2451 ± 107
	Male	2082 ± 82	2117 ± 78	1946 ± 109

Cells were treated for 5 days prior to measuring iCGRP release (pre-treatment) and additionally treated during the experiment to measure basal and stimulated iCGRP release (acute treatment). iCGRP release was measured from sequential 10-minute incubations during which cells were exposed to HEPES buffer in the presence of the indicated acute treatment (basal release), then 30nM capsaicin in the presence of the indicated acute treatment (stimulated release). Basal and stimulated iCGRP release are presented as the mean ± S.E.M. of iCGRP released as percent of total content per well (N=6-12 per condition). Total iCGRP content is the sum of iCGRP released during the experiment and remaining iCGRP measured from cells lysed with 0.1N HCl. Total iCGRP content is represented as mean ± S.E.M. femtomoles (fmol) of iCGRP per well (N=6-12 per condition). Crosses indicate enhanced iCGRP release stimulated by 30 nM capsaicin relative to basal release. Asterisks indicate significant difference in capsaicin-stimulated iCGRP release in the presence of the indicated treatment versus vehicle-treated controls.

Letrozole does not sensitize iCGRP release from sensory neuron cultures isolated from OVX rats following serum deprivation

While 10 μM letrozole sensitized DRG cultures derived from OVX rats, this effect was generally not observed in the other cultures (intact female and male) and there was no apparent concentration-dependent effect. Sensory neuron cultures used for experiments described in Figure 19 and Table 2 were maintained in F12 media, supplemented with 30 ng/mL NGF and 10% horse serum. Steroids present in the horse serum (collected from a donor herd, per manufacturer's specifications) may include estrogens or high concentrations of androgens that could be metabolized to estrogens by aromatase, thereby masking our ability to detect changes in iCGRP release secondary to aromatase inhibition. To evaluate whether the effect of letrozole could be determined using DRG cultures maintained in serum-free conditions, I first evaluated the effect of serum deprivation on basal and capsaicin-stimulated iCGRP release, as well as total iCGRP content. Cells were maintained in 12-well plates in F12 media (supplemented with 30 ng/mL NGF and 10% horse serum) that was changed the day following DRG harvest (day 1) and every other day. On culture day 9, media in 3 wells was exchanged for F12 media, supplemented with only 30 ng/mL NGF, while the other 9 wells received F12 media, supplemented with 30 ng/mL NGF and 10% horse serum. On culture days 10 and 11, media was changed for all wells and an additional 3 wells received F12 media, supplemented with only 30 ng/mL NGF. Cells receiving media without serum were maintained in serum-free conditions until the release experiment.

Maintaining DRG cultures in serum-free conditions for 48 and 72 hours resulted in a significant increase in basal and capsaicin-stimulated iCGRP release when compared to cells maintained in 10% serum (Figure 20A). Capsaicin-stimulated iCGRP release was also augmented by 24 hours of serum-free conditions, however, basal

release was not different from controls (Figure 20A). Additionally, iCGRP content in DRG cultures was sensitive to serum deprivation. As shown in Figure 20B, serum deprivation significantly reduced the total iCGRP content in cultured sensory neurons, with significant reductions in cells grown in serum-free conditions for 48 and 72 hours.

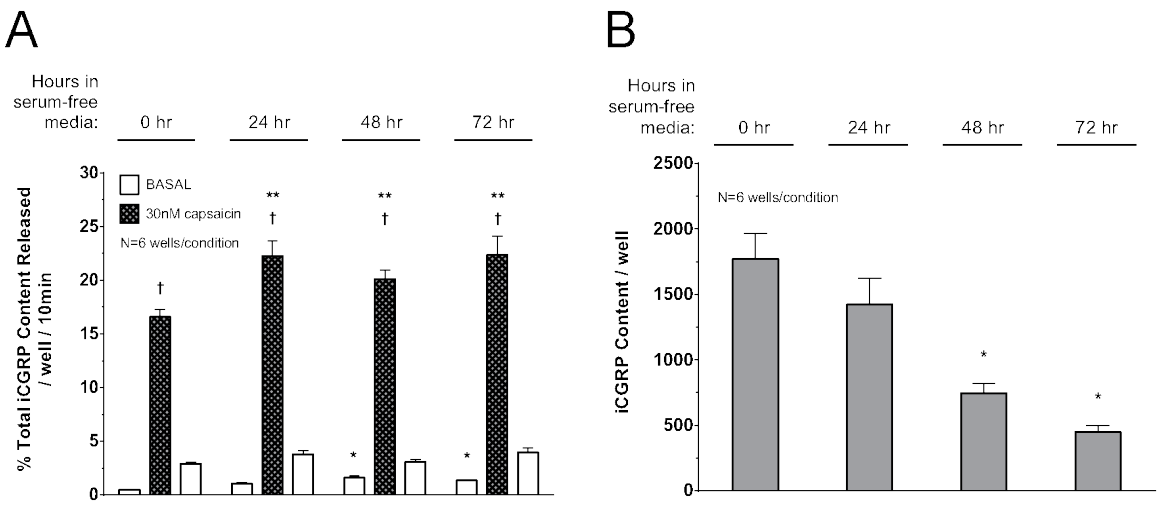

Figure 20. Capsaicin-stimulated release of iCGRP is augmented and iCGRP content is reduced in sensory neuron cultures maintained in the absence of serum

A: The ordinate represent the mean ± S.E.M. release of iCGRP as percent of total content per well. Cells were maintained in serum free media for 0, 24, 48, or 72 hours prior to measuring iCGRP release (indicated above the bar graphs) in the absence (Basal; open columns) or presence of 30 nM capsaicin (hatched columns). Within each treatment group, a cross indicates a significant difference in capsaicin-stimulated release from basal release. An asterisk indicates a significant difference in basal release, whereas and double asterisks indicate a significant difference in capsaicin-stimulated release in serum-deprived cells compared to controls. **B:** Total iCGRP content measured from each treatment group following the release experiment. An asterisk indicates a significant difference in total content in serum-deprived cells compared to controls.

To evaluate whether 10μM letrozole alters iCGRP release from sensory neurons in serum-free conditions, cells were initially maintained in F12 media, supplemented with 30 ng/mL NGF and 10% horse serum. On culture day 11, media was exchanged for F12 media, supplemented with only 30 ng/mL NGF, and treated with 10 μM letrozole or vehicle (1:10,000 dilution of MPL). After 24 hours in culture, basal and capsaicin-stimulated iCGRP release was measured with letrozole or vehicle treatments maintained during the release experiment. As shown in Figure 21, iCGRP release stimulated by 30 nM capsaicin was not sensitized by 10 μM letrozole in neuronal cultures maintained in the absence of serum, suggesting horse serum may not significantly influence the effect of letrozole on this endpoint.

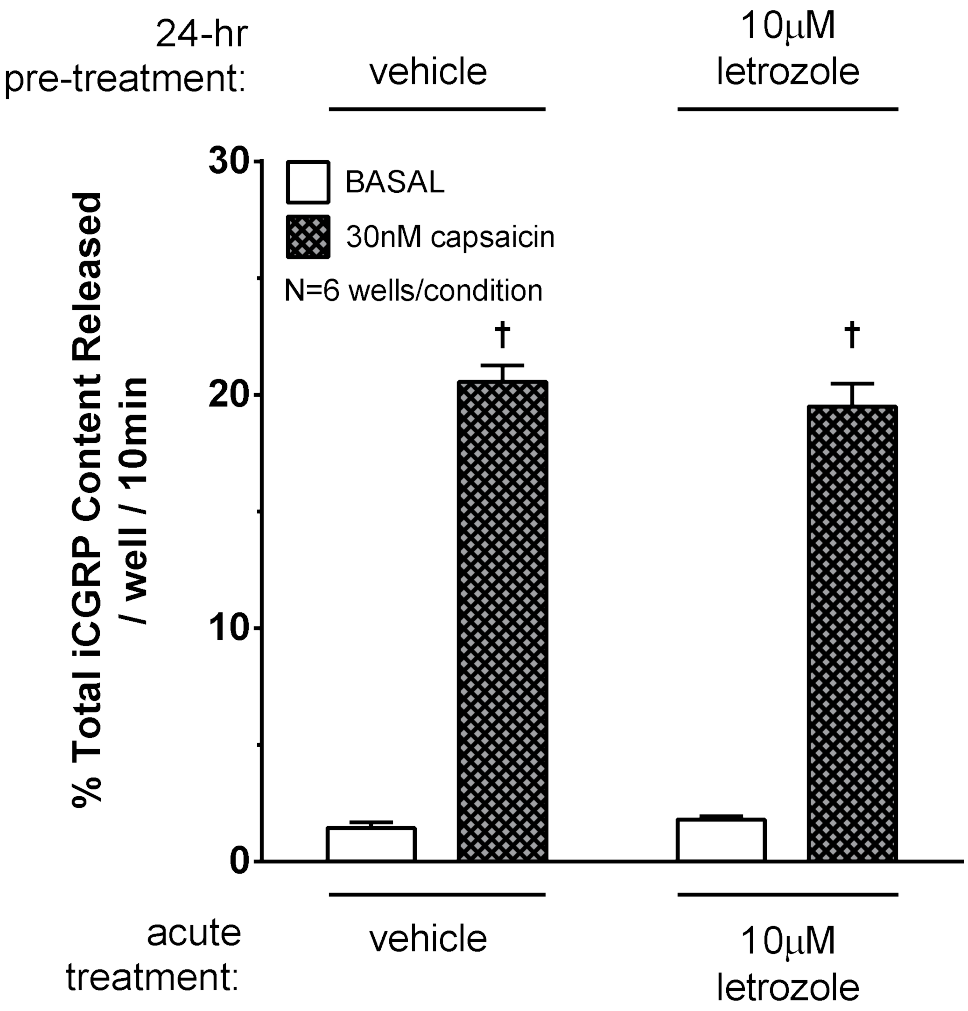

Figure 21. Letrozole does not alter basal or capsaicin-stimulated iCGRP release from sensory neuron cultures maintained for 24 hours in serum-free media
Sensory neurons were maintained in serum-free media for 24 hours prior to measuring peptide release. Cells were treated with vehicle or 10 μM letrozole for 24 hours prior to measuring iCGRP release (indicated above the bar graphs) and then were exposed to vehicle or 10 μM letrozole in the absence (BASAL; open columns) or presence of 30 nM capsaicin (hatched columns). Within each treatment group, a cross indicates a significant difference from basal release.

Letrozole does not sensitize iCGRP release from sensory neuron cultures isolated from male rats, grown in phenol-red free conditions

In addition to the potential influence of exogenous steroids present in horse serum, F12 media contains the pH indicator dye phenol red, a known estrogen receptor agonist that is also a non-competitive antagonist of P2X channels [Berthois Proc Natl Acad Sci U S A 1986; King Br J Pharmacol 2005]. To determine whether letrozole alters basal or stimulated release of iCGRP in sensory neurons maintained in the absence of phenol red, dissociated DRG neuronal cultures were maintained in DMEM-F12 media. As described in the methods, antibiotics and mitotic inhibitors were added at the same concentrations as used in F12 media and DMEM-F12 media was supplemented with 10% horse serum and 30 ng/mL NGF. Since mechanical hypersensitivity was observed in letrozole-treated animals and CGRP has been localized to TRPV1+ and TRPV1- mechano-sensitive DRG neurons, the effect of letrozole on non-selective stimulation of iCGRP release from neurons with high extracellular potassium was determined and compared to the effect of letrozole on capsaicin-stimulated iCGRP release.

In contrast to capsaicin, high extracellular concentrations of potassium ions result in non-selective depolarization of all neurons in a concentration-dependent manner. While raising the extracellular potassium concentration evokes depolarization in all neurons, depolarization of large diameter neurons that express tetrodotoxin-sensitive sodium channels does not generate action potentials, presumably due to depolarization block. On the other hand, K+-evoked depolarization generated action potentials in slowly conducting nociceptors expressing tetrodotoxin-resistant sodium channels (Jeftinija et al., 1993). Thus, it is expected that high extracellular potassium concentrations will stimulate the release of CGRP from small diameter neurons expressing this neuropeptide.

In preliminary experiments, sensory neuron cultures grown in DMEM-F12 media developed grape-like clusters of small, round inclusions when cells were maintained for more than 9 days. The inclusions appeared to be a result of degradation of the laminin/poly-D-lysine substrate. While these changes did not appear to alter neuron or support cell morphology, iCGRP release experiments with DRG neurons maintained in DMEM-F12 were performed no later than 9 days after harvesting and plating the cells.

At 72 hours preceding the release experiment, cells were exposed to 10 μM letrozole or vehicle (1:10,000 dilution of MPL) by direct addition to the culture media. At 48 and 24 hours prior to the experiment, media was exchanged containing 10 μM letrozole or vehicle. Thus, cells were exposed to the drug or vehicle for 3 days. The cultures were washed and then treated with vehicle (1:10,000 dilution of MPL) or 10 μM letrozole for 10 min prior to and throughout exposure to 30 nM capsaicin or HEPES buffer containing 30 mM KCl. As a positive control for augmentation of capsaicin and KCl-stimulated iCGRP release, additional cells in each experiment were treated with 1 μM PGE_2.

Although exposing sensory neuron cultures to 30 nM capsaicin or 30 mM KCl resulted in an 8-fold increase in peptide release over release in HEPES buffer, treatment with 10 μM letrozole did not alter basal or stimulated iCGRP release (Table 3). Acute exposure of neuronal cultures to PGE_2 sensitized iCGRP release in response to both depolarizing stimuli (Table 3). The content of iCGRP in sensory neuron cultures exposed to 10 μM letrozole acutely (560 ± 26 fmol/well) or chronically (606 ± 23 fmol/well) was not significantly different from vehicle-treated cultures (588 ± 19 fmol/well) (Table 3).

Table 3. Basal and stimulated release of iCGRP from male rat sensory neuron cultures treated with 10μM letrozole.

3 days pre-treatment:	Vehicle	Vehicle	10 μM letrozole	Vehicle
Acute treatment:	Vehicle	10 μM letrozole	10 μM letrozole	1 μM PGE_2
Basal iCGRP release (N=5-18/condition)	1.4 ± 0.2	1.4 ± 0.1	1.2 ± 0.0	1.6 ± 0.1
iCGRP release stimulated by 30 nM capsaicin (N=8-9/condition)	8.5 ± 0.3 †	8.6 ± 0.3 †	8.9 ± 0.4 †	15.9 ± 0.6 †,*
iCGRP release stimulated by 30 mM KCl (N=6-9/condition)	8.4 ± 0.9 †	8.4 ± 0.6 †	7.5 ± 0.5 †	12.5 ± 0.9 †,*
Total iCGRP content (fmol) (N=18/condition)	588 ± 19	560 ± 26	606 ± 23	599 ± 20

Cells were treated for 3 days prior to measuring iCGRP release (pre-treatment) and additionally treated during the experiment to measure basal and stimulated iCGRP release (acute treatment). iCGRP release was measured from sequential 10-minute incubations during which cells were exposed to HEPES buffer in the presence of the indicated acute treatment (basal release), then 30nM capsaicin or 30mM potassium in the presence of the indicated acute treatment (stimulated release). Basal and stimulated iCGRP release are presented as the mean ± S.E.M. of iCGRP released as percent of total content per well. Total iCGRP content is the sum of iCGRP released during the experiment and remaining iCGRP measured from cells lysed with 0.1N HCl. Total iCGRP content is represented as mean ± S.E.M. femtomoles (fmol) of iCGRP per well. Crosses indicate enhanced iCGRP release stimulated by 30 nM capsaicin relative to basal release. Asterisks indicate significant difference in capsaicin-stimulated iCGRP release in the presence of the indicated treatment versus vehicle-treated controls.

α,β-meATP does not alter iCGRP release from male sensory neuron cultures

Though letrozole did not directly sensitize iCGRP release stimulated by capsaicin or high extracellular potassium, AIs may enhance sensory neuron sensitization by algogens. As letrozole and exemestane augmented overt hypernociception in response to intraplantar ATP, I hypothesized that letrozole alters sensitization of iCGRP release by purinergic receptor agonists. In DRG neurons, estradiol and the GPR30 agonist G1 have been shown to reduce α,β-meATP-evoked currents [Ma LifeSci 2005, Lu Endocrinology 2013]. Therefore, reduced intracellular estrogens as a consequence of aromatase inhibition may augment P2X currents in DRG neurons, resulting in changes in stimulated release of iCGRP.

In previous studies using sensory neurons cultured from neonatal rats, Huang et al. showed that purinergic receptor agonists differentially affected capsaicin-stimulated iCGRP release: while the non-selective agonist ATP augmented iCGRP release in a concentration-dependent manner, the P2X-selective agonist α,β-meATP inhibited capsaicin-stimulated iCGRP release [Huang J Pharmacol Exp Ther 2003]. In acutely dissociated DRG neurons from adult rats, α,β-meATP evokes currents in approximately 70% of capsaicin-sensitive neurons that exhibit bi-exponential decay, characteristic of homomeric $P2X_3$ receptors [Ueno BrJPharmacol 1999, Lewis Nature 1995]. This current is rapidly desensitized (< 100 milliseconds), displays slow recovery from inactivation, and is rapidly run down upon repeated agonist application [Lewis Nature 1995]. Thus, the kinetics of the $P2X_3$ receptor current make it unlikely that $P2X_3$ activation can sensitize nociceptors. In contrast, α,β-meATP evokes sustained currents in approximately 50% of capsaicin-insensitive neurons and the currents retain responsiveness to repeated applications of α,β-meATP [Ueno BrJPharmacol 1999]. α,β-meATP-evoked currents in these neurons resemble those of heteromeric $P2X_2$ and $P2X_3$

channels [Lewis Nature 1995]. These data suggest that if α,β-meATP can sensitize sensory neurons, it is likely due to actions on capsaicin-insensitive cells. Thus, I characterized the effect of α,β-meATP on iCGRP release stimulated by non-selective depolarization of all neurons using 30 mM KCl. Given that the EC50 for α,β-meATP-evoked currents is similar between capsaicin-sensitive cells (10 μM) and capsaicin-insensitive neurons (66 μM), α,β-meATP concentrations for this experiment bounded these effective concentrations [Ueno BrJPharmacol 1999].

Neuronal cultures were prepared from DRGs isolated from male rats and maintained in F12 media for 12 days, supplemented with 10% horse serum and 30 ng/mL NGF. The cultures were washed and then treated with vehicle (HEPES buffer) or 0.01 to 100 μM α,β-meATP for 10 min to prior to and throughout exposure to 30 mM KCl. Basal iCGRP release was not altered at α,β-meATP concentrations up to 100 μM, suggesting that activation of homomeric $P2X_3$ channels and heteromeric $P2X_2/P2X_3$ channels does not directly simulate iCGRP release (Figure 22). Exposing cells to 30 mM KCl enhanced iCGRP release 7-fold relative to baseline. While KCl-stimulated iCGRP release was enhanced by 0.01 μM α,β-meATP, increasing concentrations of α,β-meATP did not have a similar effect.

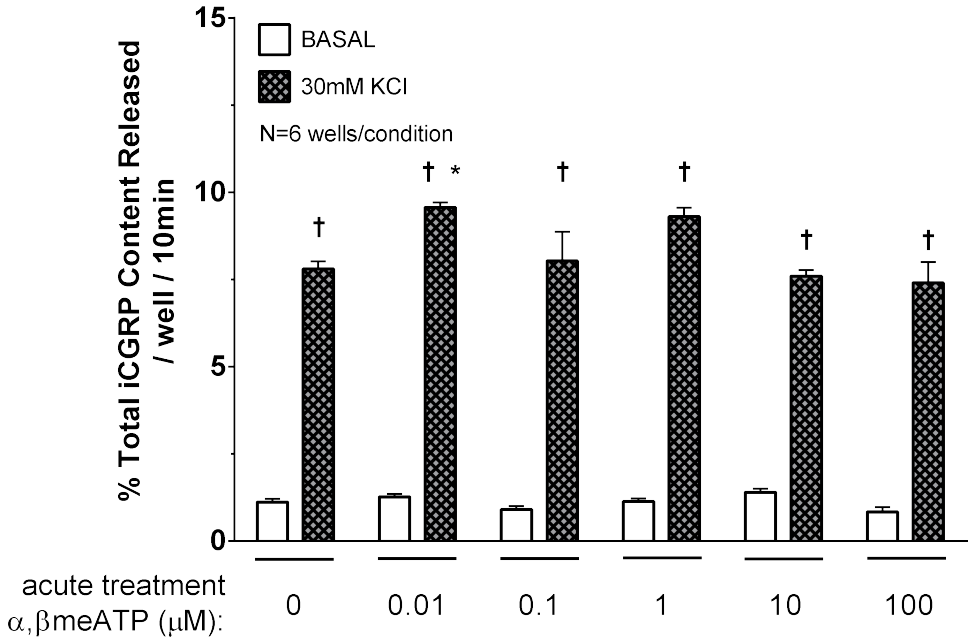

Figure 22. α,β-meATP does not alter iCGRP release from rat sensory neurons under basal conditions or following stimulation with high potassium.
The ordinate represent the mean ± S.E.M. release of iCGRP as percent of total content per well. iCGRP release was measured from cells sequentially exposed for ten minutes to buffer alone (BASAL; open columns), then 30 mM KCl (hatched columns) in the presence of vehicle or 0.01 to 100 μM α,β-meATP. Within each treatment group, a cross indicates a significant difference in iCGRP release in response to high extracellular potassium. An asterisk indicates a difference in cells treated with α,β-meATP versus those treated with only 30 mM KCl.

Capsaicin-stimulated release of iCGRP from male sensory neuron cultures is sensitized by ATP, but not α,β-meATP

In the previous experiment to determine the effect of α,β-meATP on KCl-stimulated iCGRP release, the culture media contained phenol red, a known estrogen receptor agonist that was subsequently found to also non-competitively antagonize P2X channels [Berthois Proc Natl Acad Sci U S A 1986; King Br J Pharmacol 2005]. Media containing phenol red was also used in experiments investigating the effects of α,β-meATP on release of neuropeptides in embryonic DRG neurons reported by Huang et al. [Huang JPET 2003]. Maintaining neuronal cultures in media containing phenol red may alter the response to P2X channel activation, thus I determined whether α,β-meATP alters iCGRP release under basal conditions and when stimulated by 30nM capsaicin or 30 mM KCl using sensory neurons isolated from adult rats cultured in phenol red-free culture media. Although ATP has been shown to sensitize capsaicin-stimulated iCGRP release in a concentration-dependent manner, it is unknown whether it also augments iCGRP release in response to high concentrations of extracellular potassium. Therefore, I also examined whether ATP sensitizes capsaicin or KCl-stimulated release of iCGRP under phenol-red free conditions.

Neuronal cultures were prepared from DRGs isolated from male rats and maintained in DMEM/F12 media for 9 days, supplemented with 10% horse serum and 30 ng/mL NGF. The cultures were washed and then treated with vehicle (HEPES buffer), 10 μM α,β-meATP, or 10 μM ATP for 10 min to prior to and throughout exposure to 30nM capsaicin or 30 mM KCl. As a positive control for augmentation of capsaicin and KCl-stimulated iCGRP release, additional cells in each experiment were treated with 1 μM PGE_2. Basal iCGRP release was not altered by exposing cells to 10 μM ATP or 10 μM α,β-meATP, but was slightly augmented in cells exposed to 1 μM PGE_2 (Figure 23).

In vehicle-treated cells, iCGRP release was significantly enhanced by stimulation with 30 mM KCl and 30 nM capsaicin (difference of 4.9% and 8.3% from baseline, respectively) (Figure 23).

Exposing sensory neuron cultures to 30 nM capsaicin resulted in a significant increase in iCGRP release from baseline in all culture types (difference of 6.1% to 9.4% from baseline; Table 2). Exposing sensory neurons to 10 μM ATP prior to and throughout stimulation with 30 nM capsaicin (CAP) increased iCGRP release relative to stimulation with 30 nM capsaicin alone (Figure 23). In contrast, 30 mM KCl-stimulated iCGRP release (KCl) was unaltered by treatment with 10 μM ATP (Figure 23). In comparison to ATP-mediated sensitization of iCGRP release, 10 μM α,β-meATP did not alter capsaicin-stimulated iCGRP release or KCl-stimulated iCGRP release (Figure 23). Capsaicin and KCl-stimulated iCGRP release was augmented by exposing the same neuronal cultures to 1 μM PGE_2 (Figure 23). There were no significant differences in iCGRP content in response these acute drug exposures (vehicle: 827 ± 39 fmol (n=21), 10 μM ATP: 759 ± 28 fmol (n=21), 10 μM α,β-meATP: 766 ± 34 fmol (n=21), 1 μM PGE_2: 763 ± 21 fmol (n=21); one-way ANOVA).

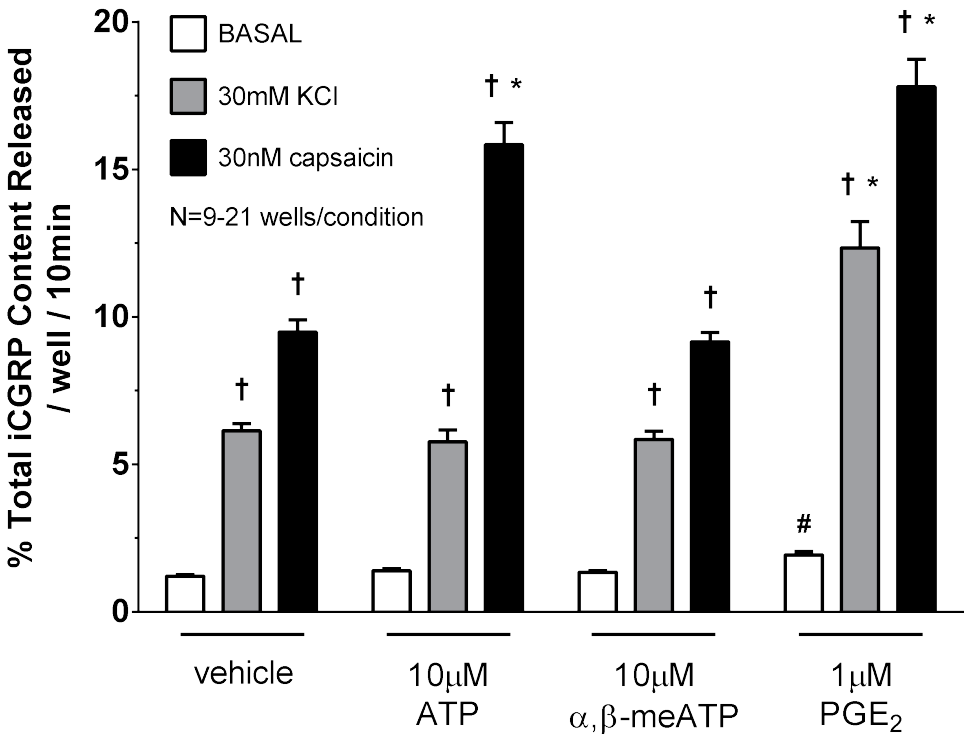

Figure 23. ATP enhances iCGRP release stimulated by capsaicin, but not high potassium.
The ordinates represent the mean ± S.E.M. release of iCGRP as percent of total content per well. iCGRP release was measured from cells sequentially exposed for ten minutes to buffer alone (BASAL; open columns), then 30 mM KCl (grey columns) or 30 nM capsaicin (black columns) in the presence of vehicle, 10 μM ATP, 10 μM α,β-meATP, or 1 μM PGE_2. Within each treatment group, crosses indicate enhanced iCGRP release in response to 30 mM KCl or 30 nM capsaicin treatment under control conditions. A pound symbol indicates augmented basal iCGRP release in the presence of the indicated treatment versus controls. Asterisks indicate significant differences in capsaicin or KCl-stimulated iCGRP release in the presence of the indicated treatment versus controls.

Letrozole does not potentiate the ability of ATP to sensitize sensory neurons in culture

Given that letrozole augmented hypernociception in response to intraplantar ATP, I sought to examine whether letrozole alters sensitization of iCGRP release secondary to purinergic receptor activation. Since α,β-meATP does not directly stimulate iCGRP release or alter capsaicin- or KCl-stimulated iCGRP release in DRG cultures, and because ATP selectively alters response to capsaicin, I chose to examine the potential interaction between ATP and letrozole exposure on capsaicin-stimulated iCGRP release. Secondly, to avoid potential ceiling effects when examining potentiation of ATP-induced sensitization by letrozole, cells were exposed to lower ATP concentrations and stimulated using lower capsaicin concentrations.

Neuronal cultures were prepared from DRGs isolated from male rats and maintained in DMEM/F12 media for 9 days, supplemented with 10% horse serum and 30 ng/mL NGF. To examine the effects of acute letrozole exposure on ATP-induced sensitization, cells were washed and then exposed to vehicle (1:10,000 dilution of MPL), 10 μM letrozole, 1 μM ATP, and the combination for ten minutes prior to and throughout stimulation with 10 nM capsaicin. Exposing sensory neurons to 1 μM ATP alone did not alter basal iCGRP release, but augmented capsaicin-stimulated release, as evidenced by an increase in iCGRP release relative to controls (Figure 24A). Exposing sensory neurons to 10 μM letrozole caused a small enhancement of basal iCGRP release relative to controls (vehicle: 0.9% ± 0.1, LET: 1.3% ± 0.1), but did not alter capsaicin-stimulated iCGRP release relative to vehicle-treated cells (Figure 24A). While letrozole treatment alone did not alter capsaicin-induced release of iCGRP, co-treatment with 10 μM letrozole and 1 μM ATP increased capsaicin-stimulated iCGRP release relative to cells treated with 1 μM ATP alone (CAP + ATP: 3.3% ± 0.1, CAP + ATP + LET: 4.0% ±

0.2) (Figure 24A). However, similar to letrozole treatment alone, basal iCGRP release from cells treated with letrozole and ATP was significantly increased relative to controls (Figure 24A). Thus, a secondary analysis was performed, accounting for the enhanced basal release in letrozole-treated cells. After subtracting basal release from capsaicin-stimulated iCGRP release from each well, letrozole exposure did not enhance the effect of ATP alone (CAP + ATP: 2.2% ± 0.1, CAP + ATP + LET: 2.6% ± 0.1) (Figure 24B). Finally, iCGRP content was not different between treatment groups (vehicle: 1256 ± 74 fmol, LET: 1101 ± 77 fmol, ATP: 1147 ± 90 fmol, ATP + LET: 1189 ± 71 fmol; one-way ANOVA).

I additionally examined whether long-term letrozole treatment alters ATP-mediated sensitization of iCGRP release. Cultures were treated with vehicle or 10 μM letrozole for three days prior to measuring iCGRP release. During the release experiment, cells pre-treated with vehicle were re-exposed to vehicle or 1 μM ATP prior to and throughout stimulation with 10 nM capsaicin. Cells pre-treated with letrozole were re-exposed to 10 μM letrozole alone or in combination with 1 μM ATP prior to and throughout stimulation with 10 nM capsaicin. Capsaicin-stimulated release of iCGRP was significantly enhanced by 1 μM ATP from 2.7 ± 0.2 % of total content to 5.2 ± 0.3 % of total content (Figure 24C). However, neither basal or capsaicin-stimulated iCGRP release was altered in cells treated with 10 μM letrozole and 1 μM ATP relative to cells treated with 1 μM ATP alone (Figure 24C). As observed in prior experiments, long-term exposure to letrozole did not significantly alter the content of iCGRP in the cultures. Total iCGRP content in cultures exposed to vehicle for 3 days was 993 ± 84 fmol/well, whereas in cultures exposed to 10 μM letrozole for 3 days, iCGRP content was 885 ± 71 fmol/well.

A

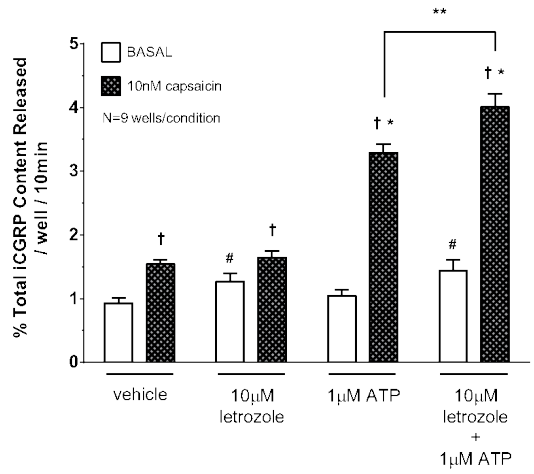
% Total iCGRP Content Released / well / 10min
BASAL
10nM capsaicin
N=9 wells/condition
**
† *
†
#
vehicle
10μM letrozole
1μM ATP
10μM letrozole + 1μM ATP

B

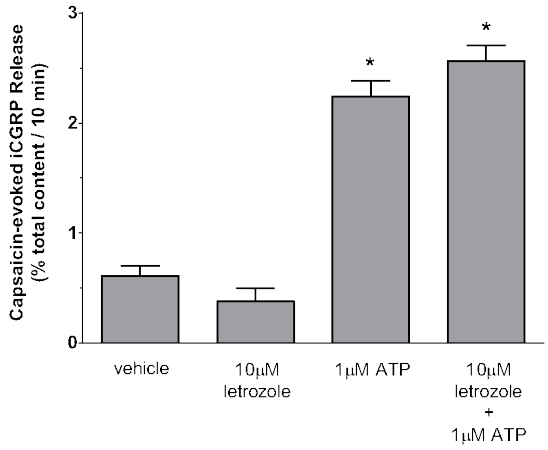
Capsaicin-evoked iCGRP Release (% total content / 10 min)
*
vehicle
10μM letrozole
1μM ATP
10μM letrozole + 1μM ATP

C

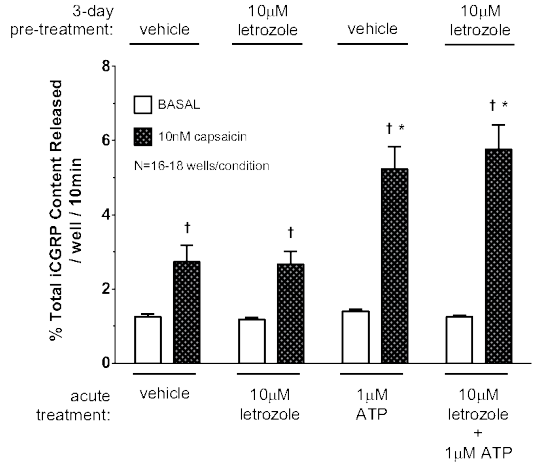
3-day pre-treatment:
vehicle
10μM letrozole
% Total iCGRP Content Released / well / 10min
BASAL
10nM capsaicin
N=16-18 wells/condition
† *
†
acute treatment:
1μM ATP
10μM letrozole + 1μM ATP

Figure 24. ATP-mediated sensitization of iCGRP release from sensory neurons is not altered by acute or long-term letrozole treatment.
The ordinates represent the mean ± S.E.M. release of iCGRP as percent of total content per well. **A:** During sequential ten minute incubations, cells were exposed to vehicle, 10 μM letrozole, 1 μM ATP, or the combination, in the absence (BASAL; open columns) or presence of 10 nM capsaicin (hatched columns). **B:** The evoked release of iCGRP is calculated by subtracting the basal release prior to stimulus exposure from the capsaicin-stimulated release. Asterisks indicate significant differences in capsaicin-evoked iCGRP release in the presence of the indicated treatment versus controls. **C:** Cells were treated with vehicle or letrozole for three days prior to measuring iCGRP release (indicated above the bar graphs) and then exposed to vehicle, 10 μM letrozole, 1 μM ATP, or the combination during the release experiment (indicated below the bar graphs) in the absence (BASAL; open columns) and presence of capsaicin (hatched columns). **In (A) and (C):** Within each treatment group, a cross indicates a significant difference from basal release. A pound symbol indicates augmented basal release versus vehicle controls, whereas an asterisk indicates a difference in cells treated with ATP versus those treated with only capsaicin. A double asterisk indicates a significant difference in capsaicin-stimulated iCGRP release in the presence of ATP versus ATP and letrozole.

Neuropeptide release from spinal cord slices is not altered in male rats treated with letrozole

To determine whether letrozole altered release of iCGRP into the spinal cord from sensory neuron central terminals, male rats were treated with 5 mg/kg letrozole (n = 6) or vehicle (750 mg/kg HPβCD; n = 7) daily for 7 to 8 days (Figure 25A). To ensure animals used in the slice release experiment had developed mechanical hypersensitivity as a result of letrozole treatment, PWT was measured at baseline and following 1, 3, and 6 days of treatment in all animals that were used in release experiments. Consistent with our previous results, 5 mg/kg letrozole significantly reduced the PWT compared to vehicle treated controls from 7.0 ± 1.0 grams to 2.7 ± 0.9 grams and 1.6 ± 0.2 at days 3 and 6 following initiation of treatment (Figure 25B). The day after the last drug dose, iCGRP release from spinal cord slices was measured under basal conditions and during depolarization with 30 mM KCl. Basal iCGRP release from spinal cord slices isolated from letrozole-treated rats (0.040 ± 0.004 % of total content per min) was not significantly different from that observed in vehicle-treated rats (0.040 ± 0.003 % of total content per min; Figure 26A and Figure 26B). Furthermore, iCGRP release during exposure to 30 mM KCl was not altered in spinal cord slices from rats treated with letrozole compared to vehicle (vehicle: 0.049 ± 0.005 versus letrozole: 0.048 ± 0.005 % of total content per min (Figure 26A and Figure 26B). Consequently, evoked iCGRP release from letrozole treated rats (0.008 ± 0.002 % of total content per min) was not different from that observed in vehicle treated rats (0.009 ± 0.003 % of total content per min; Figure 26B). Additionally, iCGRP content in the lumbar spinal cord was not different in male rats administered 5 mg/kg letrozole (407.1 ± 18.99 fmol/mg) versus vehicle (433.4 ± 35.56 fmol/mg) (Figure 26C).

As a positive control for sensitization of KCl-stimulated iCGRP release, spinal cord slices from additional treatment-naïve rats were acutely exposed to 30 μM PGE_2 (n = 4) or vehicle (1:2000 dilution of MPL; n = 14). PGE_2 augmented basal (0.103 ± 0.009 % of total content per min), 30 mM KCl stimulated (0.197 ± 0.017 % of total content per min), and evoked iCGRP release (0.095 ± 0.024 % of total content per min) relative to vehicle controls (basal: 0.051 ± 0.004 % of total content per min, 30 mM KCl: 0.086 ± 0.011 % of total content per min, evoked: 0.035 ± 0.010 % of total content per min; Figure 26D).

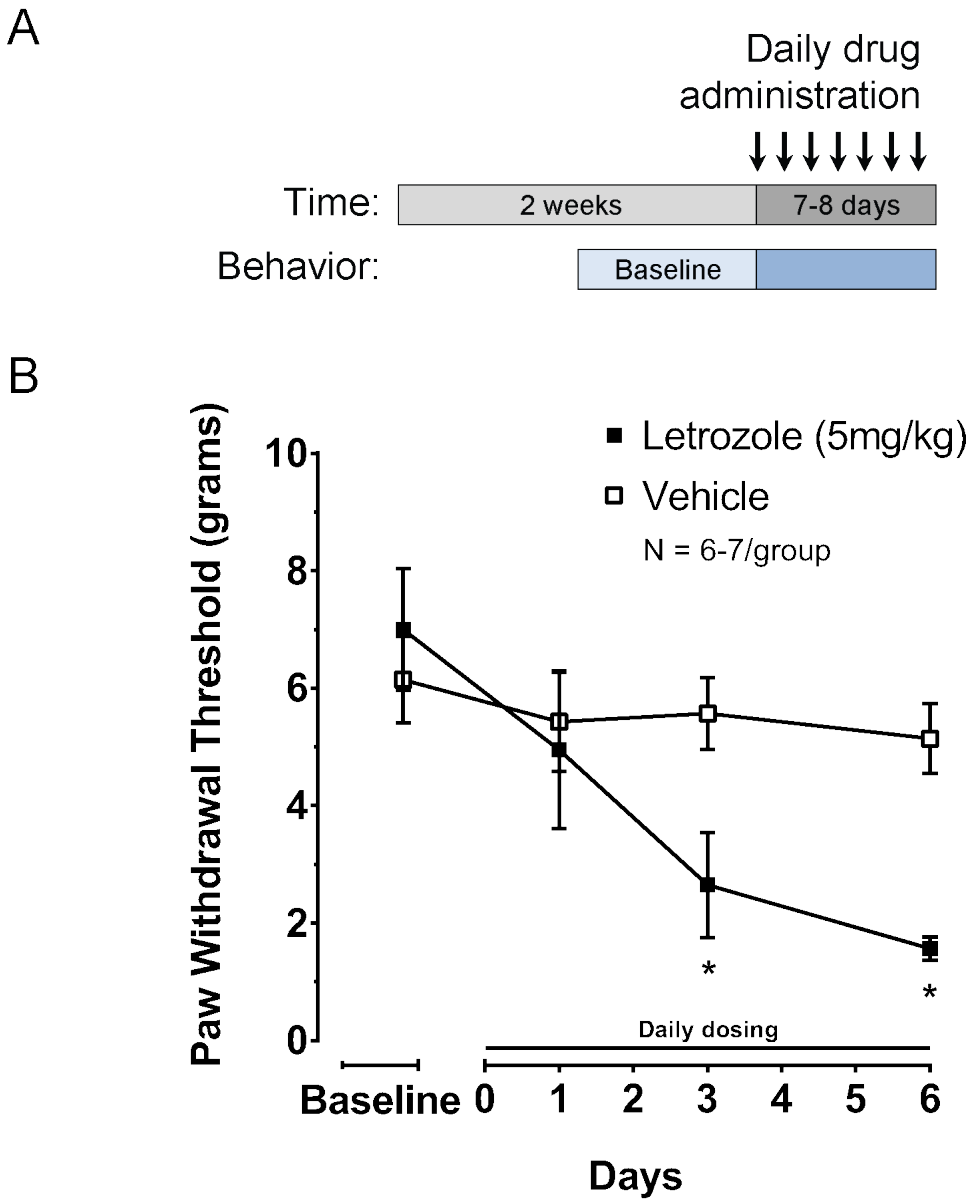

Figure 25. Daily dosing of 5 mg/kg letrozole induces mechanical hypersensitivity in male rats.
A: Depiction of the experimental design. **B:** Each point represents the mean ± S.E.M. of paw withdrawal thresholds (PWT) in grams. Letrozole or vehicle was administered daily on days 0 through 6 or 7 (7-8 total doses) during which behavior was measured. An asterisk represents significant differences in PWT between treatment groups ($P < 0.05$; t-test).

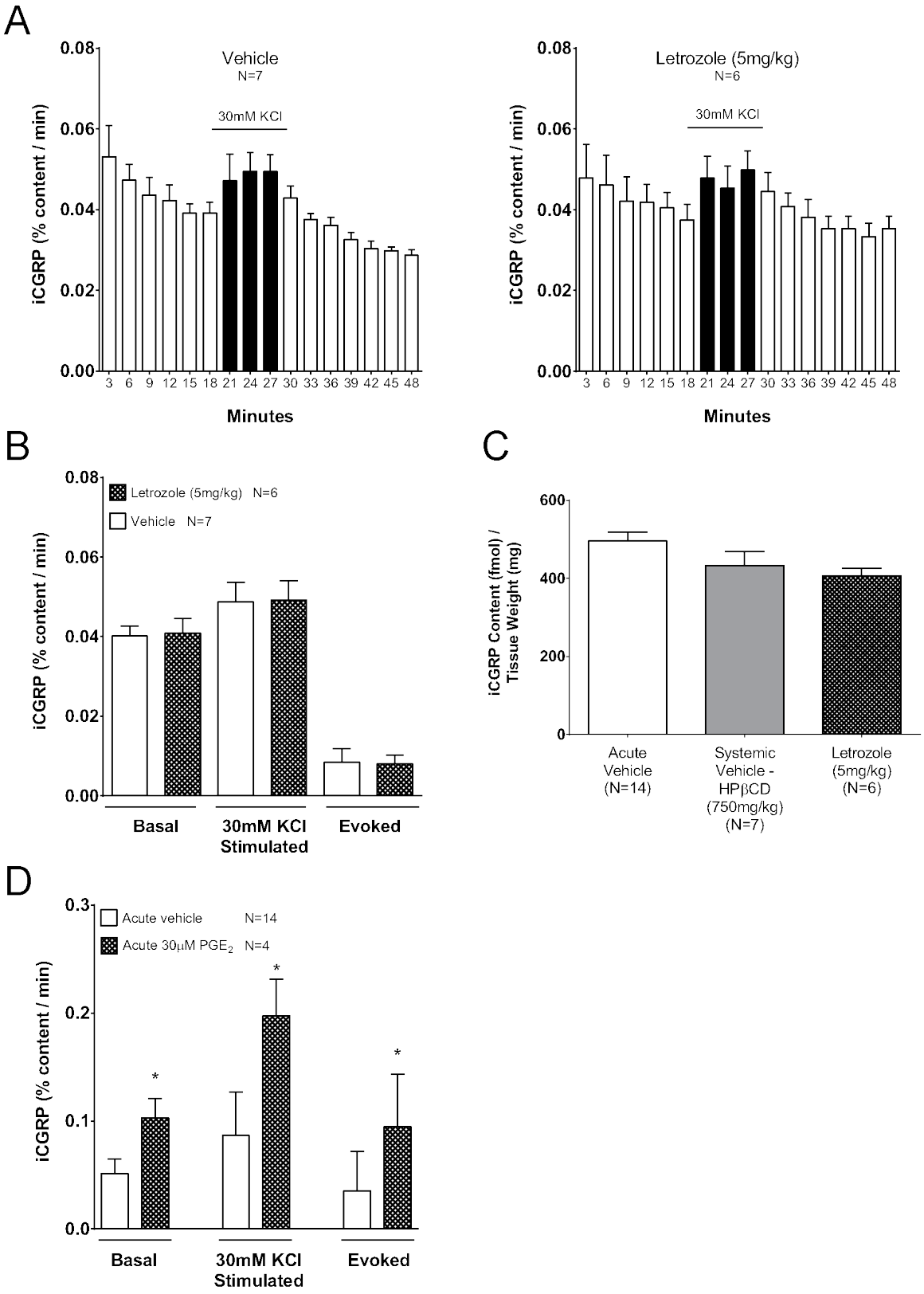
A
Vehicle
N=7
30mM KCl
iCGRP (% content / min)
Minutes
Letrozole (5mg/kg)
N=6
30mM KCl
iCGRP (% content / min)
Minutes
B
Letrozole (5mg/kg) N=6
Vehicle N=7
iCGRP (% content / min)
Basal
30mM KCl Stimulated
Evoked
C
iCGRP Content (fmol) / Tissue Weight (mg)
Acute Vehicle (N=14)
Systemic Vehicle - HPβCD (750mg/kg) (N=7)
Letrozole (5mg/kg) (N=6)
D
Acute vehicle N=14
Acute 30μM PGE2 N=4
iCGRP (% content / min)
Basal
30mM KCl Stimulated
Evoked

Figure 26. Release of iCGRP is not altered in spinal cord slices from male rats with letrozole-induced mechanical hypersensitivity.
A: Basal and potassium-stimulated release of iCGRP was measured from spinal cord slices isolated from rats following treatment with vehicle or 5 mg/kg letrozole for 7-8 days. Open columns represent iCGRP released from spinal cord slices perfused with HEPES buffer alone for successive 3-minute intervals, whereas black columns represent iCGRP released when tissues were perfused with HEPES buffer containing 30 mM potassium. The ordinate represents the mean ± S.E.M. of iCGRP released per minute, expressed as the percent of total iCGRP content in the spinal cord slice. **B:** Summary of mean ± S.E.M. of iCGRP release as percent of total content/min during basal (minutes 9-18) and high potassium stimulation (minutes 18-27) in vehicle or letrozole-treated rats from (A). Evoked release is calculated as stimulated release minus basal release. **C:** iCGRP content of the perfused slices, normalized by tissue wet weight. iCGRP content is sum of peptide released during the release experiment and residual peptide measured at the conclusion of the experiment. **D:** Summary of the mean ± S.E.M. of iCGRP release as percent of total content/min from acutely treated spinal cord slices from naïve male rats. Spinal cord slices from naïve male rats were perfused with HEPES buffer alone for 3 successive 3-minute intervals (minutes 0-9) and then perfused with HEPES buffer containing vehicle or 30 μM PGE_2 for 9 minutes prior to (minutes 9-18; basal) and throughout stimulation with 30 mM KCl (minutes 18-27; stimulated). Evoked release is calculated as stimulated release minus basal release.

DISCUSSION

Conclusions

Much circumstantial evidence suggests that AI-induced arthralgia is linked to the ability of these drugs to reduce estrogen concentrations secondary to blocking aromatase activity (Felson and Cummings, 2005; Henry et al., 2007). This notion is supported by clinical observations that painful musculoskeletal syndromes develop in patients during periods of low or declining systemic estrogens, such as during the transition into menopause (Berecki-Gisolf et al., 2009; Cecil and Archer, 1925; Meriggiola et al., 2012) or following discontinuation of estrogen replacement therapy (Brunner et al., 2010; Ockene et al., 2005). In addition, studies using male and female rats show that estrogen administration produces antinociception in animal models of pain (Kuba et al., 2005; Liu and Gintzler, 2000; Mannino et al., 2007; Tsao et al., 1999), suggesting that reducing systemic estrogens diminishes endogenous pain suppression. Despite the clinical significance of AI-induced arthralgia, few studies have attempted to determine the effects of AIs in animal models of nociception. Consequently, I explored the hypothesis that AIs produce hypersensitivity to potentially noxious stimuli in rats. The behavioral models that I chose to investigate the effect of AIs were among those previously shown to be sensitive to estrogen deprivation. To examine whether the effects of AIs on nociceptive behaviors are mediated by activation or sensitization of sensory neurons, I determined whether letrozole exposure alters release of CGRP from isolated sensory neurons and from sensory nerve endings in spinal cord slices. CGRP release was examined, in part, because previous studies suggest that estrogens regulate CGRP expression in sensory neurons (Gangula et al., 2000).

I first determined the effect of letrozole exposure on nociceptive behaviors using ovariectomized (OVX) rats, since these rats exhibit many hormonal and physiological alterations consistent with those that occur during menopausal transition in women (Hoegh-Andersen et al., 2004; Kalu, 1991; Kobayashi et al., 2000). In OVX rats, sensitivity to mechanical stimulation of hind paws was significantly augmented by administration of a single dose of 1 or 5 mg/kg letrozole and this effect was maintained during thirty subsequent days of behavioral evaluation. In contrast, letrozole treated rats did not have altered nocifensive responses to noxious thermal stimulation, suggesting that the mechanism by which letrozole augments the nociceptive behavior is limited to mechanically sensitive neuronal pathways. I also observed that the PWTs in control OVX rats were significantly reduced from baseline throughout the testing period, a finding that is consistent with previous studies using OVX animals to examine mechanical hypernociception secondary to loss of ovarian-derived estrogens (Dina et al., 2001; Ma et al., 2011; Sanoja and Cervero, 2005). Similar to the differential effect of AI treatment on hypernociception, responses to noxious thermal stimulation did not change over the month of evaluating vehicle-treated OVX rats. Given the impact of OVX on basal nociception and its potential to complicate the interpretation of experiments involving drug administration after OVX, I evaluated the effect of systemic AI administration in male rats, an alternative rat model with very low circulating estrogens.

Similar to OVX rats, male rats treated with letrozole daily for 15 days showed a significant reduction in the paw withdrawal threshold to mechanical stimuli without any change in withdrawal latency to thermal stimuli. Unlike OVX rats, when letrozole injections were stopped in males, mechanical hypersensitivity was reversed within seven days. Of interest, the onset of the mechanical sensitivity was similar in male and OVX rats despite differences in the amount of cumulative drug administered.

Differences in the duration of letrozole-induced mechanical hypersensitivity between the sexes may, in part, be a consequence of pharmacokinetic differences between the sexes. The sparse pharmacokinetic measurements of letrozole in serum, brain, and DRGs performed in this study are consistent with the long elimination half-life of cyclodextrin-complexed letrozole in female rats (Wempe et al., 2007). Median letrozole concentrations measured in whole-brain homogenates four days after a single dose of 1 mg/kg in OVX rats were over 20,000-fold higher than the reported IC50 for aromatase inhibition in cell lines (413 pg/mg in brain versus an IC50 of 70 pM) (Bhatnagar et al., 2001). Assuming a conservative elimination half-life of 40 hours and first-order elimination kinetics from brain tissue, letrozole concentrations lower than 70 pM and increasing aromatase activity in peripheral tissues would hypothetically be achieved at 15 half-lives, or 25 days, following a single dose of 1 mg/kg in OVX rats. A detailed description of tissue drug exposure in OVX and male rats, and preferentially, aromatase activity measurements, are needed to verify these approximations. Additionally, different mechanisms mediating hypersensitivity in the different sexes may contribute to sex differences in drug-induced hypersensitivity. For example, inhibiting aromatase eliminates one metabolic pathway of androgen metabolism, and therefore AI treatment could alter concentrations or dynamics of other tissue steroids that might contribute to hypersensitivity. Indeed, AIs are known to increase blood concentrations of the aromatase substrate testosterone in men (Burnett-Bowie et al., 2009; Mauras et al., 2000), but have a small or no effect in women (Gallicchio et al., 2011; Ingle et al., 2010a; Rossi et al., 2009). Understanding changes in sex steroid *precursors* and their impact on nociception may be important to understanding AI-induced hypersensitivity.

Experimentally induced joint inflammation or trauma in animals is consistently associated with the development of mechanical hypersensitivity (Malfait et al., 2013).

Arthritic rats and mice display reduced thresholds for hind limb withdrawal reflexes evoked by compression of the knee, however, mechanical sensitivity in these models is more commonly measured by changes in the reflexive response to application of von Frey hairs to the dorsal surface of the hind paw (Neugebauer et al., 2007). Since the experimental lesions are typically induced in the knee joint and von Frey sensitivity is measured at the paw, mechanical sensitivity in these models is thought to reflect referred pain or secondary allodynia. While this logic applies to experimental models where the involved joint has been specifically manipulated by the experimenter and joint pathology can be shown to be limited to that joint, in the case of AI-induced hypersensitivity, potential pathological changes in joints have not yet been characterized. Given that the clinical manifestations of the toxicity significantly impact the joints, we may speculate that a component of AI-induced hypersensitivity observed in rats reflects secondary hyperalgesia. Investigating histopathological changes of the joints and muscles of AI-treated rats may lend support to this hypothesis. Interestingly, hypersensitivity to noxious thermal temperatures in the hind paw are often detected in models associated with involvement of inflammatory mediators, such as carrageenan-induced arthritis and collagen-induced arthritis (Inglis et al., 2007; Malfait et al., 2013; Zhang et al., 2001), but not in models of surgically-induced joint instability (Malfait et al., 2013). Here I report that OVX and male rats treated with letrozole do not develop thermal hypernociception. If distinct hypernociceptive behaviors are associated with different types of musculoskeletal lesions, they may share common pathological features. Therefore, future mechanistic studies of AI-induced mechanical hypersensitivity may utilize prior information on molecular and neuronal pathways known to be engaged in mediating other types of musculoskeletal pain that are not associated with changes in cutaneous thermal sensation.

Activation of G-protein-coupled P2Y and ionotropic P2X nucleotide receptors contributes to inflammatory and neuropathic pain behaviors in rodents and may be an important mediator of enhanced mechanosensory transduction in these models (Chen et al., 2005; Cockayne et al., 2000; McGaraughty et al., 2003; Souslova et al., 2000; Tsuda et al., 1999). Pharmacological activation of purinergic receptors by ATP or α,β-meATP in the dermis rapidly induces nocifensive behavioral responses and reduces hind paw withdrawal thresholds to von Frey hair stimulation, which is also induced by intrathecal administration of either agent (Nakagawa et al., 2007; Okada et al., 2002; Tsuda et al., 2000). Consistent with previous reports, I observed augmented responses to intraplantar ATP injections in OVX rats when compared to intact females (Ma et al., 2011). This differential effect of ATP in OVX rats is partially attributed to loss of an inhibitory effect of estrogens, as systemic estradiol treatment partially attenuates overt nociceptive behaviors in OVX rats induced by ATP (Ma et al., 2011). Estradiol similarly attenuates overt nociception induced by the P2X-selective agonist, α,β-me-ATP, when the compounds are co-administered in the paw (Lu et al., 2013). Conversely, intraplantar administration of estradiol prior to bradykinin injections has also been shown to enhance bradykinin-induced thermal sensitivity in OVX rats (Rowan et al., 2010). Intraplantar co-injection of estradiol with capsaicin potentiates capsaicin-induced nocifensive response in male rats (Lu et al., 2009). These experiments do not indicate whether estradiol modulates algogen actions at the level of the nociceptive fiber, but do suggest that manipulation of sex steroid concentrations in specific anatomical and temporal contexts can dramatically influence the activation of nociceptive sensory neurons. Experiments presented in this thesis demonstrate that treating male rats systemically with letrozole and exemestane augments overt nociceptive responses to intraplantar injection of ATP. These data raise the possibility that AIs potentiate nociceptive behavior evoked by ATP exposure in the paw by altering physiologic hormone concentrations, either in the paw,

or in other cells responsible for the integrated behavioral response to ATP. My findings are consistent with prior studies showing pharmacologic inhibition of aromatase in rats and genetic ablation of *CYP19* in aromatase knockout mice enhances formalin-induced nocifensive behavior. In naïve and OVX female rats, subcutaneous letrozole dosing (5 mg/kg) enhanced scored phase II behavior to low concentrations, but not high concentrations of formalin injected in the hindpaw (Moradi-Azani et al., 2011). Similarly, aromatase knockout mice displayed increased grooming during interphase and phase II following formalin injections in the lip (Multon et al., 2005). Purinergic signaling is implicated in the behavioral response to formalin as $P2X_2$ and $P2X_3$ knockout mice and P2X receptor antagonists reduce phases I and II of formalin-induced flinching behavior (Cockayne et al., 2000; McGaraughty et al., 2003; Souslova et al., 2000). It is possible that the ability of AIs to augment nociceptive response to formalin is mechanistically related to enhanced response to the inflammatory mediator ATP.

In studies by Ma et al., mechanical hypernociception in OVX rats was reversed by intraplantar injection of the purinoreceptor antagonists 2′,3′-O-(2,4,6-trinitrophenyl) adenosine-5′-triphosphate (TNP-ATP) and A-317491, implicating P2X receptor activation in the maintenance of mechanical hypersensitivity following ovariectomy (Ma et al., 2011). Given that activation of P2X receptors by α,β-me-ATP in the dermis or in the spinal cord induces tactile hypersensitivity (Tsuda et al., 2000) and that inhibition of P2X receptors attenuates tactile allodynia following spinal cord injury and inflammation (Chadwick et al., 2004), the data in OVX rats suggests that estrogens may suppress mechanoreceptor activation by purines subsequent to purine release by the mechanical stimulation. Physical or mechanical forces acting at the membrane, such as stretch or distention, pressure, and deformation are known to be potent stimuli for ATP release from many cell types, including epithelial cells and neurons (Jo and Schlichter, 1999;

Knight et al., 2002; Patel et al., 2005; Wang et al., 2005; Xia et al., 2012). If hypernociceptive behaviors induced by AI described here are mechanistically related, a component of mechanosensitivity of the hindpaws during AI administration may be mediated by enhanced ATP release or enhanced purinergic receptor activation by endogenous purines secondary to mechanical stimulation. Additional experiments are needed to determine whether mechanical hypersensitivity in letrozole-treated rats is a result of enhanced purinergic receptor activation, either centrally or peripherally.

In the current work, I show that AIs alter nociceptive responses in both OVX and male rats. If these effects are mediated by altered endocrine actions of circulating estrogens, they result from a reduction in the already very low blood estrogen concentrations in both animal models. Alternatively, the AI effects may be a consequence of inhibiting the production of estrogens in tissues that disrupts their paracrine actions. For example, although blood estrogen concentrations in ovariectomized rodents are reduced to concentrations observed in males (i.e., near or below sensitivity for analytical detection), (Davidge et al., 2001; Farrell et al., 1988; Zhao et al., 2004) aromatase expression and activity in extra-gonadal tissues persists following OVX (Zhao et al., 2004). In cells of the vertebrate nervous system, *de novo* synthesis of estrogens also occurs due to aromatase expression (Naftolin et al., 1996). In aromatase expressing brain regions, low levels of constitutive basal activity contribute to steady-state estrogen exposure. Additionally, aromatase activity and estradiol content have been shown to fluctuate in response to physiologic or experimentally induced changes in neuronal activity, such as song-driven neuronal responses in the zebra finch brain (Remage-Healey et al., 2009). Activity-dependent aromatase activity may contribute to the variability in estradiol concentrations in the rat brain regions expressing aromatase, which by definition, are not strongly correlated with blood estradiol

concentrations (Konkle and McCarthy, 2011b). Therefore, estrogen-dependent signaling processes activated in aromatase-expressing tissues in the nervous system are expected to be asynchronous with those mediated by ′endocrine′ sources of estrogens from blood. If side effects of AI therapies are secondary to aromatase inhibition, neuronal processes modulated by local aromatase activity are likely to be significantly altered during AI administration.

In the peripheral nervous system, aromatase immunoreactivity and synthesis of ^{3}H-estradiol from the steroid precursor ^{3}H-pregnenolone was shown in lumbosacral DRGs from rats (Schaeffer et al., 2010). Results presented in this thesis support the expression of mRNA encoding *CYP19A1* and translation of these transcripts. However, given the high C_T values obtained for *CYP19A1* mRNA in total RNA isolated from DRGs and DRG cultures, *CYP19A1* transcripts can be described as low abundance under physiological conditions. Despite their low abundance, aromatase immunoreactive bands corresponding to the predicted molecular weight of the aromatase enzyme, were detected in DRG lysates from both OVX female and male rats. Aromatase immunoreactive bands were also detected in DRG cultures after 24 hours, and up to 12 days in culture, suggesting that factors contributing to basal expression of the enzyme were maintained in cultures. In DRGs and in DRG cultures, aromatase expression coincides with expression of classical nuclear estrogen receptors, ERα and ERβ, and of GPR30 (Papka and Storey-Workley, 2002; Takanami et al., 2010; Taleghany et al., 1999; Vanderhorst et al., 2005). The expression of aromatase and estrogen receptors in DRGs and the spinal cord raises the interesting possibility that aromatase activity in pain-transduction pathways may modulate the processing of afferent sensory information via autocrine or paracrine signaling. Consequently, I first examined whether letrozole could augment the release of the peptide neurotransmitter CGRP from sensory

neurons. The use of sensory neuron cultures for these experiments controls for circulating sources of endogenous sex steroids and minimizes the contribution of inflammatory mediators and other factors that may be altered following administration of AIs to animals. The rationale for examining CGRP release was as follows. 1) CGRP is synthesized and released from a number of nociceptive sensory neurons including mechanosensitive C-fibers (Dubin and Patapoutian, 2010; Lawson et al., 2002; Lawson et al., 1997). 2) Sensory fibers that discharge in response to nonnoxious and noxious movements of the knee joint and also express CGRP are particularly abundant in joints, where about one-third of articular afferents contain CGRP (Hukkanen et al., 1991; Konttinen et al., 1990; Schaible et al., 1986). 3) Release of this peptide in the periphery augments inflammation (Brain and Williams, 1985; Richardson and Vasko, 2002) and CGRP release is enhanced in experimental models of joint inflammation (Fehrenbacher et al., 2003; Ogbonna et al., 2013). 4) Lastly, ERα is co-expressed with CGRP in sensory neurons and estradiol increases CGRP mRNA and CGRP content in a concentration and time-dependent manner (Gangula et al., 2000; Mowa et al., 2003b).

Contrary to my hypothesis, I did not observe any alterations in basal, capsaicin-evoked or high extracellular potassium-evoked iCGRP release in sensory neuronal cultures after acute exposure to letrozole or after chronic treatment with the AI. These results were not impacted by removing media components with known (phenol red) and potentially (serum) estrogenic properties that could have interfered with the ability to detect the effects of estrogen depletion by letrozole. Additionally, there were no sex-dependent effects of letrozole exposure on iCGRP release in sensory neuron cultures as the drug did not significantly alter iCGRP release in cultures derived from OVX female rats or male rats. On the other hand, capsaicin-stimulated release of iCGRP was significantly greater in sensory neuron cultures from OVX rats, when compared to

cultures from intact female or male rats. These data suggest that ovariectomy results in a significant change in the mechanism of nociceptor excitation or neurotransmitter release due to capsaicin stimulation. The effect of OVX to enhance capsaicin sensitivity in 12-day old neuronal cultures suggests a permanent change that is independent of sustained blood steroid or inflammatory changes that follow ovariectomy *in vivo*.

Given the effect of systemically administered AIs to augment ATP-induced nociception *in vivo*, I tested whether the effect of purines on sensory neurons in culture might also be altered by letrozole exposure. Preliminary experiments to determine whether the nonselective (ATP) or $P2X_3$-selective (α,β-meATP) purinergic receptor agonists stimulate or sensitize iCGRP release, showed that the ability of these agents to alter iCGRP release was dependent on the agonist and on the type of excitation. Although exposing isolated sensory neurons to ATP significantly increased capsaicin-evoked release of iCGRP in the cultures, exposure to ATP did not alter iCGRP release stimulated by high extracellular potassium. Furthermore, α,β-meATP had no direct effect on iCGRP release and did not sensitize the nociceptors. These results are consistent with the ability of ATP and UTP to sensitize CGRP release through $P2Y_2$ receptor activation in sensory neuron cultures from embryonic DRGs (Huang et al., 2003). $P2X_3$ receptors, the primary P2X receptor expressed in small-diameter capsaicin-sensitive neurons, are known to rapidly desensitize (<100 ms) following activation by ATP or α,β-meATP and slowly recover activity (> 20 min) (Lewis et al., 1995; Ueno et al., 1999). Although activation of $P2X_3$ receptors by α,β-meATP can induce short bursts of action potentials in nociceptors, the inactivation kinetics may limit the ability of this activation to stimulate or sensitize the release of neuropeptides. Further specificity for the contribution of $P2Y_2$ to sensitization of CGRP release is supported by reduced cation conductance through α,β-meATP-activated P2X channels following activation of $P2Y_2$ receptors with

UTP (Mo et al., 2013). Exposing sensory neurons to letrozole acutely or for three days prior to the release experiment did not alter basal release of iCGRP or the sensitizing actions of ATP on capsaicin-stimulated release.

While previous studies have provided strong evidence for the regulation of CGRP expression by exogenous estrogens, I observed no change in total content of iCGRP in neuronal cultures exposed to letrozole for up to five days. These results are consistent with the notion that cellular events mediated by local aromatase activity may not resemble those mediated by exogenous estrogens. However, these results may have alternative explanations. First, it is unclear whether the expression of aromatase in DRG cultures indicates constitutive enzymatic activity. If the enzyme is constitutively active, the low expression level of aromatase may not result in significant estrogen concentrations that can be impacted by pharmacologic inhibition. Alternatively, aromatase activity in the CNS has been shown to be manipulated by changes in neuronal activity, raising the intriguing possibility that the enzymatic activity is dynamically regulated in DRGs or DRG cultures. Thus, effects of AI treatments may only be observed under conditions associated with high enzymatic activity. My experiments showed aromatase immunoreactive bands corresponding to two distinct molecular weights, with higher molecular weight bands in sensory neuron cultures. Bands corresponding to these molecular weights were also found in ovary lysates from two different rats. The observations are consistent with the observation of two aromatase isoforms in human placental microsomes with approximate molecular weights of 50 to 51 and 55 kDa and may reflect differential phosphorylation or glycosylation of the enzyme (Balthazart et al., 2001; Balthazart et al., 2003b; Harada, 1988; Mendelson et al., 1985; Miller et al., 2008; Sethumadhavan et al., 1991). In addition, these isoforms may correspond to different enzymatic activities as post-translational modifications that have

been demonstrated to modulate aromatase activity in the CNS (Balthazart et al., 2001; Balthazart et al., 2003b; Miller et al., 2008; Sethumadhavan et al., 1991). Secondly, a sufficient spatial relationship between aromatase and estrogen receptors may need to be maintained within or between cells for aromatase activity to initiate estrogen-mediated signaling events. Although neurons in culture grow neurites in the presence of NGF, generating a complex network of inter-connected neurites that resembles an interlaced mat, anatomical relationships between cells that may allow aromatase-mediated signaling events may not be recapitulated in the cultures. Finally, cells were grown in horse serum that may contain sufficient quantities of estrogens to effectively nullify any effect of reduced estrogen synthesis by aromatase inhibition. Experiments to evaluate the long-term effects of letrozole exposure on iCGRP release in serum-free conditions were not feasible due to the rapid loss of iCGRP content from cultures when serum was removed.

To further evaluate the effect of AIs on sensory neurons, I examined whether chronic administration of letrozole, which produced mechanical hypersensitivity in the rat, would alter release of CGRP in spinal cord slices taken from these animals. Basal iCGRP release from spinal cord tissue of letrozole-treated rats was not different than vehicle-treated controls, suggesting that letrozole treatment does not result in activation of CGRP expressing nociceptors. Additionally, potassium-stimulated iCGRP release was not altered in rats treated with letrozole, suggesting aromatase inhibition does not sensitize CGRP-expressing sensory neurons to a depolarizing stimulus. Finally, total content of iCGRP was not altered in letrozole-treated rats compared to controls, suggesting that CGRP content in pre-synaptic terminals of primary afferents is not strongly influenced by AIs or aromatase inhibition *in vivo*.

Taken together, my results do not support the altered release of this neuropeptide into the spinal cord as a mediator of letrozole-induced mechanical hypersensitivity, but do not preclude a potential effect on other neurotransmitters or other sensory neuron populations. Indeed, a number of mechanosensitive A and C sensory neurons do not express CGRP (Dubin and Patapoutian, 2010; Lawson et al., 2002) and thus the effects we observe on mechanical nociception could be mediated by these neurons. Further studies seem warranted to examine whether letrozole alters excitability of small, nonpeptideregic C-type sensory neurons or large diameter A-type neurons and/or other neurons in the pain pathway. It also is possible that AI-induced hypernociception occurs by mechanisms other than, or in addition to, alteration in the excitability of sensory neurons.

Future Directions

Based on the results presented in this body of work, consideration should be given to the following experiments:

(1) Determine the effect of systemically administered AIs on nociceptive response to P2X or P2Y-selectve agonists.

Intraplantar administration of α,β-meATP and ATP elicit dose-dependent nociceptive responses in rats. To identify whether the effect of AIs to augment ATP-induced nociception is mediated by activation of ionotropic or metabotropic purinergic receptors, nociceptive responses should be evaluated in AI-treated rats injected with α,β-meATP (activate $P2X_{1/3}$ receptors) versus UTP (activate $P2Y_{2/4}$ receptors).

(2) Determine whether rats treated with AIs display changes in mobility or gait.

One of the symptoms most commonly reported with the therapeutic use of AIs are severe early morning stiffness and hand–wrist pain. Patients with these symptoms have severely limited mobility in the affected part of the hand or wrist (Thorne, 2007). Evaluating the unrestrained mobility or specifically measuring joint motion of AI treated animals may be a useful indication of changes in joint stiffness.

(3) Determine whether the effect of AIs to enhance mechanical sensitivity and augment ATP-induced nociception is secondary to aromatase inhibition.

The precipitating mechanism underlying AI-induced toxicities has been largely assumed to be due to a reduction in estrogens during AI therapy. However, definitive studies to address this fundamental premise are lacking and the possibility that additional pharmacologic effects of AIs may contribute to their toxicity (or efficacy) has not been given sufficient consideration. The identification of alternative pharmacologic targets of AIs could provide new therapeutic approaches to alleviate AI-induced pain or provide targets for rational development of new analgesics or agents to prevent the onset of this toxicity. In the current work, I demonstrated that rats systemically administered two AIs, letrozole and exemestane, displayed augmented nociceptive responses to intraplantar ATP injections. AI doses for these studies were chosen to achieve maximal systemic aromatase inhibition, based on previously published dose-response studies. Differences in the molecular structures and the mechanisms by which these drugs inhibit aromatase, reduces the probability that engagement of an additional, and yet common, pharmacologic target underlies the observed effects on nociceptive behaviors. Yet these observations do not exclude the possibility that AIs produce hypersensitivity by engaging pharmacological targets other than, or in addition to, aromatase. Therfore, studies aimed to determine the potential contribution of additional

pharmacologic effects of AIs should be considered as part of future experiments. To address this question, the effect of AI administration on nociceptive responses to mechanical stimulation and intraplantar ATP should be determined in *CYP19* knockout mice (Fisher et al., 1998; Honda et al., 1998). Furthermore, sensory neuron cultures produced from these mice could be used in complementary *in-vitro* experiments aimed at determining the contribution of aromatase to sensitization by ATP and measures of excitability.

(4) Determine whether aromatase expression is confined to neuronal or non-neuronal cells in rat DRGs.

While experiments investigating aromatase in the CNS and PNS have focused on neuronal expression of the enzyme, and early experiments suggest sensory neurons of the DRG express the enzyme, the exact cellular localization of this enzymatic complex within the different cell populations PNS is still uncertain (Schaeffer et al., 2010). These experiments are challenging given the low expression levels of both the mRNA transcripts and protein in the nervous system. One approach would be to utilize the recently described ′aromatase-*IRES-plap-IRES-nuclear lacZ*′ or ′aromatase-IPIN′ mouse model that has a genetically modified aromatase locus, such that all cells expressing this enzyme coexpress two reporters: nuclear targeted LacZ and placental alkaline phosphatase (Wu et al., 2009). This mouse model has been used to describe the expression pattern of aromatase in the mouse brain and may be useful for further investigations in the PNS. Understanding whether aromatase is expressed in glia and its expression pattern in neurons relative to known morphological (e.g. small, medium, large diameter) or molecular (e.g. TRPV1 positive) may direct future functional studies.

(5) Determine the enzymatic activity of aromatase in excised DRGs and sensory neuron cultures, and additionally, whether its activity is altered by depolarizing stimuli.

The ability of depolarizing stimuli to alter aromatase activity has been demonstrated in three separate model systems and preparations: quail hypothalamus (Balthazart et al., 2003a), rat hippocampus (Hojo et al., 2004), and zebra finch cortex (Remage-Healey et al., 2011; Remage-Healey et al., 2008). Understanding the potential dynamic control of estrogen synthesis under excitatory conditions in DRG neurons will guide future investigations into the role of aromatase in sensory neurons and the potential impact of aromatase inhibitors. Since several inflammatory molecules relevant to studies of pain are known to regulate *CYP19A1* transcription in other tissues (e.g. PGE_2), these studies could be coupled with induction or suppression of aromatase activity by activating various second messenger cascades (Bulun et al., 2005).

(6) Determine whether sensory neurons exposed to AIs have altered release of neurotransmitters other than CGRP and whether they alter the excitability of sensory neurons.

While experiments in this report focused on CGRP release as an endpoint to measure sensitization, further insight into the potential effects of AIs may be gained by investigating the release of additional neurotransmitters. The amino acid glutamate is the major excitatory neurotransmitter in the mammalian central nervous system and it is likely synthesized released from the majority of DRG neurons (Hoffman et al., 2010). Release of glutamate and neuropeptides are enhanced in the spinal cord in response to peripheral injections of algogens (e.g. capsaicin) or inflammation (Sluka and Willis, 1998; Warsame Afrah et al., 2004). However, glutamate and CGRP release from sensory neurons in culture is known to be differentially influenced by various algogens, such as ATP (Gu and MacDermott, 1997; Khodorova et al., 2009). Thus, additional experiment

are warranted to address whether AIs alter release of additional neurotransmitters, such as glutamate, from sensory neuron in culture.

(7) Determine whether sensory neurons exposed to AIs have altered excitability, as measured by patch-clamp electrophysiology.

Current-clamp electrophysiology is an additional technique that may be used to study the effects of AIs on the excitability of sensory neurons. The ability AIs to alter the excitability of sensory neurons *in vitro* should be examined using current clamp electrophysiology.

Summary

A significant fraction of breast cancer patients treated with AIs develop pain in joints and/or muscles that results in approximately one-fourth of the afflicted patients discontinuing therapy (Henry et al., 2012). Furthermore, AIs are currently being studied in the chemoprevention setting and initial trial results have shown that exemestane lowers the risk of a new breast cancer in postmenopausal women at high risk (Goss et al., 2011). It is expected that AI-induced musculoskeletal pain will also significantly impact patient compliance during AI treatment for breast cancer prevention. Critically, mechanistic insight and guided interventions are needed to alleviate musculoskeletal pain in these patients and allow these patients to persist on AI therapy. Taken together, the experiments conducted in this dissertation have provided new experimental models for AI-induced hypersensitivity that could be beneficial in delineating the mechanism by which AIs augment nociception and developing interventions to prevent or reverse AI-induced musculoskeletal pain. Additionally, these studies do not support a significant role for CGRP expressing small diameter sensory neurons in the pathogenesis of AI-

induced pain. These studies provide a scientific basis to direct future investigations into altered function of additional sensory neuron populations and the biochemical and pharmacologic mechanisms that underlie the effects of estrogens and their modulators on musculoskeletal pain.

REFERENCES

Abu-Taha, M., Rius, C., Hermenegildo, C., Noguera, I., Cerda-Nicolas, J.M., Issekutz, A.C., Jose, P.J., Cortijo, J., Morcillo, E.J., and Sanz, M.J. (2009). Menopause and ovariectomy cause a low grade of systemic inflammation that may be prevented by chronic treatment with low doses of estrogen or losartan. J Immunol *183*, 1393-1402.

Aebi, S., Davidson, T., Gruber, G., Cardoso, F., and Group, E.G.W. (2011). Primary breast cancer: ESMO Clinical Practice Guidelines for diagnosis, treatment and follow-up. Ann Oncol *22 Suppl 6*, vi12-24.

Aletaha, D., Neogi, T., Silman, A.J., Funovits, J., Felson, D.T., Bingham, C.O., 3rd, Birnbaum, N.S., Burmester, G.R., Bykerk, V.P., Cohen, M.D.*, et al.* (2010). 2010 Rheumatoid arthritis classification criteria: an American College of Rheumatology/European League Against Rheumatism collaborative initiative. Arthritis Rheum *62*, 2569-2581.

Altman, R., Alarcon, G., Appelrouth, D., Bloch, D., Borenstein, D., Brandt, K., Brown, C., Cooke, T.D., Daniel, W., Gray, R.*, et al.* (1990). The American College of Rheumatology criteria for the classification and reporting of osteoarthritis of the hand. Arthritis Rheum *33*, 1601-1610.

Amara, S.G., Arriza, J.L., Leff, S.E., Swanson, L.W., Evans, R.M., and Rosenfeld, M.G. (1985). Expression in brain of a messenger RNA encoding a novel neuropeptide homologous to calcitonin gene-related peptide. Science *229*, 1094-1097.

Amara, S.G., Jonas, V., Rosenfeld, M.G., Ong, E.S., and Evans, R.M. (1982). Alternative RNA processing in calcitonin gene expression generates mRNAs encoding different polypeptide products. Nature *298*, 240-244.

Aronica, S.M., Kraus, W.L., and Katzenellenbogen, B.S. (1994). Estrogen action via the cAMP signaling pathway: stimulation of adenylate cyclase and cAMP-regulated gene transcription. Proc Natl Acad Sci U S A *91*, 8517-8521.

Babes, A., Zorzon, D., and Reid, G. (2004). Two populations of cold-sensitive neurons in rat dorsal root ganglia and their modulation by nerve growth factor. Eur J Neurosci *20*, 2276-2282.

Baggett, B., Dorfman, R.I., Engel, L.L., and Savard, K. (1956). The conversion of testosterone-3-C14 to C14-estradiol-17beta by human ovarian tissue. J Biol Chem *221*, 931-941.

Balthazart, J., Baillien, M., and Ball, G.F. (2001). Phosphorylation processes mediate rapid changes of brain aromatase activity. J Steroid Biochem Mol Biol *79*, 261-277.

Balthazart, J., Baillien, M., Charlier, T.D., and Ball, G.F. (2003a). Calcium-dependent phosphorylation processes control brain aromatase in quail. Eur J Neurosci *17*, 1591-1606.

Balthazart, J., Baillien, M., Charlier, T.D., Cornil, C.A., and Ball, G.F. (2003b). Multiple mechanisms control brain aromatase activity at the genomic and non-genomic level. J Steroid Biochem Mol Biol *86*, 367-379.

Banks, P.K., Meyer, K., and Brodie, A.M. (1991). Regulation of ovarian steroid biosynthesis by estrogen during proestrus in the rat. Endocrinology *129*, 1295-1304.

Basbaum, A.I., Bautista, D.M., Scherrer, G., and Julius, D. (2009). Cellular and molecular mechanisms of pain. Cell *139*, 267-284.

Baum, M., Budzar, A.U., Cuzick, J., Forbes, J., Houghton, J.H., Klijn, J.G., Sahmoud, T., and Group, A.T. (2002). Anastrozole alone or in combination with tamoxifen versus tamoxifen alone for adjuvant treatment of postmenopausal women with early breast cancer: first results of the ATAC randomised trial. Lancet *359*, 2131-2139.

Beatson, G.T. (1896). On the Treatment of Inoperable Cases of Carcinoma of the Mamma: Suggestions for a New Method of Treatment, With Illustrative Cases. Lancet *148*, 162-165.

Beis, I., and Newsholme, E.A. (1975). The contents of adenine nucleotides, phosphagens and some glycolytic intermediates in resting muscles from vertebrates and invertebrates. Biochem J *152*, 23-32.

Berecki-Gisolf, J., Begum, N., and Dobson, A.J. (2009). Symptoms reported by women in midlife: menopausal transition or aging? Menopause *16*, 1021-1029.

Bessou, P., and Perl, E.R. (1969). Response of cutaneous sensory units with unmyelinated fibers to noxious stimuli. J Neurophysiol *32*, 1025-1043.

Bhatnagar, A.S., Brodie, A.M., Long, B.J., Evans, D.B., and Miller, W.R. (2001). Intracellular aromatase and its relevance to the pharmacological efficacy of aromatase inhibitors. J Steroid Biochem Mol Biol *76*, 199-202.

Bhatnagar, A.S., Hausler, A., Schieweck, K., Lang, M., and Bowman, R. (1990). Highly selective inhibition of estrogen biosynthesis by CGS 20267, a new non-steroidal aromatase inhibitor. J Steroid Biochem Mol Biol *37*, 1021-1027.

Bland-Ward, P.A., and Humphrey, P.P. (1997). Acute nociception mediated by hindpaw P2X receptor activation in the rat. Br J Pharmacol *122*, 365-371.

Bleehen, T., and Keele, C.A. (1977). Observations on the algogenic actions of adenosine compounds on the human blister base preparation. Pain *3*, 367-377.

Bonneterre, J., Thurlimann, B., Robertson, J.F., Krzakowski, M., Mauriac, L., Koralewski, P., Vergote, I., Webster, A., Steinberg, M., and von Euler, M. (2000). Anastrozole versus tamoxifen as first-line therapy for advanced breast cancer in 668 postmenopausal women: results of the Tamoxifen or Arimidex Randomized Group Efficacy and Tolerability study. J Clin Oncol *18*, 3748-3757.

Bradbury, E.J., Burnstock, G., and McMahon, S.B. (1998). The expression of P2X3 purinoreceptors in sensory neurons: effects of axotomy and glial-derived neurotrophic factor. Mol Cell Neurosci *12*, 256-268.

Brain, S.D., and Williams, T.J. (1985). Inflammatory oedema induced by synergism between calcitonin gene-related peptide (CGRP) and mediators of increased vascular permeability. Br J Pharmacol *86*, 855-860.

Braun, H.J., and Gold, G.E. (2012). Diagnosis of osteoarthritis: imaging. Bone *51*, 278-288.

Briot, K., Tubiana-Hulin, M., Bastit, L., Kloos, I., and Roux, C. (2010). Effect of a switch of aromatase inhibitors on musculoskeletal symptoms in postmenopausal women with hormone-receptor-positive breast cancer: the ATOLL (articular tolerance of letrozole) study. Breast Cancer Res Treat *120*, 127-134.

Brodie, A.M., Schwarzel, W.C., Shaikh, A.A., and Brodie, H.J. (1977). The effect of an aromatase inhibitor, 4-hydroxy-4-androstene-3,17-dione, on estrogen-dependent processes in reproduction and breast cancer. Endocrinology *100*, 1684-1695.

Brooks, S.C., Horn, L., and Horwitz, J.P. (1965). The conjugation of estrogen metabolites by liver slices. Biochim Biophys Acta *104*, 250-260.

Brufsky, A., Harker, W.G., Beck, J.T., Carroll, R., Tan-Chiu, E., Seidler, C., Hohneker, J., Lacerna, L., Petrone, S., and Perez, E.A. (2007). Zoledronic acid inhibits adjuvant letrozole-induced bone loss in postmenopausal women with early breast cancer. J Clin Oncol *25*, 829-836.

Brunner, R.L., Aragaki, A., Barnabei, V., Cochrane, B.B., Gass, M., Hendrix, S., Lane, D., Ockene, J., Woods, N.F., Yasmeen, S.*, et al.* (2010). Menopausal symptom experience before and after stopping estrogen therapy in the Women's Health Initiative randomized, placebo-controlled trial. Menopause *17*, 946-954.

Bullock, C.M., Wookey, P., Bennett, A., Mobasheri, A., Dickerson, I., and Kelly, S. (2014). Increased peripheral calcitonin gene-related peptide receptor signalling drives mechanical sensitization of the joint in rat models of osteoarthritis pain. Arthritis Rheumatol.

Bulun, S.E., Lin, Z., Imir, G., Amin, S., Demura, M., Yilmaz, B., Martin, R., Utsunomiya, H., Thung, S., Gurates, B.*, et al.* (2005). Regulation of aromatase expression in estrogen-responsive breast and uterine disease: from bench to treatment. Pharmacol Rev *57*, 359-383.

Bulun, S.E., Sebastian, S., Takayama, K., Suzuki, T., Sasano, H., and Shozu, M. (2003). The human CYP19 (aromatase P450) gene: update on physiologic roles and genomic organization of promoters. J Steroid Biochem Mol Biol *86*, 219-224.

Burgess, P.R., and Perl, E.R. (1967). Myelinated afferent fibres responding specifically to noxious stimulation of the skin. J Physiol *190*, 541-562.

Burkey, T.H., Hingtgen, C.M., and Vasko, M.R. (2004). Isolation and culture of sensory neurons from the dorsal-root ganglia of embryonic or adult rats. Methods Mol Med *99*, 189-202.

Burnett-Bowie, S.A., McKay, E.A., Lee, H., and Leder, B.Z. (2009). Effects of aromatase inhibition on bone mineral density and bone turnover in older men with low testosterone levels. J Clin Endocrinol Metab *94*, 4785-4792.

Burnstock, G. (2007). Physiology and pathophysiology of purinergic neurotransmission. Physiol Rev *87*, 659-797.

Burstein, H.J., Prestrud, A.A., Seidenfeld, J., Anderson, H., Buchholz, T.A., Davidson, N.E., Gelmon, K.E., Giordano, S.H., Hudis, C.A., Malin, J.*, et al.* (2010). American Society of Clinical Oncology clinical practice guideline: update on adjuvant endocrine therapy for women with hormone receptor-positive breast cancer. J Clin Oncol *28*, 3784-3796.

Burstein, H.J., and Winer, E.P. (2007). Aromatase inhibitors and arthralgias: a new frontier in symptom management for breast cancer survivors. J Clin Oncol *25*, 3797-3799.

Castel, L.D., Hartmann, K.E., Mayer, I.A., Saville, B.R., Alvarez, J., Boomershine, C.S., Abramson, V.G., Chakravarthy, A.B., Friedman, D.L., and Cella, D.F. (2013). Time course of arthralgia among women initiating aromatase inhibitor therapy and a postmenopausal comparison group in a prospective cohort. Cancer *119*, 2375-2382.

Caterina, M.J., Leffler, A., Malmberg, A.B., Martin, W.J., Trafton, J., Petersen-Zeitz, K.R., Koltzenburg, M., Basbaum, A.I., and Julius, D. (2000). Impaired nociception and pain sensation in mice lacking the capsaicin receptor. Science *288*, 306-313.

Caterina, M.J., Rosen, T.A., Tominaga, M., Brake, A.J., and Julius, D. (1999). A capsaicin-receptor homologue with a high threshold for noxious heat. Nature *398*, 436-441.

Ceccarelli, I., Fiorenzani, P., Massafra, C., and Aloisi, A.M. (2003). Long-term ovariectomy changes formalin-induced licking in female rats: the role of estrogens. Reprod Biol Endocrinol *1*, 24.

Cecil, R.L., and Archer, B.H. (1925). Arthritis Of The Menopause. JAMA *84*, 75-79.

Chaban, V.V., Mayer, E.A., Ennes, H.S., and Micevych, P.E. (2003). Estradiol inhibits atp-induced intracellular calcium concentration increase in dorsal root ganglia neurons. Neuroscience *118*, 941-948.

Chaban, V.V., and Micevych, P.E. (2005). Estrogen receptor-alpha mediates estradiol attenuation of ATP-induced Ca2+ signaling in mouse dorsal root ganglion neurons. J Neurosci Res *81*, 31-37.

Chadwick, D., Goode, J., and ebrary Inc. (2004). Pathological pain from molecular to clinical aspects. In Novartis Foundation symposium 261 (Chichester, UK ; Hoboken, NJ, USA: John Wiley), pp. ix, 271 p.

Chakraborty, J., Hopkins, R., and Parke, D.V. (1972). Inhibition studies on the aromatization of androst-4-ene-3,17-dione by human placental microsomal preparations. Biochem J *130*, 19P-20P.

Chaplan, S.R., Bach, F.W., Pogrel, J.W., Chung, J.M., and Yaksh, T.L. (1994). Quantitative assessment of tactile allodynia in the rat paw. J Neurosci Methods *53*, 55-63.

Chen, B.L., Li, Y.Q., Xie, D.H., He, Q.L., and Yang, X.X. (2012). Blocking TNF-alpha with infliximab alleviates ovariectomy induced mechanical and thermal hyperalgesia in rats. Neurol Sci *33*, 527-533.

Chen, J.J., Barber, L.A., Dymshitz, J., and Vasko, M.R. (1996). Peptidase inhibitors improve recovery of substance P and calcitonin gene-related peptide release from rat spinal cord slices. Peptides *17*, 31-37.

Chen, Y., Li, G.W., Wang, C., Gu, Y., and Huang, L.Y. (2005). Mechanisms underlying enhanced P2X receptor-mediated responses in the neuropathic pain state. Pain *119*, 38-48.

Chlebowski, R.T., Cirillo, D.J., Eaton, C.B., Stefanick, M.L., Pettinger, M., Carbone, L.D., Johnson, K.C., Simon, M.S., Woods, N.F., and Wactawski-Wende, J. (2013). Estrogen alone and joint symptoms in the Women's Health Initiative randomized trial. Menopause *20*, 600-608.

Chow, J.D., Simpson, E.R., and Boon, W.C. (2009). Alternative 5'-untranslated first exons of the mouse Cyp19A1 (aromatase) gene. J Steroid Biochem Mol Biol *115*, 115-125.

Cockayne, D.A., Hamilton, S.G., Zhu, Q.M., Dunn, P.M., Zhong, Y., Novakovic, S., Malmberg, A.B., Cain, G., Berson, A., Kassotakis, L.*, et al.* (2000). Urinary bladder hyporeflexia and reduced pain-related behaviour in P2X3-deficient mice. Nature *407*, 1011-1015.

Collo, G., North, R.A., Kawashima, E., Merlo-Pich, E., Neidhart, S., Surprenant, A., and Buell, G. (1996). Cloning OF P2X5 and P2X6 receptors and the distribution and properties of an extended family of ATP-gated ion channels. J Neurosci *16*, 2495-2507.

Cook, S.P., and McCleskey, E.W. (2002). Cell damage excites nociceptors through release of cytosolic ATP. Pain *95*, 41-47.

Coombes, R.C., Hall, E., Gibson, L.J., Paridaens, R., Jassem, J., Delozier, T., Jones, S.E., Alvarez, I., Bertelli, G., Ortmann, O.*, et al.* (2004). A randomized trial of exemestane after two to three years of tamoxifen therapy in postmenopausal women with primary breast cancer. N Engl J Med *350*, 1081-1092.

Coutts, A.A., Jorizzo, J.L., Eady, R.A., Greaves, M.W., and Burnstock, G. (1981). Adenosine triphosphate-evoked vascular changes in human skin: mechanism of action. Eur J Pharmacol *76*, 391-401.

Craft, R.M. (2007). Modulation of pain by estrogens. Pain *132 Suppl 1*, S3-12.

Crew, K.D., Greenlee, H., Capodice, J., Raptis, G., Brafman, L., Fuentes, D., Sierra, A., and Hershman, D.L. (2007). Prevalence of joint symptoms in postmenopausal women taking aromatase inhibitors for early-stage breast cancer. J Clin Oncol *25*, 3877-3883.

Cuzick, J., Sestak, I., Cella, D., and Fallowfield, L. (2008). Treatment-emergent endocrine symptoms and the risk of breast cancer recurrence: a retrospective analysis of the ATAC trial. Lancet Oncol.

Dave, N., Gudelsky, G.A., and Desai, P.B. (2013). The pharmacokinetics of letrozole in brain and brain tumor in rats with orthotopically implanted C6 glioma, assessed using intracerebral microdialysis. Cancer Chemother Pharmacol *72*, 349-357.

Davidge, S.T., Zhang, Y., and Stewart, K.G. (2001). A comparison of ovariectomy models for estrogen studies. Am J Physiol Regul Integr Comp Physiol *280*, R904-907.

Desta, Z., Kreutz, Y., Nguyen, A.T., Li, L., Skaar, T., Kamdem, L.K., Henry, N.L., Hayes, D.F., Storniolo, A.M., Stearns, V.*, et al.* (2011). Plasma letrozole concentrations in postmenopausal women with breast cancer are associated with CYP2A6 genetic variants, body mass index, and age. Clin Pharmacol Ther *90*, 693-700.

Dina, O.A., Aley, K.O., Isenberg, W., Messing, R.O., and Levine, J.D. (2001). Sex hormones regulate the contribution of PKCepsilon and PKA signalling in inflammatory pain in the rat. Eur J Neurosci *13*, 2227-2233.

Diogenes, A., Patwardhan, A.M., Jeske, N.A., Ruparel, N.B., Goffin, V., Akopian, A.N., and Hargreaves, K.M. (2006). Prolactin modulates TRPV1 in female rat trigeminal sensory neurons. J Neurosci *26*, 8126-8136.

Dizdar, O., Ozcakar, L., Malas, F.U., Harputluoglu, H., Bulut, N., Aksoy, S., Ozisik, Y., and Altundag, K. (2009). Sonographic and electrodiagnostic evaluations in patients with aromatase inhibitor-related arthralgia. J Clin Oncol *27*, 4955-4960.

Dombernowsky, P., Smith, I., Falkson, G., Leonard, R., Panasci, L., Bellmunt, J., Bezwoda, W., Gardin, G., Gudgeon, A., Morgan, M.*, et al.* (1998). Letrozole, a new oral aromatase inhibitor for advanced breast cancer: double-blind randomized trial showing a dose effect and improved efficacy and tolerability compared with megestrol acetate. J Clin Oncol *16*, 453-461.

Donnellan, P.P., Douglas, S.L., Cameron, D.A., and Leonard, R.C. (2001). Aromatase inhibitors and arthralgia. J Clin Oncol *19*, 2767.

Donnelly-Roberts, D., McGaraughty, S., Shieh, C.C., Honore, P., and Jarvis, M.F. (2008). Painful purinergic receptors. J Pharmacol Exp Ther *324*, 409-415.

Dowsett, M., Cuzick, J., Ingle, J., Coates, A., Forbes, J., Bliss, J., Buyse, M., Baum, M., Buzdar, A., Colleoni, M.*, et al.* (2010). Meta-analysis of breast cancer outcomes in adjuvant trials of aromatase inhibitors versus tamoxifen. J Clin Oncol *28*, 509-518.

Dubin, A.E., and Patapoutian, A. (2010). Nociceptors: the sensors of the pain pathway. J Clin Invest *120*, 3760-3772.

Dugan, S.A., Powell, L.H., Kravitz, H.M., Everson Rose, S.A., Karavolos, K., and Luborsky, J. (2006). Musculoskeletal pain and menopausal status. Clin J Pain *22*, 325-331.

Dymshitz, J., and Vasko, M.R. (1994). Endothelin-1 enhances capsaicin-induced peptide release and cGMP accumulation in cultures of rat sensory neurons. Neurosci Lett *167*, 128-132.

Erben, R.G., Eberle, J., Stahr, K., and Goldberg, M. (2000). Androgen deficiency induces high turnover osteopenia in aged male rats: a sequential histomorphometric study. J Bone Miner Res *15*, 1085-1098.

Evans, R.J., Lewis, C., Virginio, C., Lundstrom, K., Buell, G., Surprenant, A., and North, R.A. (1996). Ionic permeability of, and divalent cation effects on, two ATP-gated cation channels (P2X receptors) expressed in mammalian cells. J Physiol *497 (Pt 2)*, 413-422.

Evrard, H., Baillien, M., Foidart, A., Absil, P., Harada, N., and Balthazart, J. (2000). Localization and controls of aromatase in the quail spinal cord. J Comp Neurol *423*, 552-564.

Evrard, H.C., and Balthazart, J. (2004a). Aromatization of androgens into estrogens reduces response latency to a noxious thermal stimulus in male quail. Horm Behav *45*, 181-189.

Evrard, H.C., and Balthazart, J. (2004b). Rapid regulation of pain by estrogens synthesized in spinal dorsal horn neurons. J Neurosci *24*, 7225-7229.

Evrard, H.C., Willems, E., Harada, N., and Balthazart, J. (2003). Specific innervation of aromatase neurons by substance P fibers in the dorsal horn of the spinal cord in quail. J Comp Neurol *465*, 309-318.

Farrell, G.C., Koltai, A., and Murray, M. (1988). Source of raised serum estrogens in male rats with portal bypass. J Clin Invest *81*, 221-228.

Fehrenbacher, J.C., Taylor, C.P., and Vasko, M.R. (2003). Pregabalin and gabapentin reduce release of substance P and CGRP from rat spinal tissues only after inflammation or activation of protein kinase C. Pain *105*, 133-141.

Felson, D.T., and Cummings, S.R. (2005). Aromatase inhibitors and the syndrome of arthralgias with estrogen deprivation. Arthritis Rheum *52*, 2594-2598.

Fernihough, J., Gentry, C., Bevan, S., and Winter, J. (2005). Regulation of calcitonin gene-related peptide and TRPV1 in a rat model of osteoarthritis. Neurosci Lett *388*, 75-80.

Filardo, E.J., and Thomas, P. (2005). GPR30: a seven-transmembrane-spanning estrogen receptor that triggers EGF release. Trends Endocrinol Metab *16*, 362-367.

Fillingim, R.B., and Ness, T.J. (2000). Sex-related hormonal influences on pain and analgesic responses. Neurosci Biobehav Rev *24*, 485-501.

Fischer, L., Torres-Chavez, K.E., Clemente-Napimoga, J.T., Jorge, D., Arsati, F., de Arruda Veiga, M.C., and Tambeli, C.H. (2008). The influence of sex and ovarian hormones on temporomandibular joint nociception in rats. J Pain *9*, 630-638.

Fisher, C.R., Graves, K.H., Parlow, A.F., and Simpson, E.R. (1998). Characterization of mice deficient in aromatase (ArKO) because of targeted disruption of the cyp19 gene. Proc Natl Acad Sci U S A *95*, 6965-6970.

Friedman, A.J., Juneau-Norcross, M., and Rein, M.S. (1993). Adverse effects of leuprolide acetate depot treatment. Fertil Steril *59*, 448-450.

Gale, S.K., and Sclafani, A. (1977). Comparison of ovarian and hypothalamic obesity syndromes in the female rat: effects of diet palatability on food intake and body weight. J Comp Physiol Psychol *91*, 381-392.

Gallicchio, L., Macdonald, R., Wood, B., Rushovich, E., and Helzlsouer, K.J. (2011). Androgens and musculoskeletal symptoms among breast cancer patients on aromatase inhibitor therapy. Breast Cancer Res Treat *130*, 569-577.

Gangula, P.R., Lanlua, P., Wimalawansa, S., Supowit, S., DiPette, D., and Yallampalli, C. (2000). Regulation of calcitonin gene-related peptide expression in dorsal root ganglia of rats by female sex steroid hormones. Biol Reprod *62*, 1033-1039.

Garcia-Giralt, N., Rodriguez-Sanz, M., Prieto-Alhambra, D., Servitja, S., Torres-Del Pliego, E., Balcells, S., Albanell, J., Grinberg, D., Diez-Perez, A., Tusquets, I.*, et al.* (2013). Genetic determinants of aromatase inhibitor-related arthralgia: the B-ABLE cohort study. Breast Cancer Res Treat.

Garrison, J.A., McCune, J.S., Livingston, R.B., Linden, H.M., Gralow, J.R., Ellis, G.K., and West, H.L. (2003). Myalgias and arthralgias associated with paclitaxel. Oncology (Williston Park) *17*, 271-277; discussion 281-272, 286-278.

Garry, M.G., and Hargreaves, K.M. (1992). Enhanced release of immunoreactive CGRP and substance P from spinal dorsal horn slices occurs during carrageenan inflammation. Brain Res *582*, 139-142.

Geisler, J., Detre, S., Berntsen, H., Ottestad, L., Lindtjorn, B., Dowsett, M., and Einstein Lonning, P. (2001). Influence of neoadjuvant anastrozole (Arimidex) on intratumoral estrogen levels and proliferation markers in patients with locally advanced breast cancer. Clin Cancer Res *7*, 1230-1236.

Geisler, J., Haynes, B., Anker, G., Dowsett, M., and Lonning, P.E. (2002). Influence of letrozole and anastrozole on total body aromatization and plasma estrogen levels in postmenopausal breast cancer patients evaluated in a randomized, cross-over study. J Clin Oncol *20*, 751-757.

Geisler, J., King, N., Anker, G., Ornati, G., Di Salle, E., Lonning, P.E., and Dowsett, M. (1998). In vivo inhibition of aromatization by exemestane, a novel irreversible aromatase inhibitor, in postmenopausal breast cancer patients. Clin Cancer Res *4*, 2089-2093.

Geisler, J., and Lonning, P.E. (2005a). Aromatase inhibition: translation into a successful therapeutic approach. Clin Cancer Res *11*, 2809-2821.

Geisler, J., and Lonning, P.E. (2005b). Endocrine effects of aromatase inhibitors and inactivators in vivo: review of data and method limitations. J Steroid Biochem Mol Biol *95*, 75-81.

Ghosh, D., Griswold, J., Erman, M., and Pangborn, W. (2009). Structural basis for androgen specificity and oestrogen synthesis in human aromatase. Nature *457*, 219-223.

Giudici, D., Ornati, G., Briatico, G., Buzzetti, F., Lombardi, P., and di Salle, E. (1988). 6-Methylenandrosta-1,4-diene-3,17-dione (FCE 24304): a new irreversible aromatase inhibitor. J Steroid Biochem *30*, 391-394.

Gnant, M., Mlineritsch, B., Schippinger, W., Luschin-Ebengreuth, G., Postlberger, S., Menzel, C., Jakesz, R., Seifert, M., Hubalek, M., Bjelic-Radisic, V.*, et al.* (2009). Endocrine therapy plus zoledronic acid in premenopausal breast cancer. N Engl J Med *360*, 679-691.

Goss, P.E., Ingle, J.N., Ales-Martinez, J.E., Cheung, A.M., Chlebowski, R.T., Wactawski-Wende, J., McTiernan, A., Robbins, J., Johnson, K.C., Martin, L.W.*, et al.* (2011). Exemestane for breast-cancer prevention in postmenopausal women. N Engl J Med *364*, 2381-2391.

Goss, P.E., Ingle, J.N., Pritchard, K.I., Ellis, M.J., Sledge, G.W., Budd, G.T., Rabaglio, M., Ansari, R.H., Johnson, D.B., Tozer, R.*, et al.* (2013). Exemestane versus anastrozole in postmenopausal women with early breast cancer: NCIC CTG MA.27--a randomized controlled phase III trial. J Clin Oncol *31*, 1398-1404.

Goss, P.E., Winer, E.P., Tannock, I.F., and Schwartz, L.H. (1999). Randomized phase III trial comparing the new potent and selective third-generation aromatase inhibitor vorozole with megestrol acetate in postmenopausal advanced breast cancer patients. North American Vorozole Study Group. J Clin Oncol *17*, 52-63.

Grodin, J.M., Siiteri, P.K., and MacDonald, P.C. (1973). Source of estrogen production in postmenopausal women. J Clin Endocrinol Metab *36*, 207-214.

Gu, J.G., and MacDermott, A.B. (1997). Activation of ATP P2X receptors elicits glutamate release from sensory neuron synapses. Nature *389*, 749-753.

Harada, N. (1988). Novel properties of human placental aromatase as cytochrome P-450: purification and characterization of a unique form of aromatase. J Biochem *103*, 106-113.

Hargreaves, K., Dubner, R., Brown, F., Flores, C., and Joris, J. (1988). A new and sensitive method for measuring thermal nociception in cutaneous hyperalgesia. Pain *32*, 77-88.

Hashem, M.G., Cleary, K., Fishman, D., Nichols, L., and Khalid, M. (2013). Effect of concurrent prescription antiarthralgia pharmacotherapy on persistence to aromatase inhibitors in treatment-naive postmenopausal females. Ann Pharmacother *47*, 29-34.

Henry, N.L., Azzouz, F., Desta, Z., Li, L., Nguyen, A.T., Lemler, S., Hayden, J., Tarpinian, K., Yakim, E., Flockhart, D.A.*, et al.* (2012). Predictors of aromatase inhibitor discontinuation as a result of treatment-emergent symptoms in early-stage breast cancer. J Clin Oncol *30*, 936-942.

Henry, N.L., Giles, J.T., Ang, D., Mohan, M., Dadabhoy, D., Robarge, J., Hayden, J., Lemler, S., Shahverdi, K., Powers, P.*, et al.* (2007). Prospective characterization of musculoskeletal symptoms in early stage breast cancer patients treated with aromatase inhibitors. Breast Cancer Res Treat.

Henry, N.L., Giles, J.T., and Stearns, V. (2008). Aromatase inhibitor-associated musculoskeletal symptoms: etiology and strategies for management. Oncology (Williston Park) *22*, 1401-1408; discussion 1416, 1424, 1426.

Henry, N.L., Jacobson, J.A., Banerjee, M., Hayden, J., Smerage, J.B., Van Poznak, C., Storniolo, A.M., Stearns, V., and Hayes, D.F. (2010a). A prospective study of aromatase inhibitor-associated musculoskeletal symptoms and abnormalities on serial high-resolution wrist ultrasonography. Cancer *116*, 4360-4367.

Henry, N.L., Pchejetski, D., A'Hern, R., Nguyen, A.T., Charles, P., Waxman, J., Li, L., Storniolo, A.M., Hayes, D.F., Flockhart, D.A.*, et al.* (2010b). Inflammatory cytokines and aromatase inhibitor-associated musculoskeletal syndrome: a case-control study. Br J Cancer *103*, 291-296.

Henry, N.L., Skaar, T.C., Dantzer, J., Li, L., Kidwell, K., Gersch, C., Nguyen, A.T., Rae, J.M., Desta, Z., Oesterreich, S.*, et al.* (2013). Genetic associations with toxicity-related discontinuation of aromatase inhibitor therapy for breast cancer. Breast Cancer Res Treat *138*, 807-816.

Hingtgen, C.M., and Vasko, M.R. (1994). Prostacyclin enhances the evoked-release of substance P and calcitonin gene-related peptide from rat sensory neurons. Brain Res *655*, 51-60.

Hoegh-Andersen, P., Tanko, L.B., Andersen, T.L., Lundberg, C.V., Mo, J.A., Heegaard, A.M., Delaisse, J.M., and Christgau, S. (2004). Ovariectomized rats as a model of postmenopausal osteoarthritis: validation and application. Arthritis research & therapy *6*, R169-180.

Hoffman, E.M., Schechter, R., and Miller, K.E. (2010). Fixative composition alters distributions of immunoreactivity for glutaminase and two markers of nociceptive neurons, Nav1.8 and TRPV1, in the rat dorsal root ganglion. J Histochem Cytochem *58*, 329-344.

Hojo, Y., Hattori, T.A., Enami, T., Furukawa, A., Suzuki, K., Ishii, H.T., Mukai, H., Morrison, J.H., Janssen, W.G., Kominami, S.*, et al.* (2004). Adult male rat hippocampus synthesizes estradiol from pregnenolone by cytochromes P45017alpha and P450 aromatase localized in neurons. Proc Natl Acad Sci U S A *101*, 865-870.

Holler, M., Grochtmann, W., Napp, M., and Breuer, H. (1977). Studies on the metabolism of oestrone sulphate. Comparative perfusions of oestrone and oestrone sulphate through isolated rat livers. Biochem J *166*, 363-371.

Honda, J., Kanematsu, M., Nakagawa, M., Takahashi, M., Nagao, T., Tangoku, A., and Sasa, M. (2011). Joint symptoms, aromatase inhibitor-related adverse reactions, are indirectly associated with decreased serum estradiol. Int J Surg Oncol *2011*, 951260.

Honda, S., Harada, N., Ito, S., Takagi, Y., and Maeda, S. (1998). Disruption of sexual behavior in male aromatase-deficient mice lacking exons 1 and 2 of the cyp19 gene. Biochem Biophys Res Commun *252*, 445-449.

Huang, H., Wu, X., Nicol, G.D., Meller, S., and Vasko, M.R. (2003). ATP augments peptide release from rat sensory neurons in culture through activation of P2Y receptors. J Pharmacol Exp Ther *306*, 1137-1144.

Hukkanen, M., Gronblad, M., Rees, R., Kottinen, Y.T., Gibson, S.J., Hietanen, J., Polak, J.M., and Brewerton, D.A. (1991). Regional distribution of mast cells and peptide containing nerves in normal and adjuvant arthritic rat synovium. J Rheumatol *18*, 177-183.

Ingle, J.N., Buzdar, A.U., Schaid, D.J., Goetz, M.P., Batzler, A., Robson, M.E., Northfelt, D.W., Olson, J.E., Perez, E.A., Desta, Z*., et al.* (2010a). Variation in anastrozole metabolism and pharmacodynamics in women with early breast cancer. Cancer Res *70*, 3278-3286.

Ingle, J.N., Schaid, D.J., Goss, P.E., Liu, M., Mushiroda, T., Chapman, J.A., Kubo, M., Jenkins, G.D., Batzler, A., Shepherd, L*., et al.* (2010b). Genome-Wide Associations and Functional Genomic Studies of Musculoskeletal Adverse Events in Women Receiving Aromatase Inhibitors. J Clin Oncol.

Inglis, J.J., Notley, C.A., Essex, D., Wilson, A.W., Feldmann, M., Anand, P., and Williams, R. (2007). Collagen-induced arthritis as a model of hyperalgesia: functional and cellular analysis of the analgesic actions of tumor necrosis factor blockade. Arthritis Rheum *56*, 4015-4023.

Islander, U., Jochems, C., Lagerquist, M.K., Forsblad-d'Elia, H., and Carlsten, H. (2011). Estrogens in rheumatoid arthritis; the immune system and bone. Mol Cell Endocrinol *335*, 14-29.

Iveson, T.J., Smith, I.E., Ahern, J., Smithers, D.A., Trunet, P.F., and Dowsett, M. (1993). Phase I study of the oral nonsteroidal aromatase inhibitor CGS 20267 in healthy postmenopausal women. J Clin Endocrinol Metab *77*, 324-331.

Jahr, C.E., and Jessell, T.M. (1983). ATP excites a subpopulation of rat dorsal horn neurones. Nature *304*, 730-733.

Jeftinija, S., Urban, L., and Kojic, L. (1993). The selective activation of dorsal horn neurons by potassium stimulation of high threshold primary afferent neurons in vitro. Neuroscience *56*, 473-484.

Jimenez-Andrade, J.M., Herrera, M.B., Ghilardi, J.R., Vardanyan, M., Melemedjian, O.K., and Mantyh, P.W. (2008). Vascularization of the dorsal root ganglia and peripheral nerve of the mouse: implications for chemical-induced peripheral sensory neuropathies. Mol Pain *4*, 10.

Jo, Y.H., and Schlichter, R. (1999). Synaptic corelease of ATP and GABA in cultured spinal neurons. Nat Neurosci *2*, 241-245.

Kalu, D.N. (1991). The ovariectomized rat model of postmenopausal bone loss. Bone Miner *15*, 175-191.

Kamdem, L.K., Flockhart, D.A., and Desta, Z. (2011). In vitro cytochrome P450-mediated metabolism of exemestane. Drug Metab Dispos *39*, 98-105.

Kanematsu, M., Morimoto, M., Honda, J., Nagao, T., Nakagawa, M., Takahashi, M., Tangoku, A., and Sasa, M. (2011). The time since last menstrual period is important as a clinical predictor for non-steroidal aromatase inhibitor-related arthralgia. BMC Cancer *11*, 436.

Khakh, B.S., Burnstock, G., Kennedy, C., King, B.F., North, R.A., Seguela, P., Voigt, M., and Humphrey, P.P. (2001). International union of pharmacology. XXIV. Current status of the nomenclature and properties of P2X receptors and their subunits. Pharmacol Rev *53*, 107-118.

Khan, Q.J., O'Dea, A.P., and Sharma, P. (2010). Musculoskeletal Adverse Events Associated with Adjuvant Aromatase Inhibitors. J Oncol *2010*.

Khodorova, A., Richter, J., Vasko, M.R., and Strichartz, G. (2009). Early and late contributions of glutamate and CGRP to mechanical sensitization by endothelin-1. J Pain *10*, 740-749.

Kley, H.K., Deselaers, T., Peerenboom, H., and Kruskemper, H.L. (1980). Enhanced conversion of androstenedione to estrogens in obese males. J Clin Endocrinol Metab *51*, 1128-1132.

Knight, G.E., Bodin, P., De Groat, W.C., and Burnstock, G. (2002). ATP is released from guinea pig ureter epithelium on distension. Am J Physiol Renal Physiol *282*, F281-288.

Kobayashi, T., Tamura, M., Hayashi, M., Katsuura, Y., Tanabe, H., Ohta, T., and Komoriya, K. (2000). Elevation of tail skin temperature in ovariectomized rats in relation to menopausal hot flushes. Am J Physiol Regul Integr Comp Physiol *278*, R863-869.

Koltzenburg, M., Stucky, C.L., and Lewin, G.R. (1997). Receptive properties of mouse sensory neurons innervating hairy skin. J Neurophysiol *78*, 1841-1850.

Konkle, A.T., and McCarthy, M.M. (2011a). Developmental time course of estradiol, testosterone, and dihydrotestosterone levels in discrete regions of male and female rat brain. Endocrinology *152*, 223-235.

Konkle, A.T.M., and McCarthy, M.M. (2011b). Developmental Time Course of Estradiol, Testosterone, and Dihydrotestosterone Levels in Discrete Regions of Male and Female Rat Brain. Endocrinology *152*, 223-235.

Konttinen, Y.T., Rees, R., Hukkanen, M., Gronblad, M., Tolvanen, E., Gibson, S.J., Polak, J.M., and Brewerton, D.A. (1990). Nerves in inflammatory synovium: immunohistochemical observations on the adjuvant arthritis rat model. J Rheumatol *17*, 1586-1591.

Kuba, T., Kemen, L.M., and Quinones-Jenab, V. (2005). Estradiol administration mediates the inflammatory response to formalin in female rats. Brain Res *1047*, 119-122.

Kuba, T., Wu, H.B., Nazarian, A., Festa, E.D., Barr, G.A., Jenab, S., Inturrisi, C.E., and Quinones-Jenab, V. (2006). Estradiol and progesterone differentially regulate formalin-induced nociception in ovariectomized female rats. Horm Behav *49*, 441-449.

Kumazawa, T. (1996). The polymodal receptor: bio-warning and defense system. Prog Brain Res *113*, 3-18.

Kumazawa, T., Kruger, L., and Mizumura, K. (1996). The polymodal receptor : a gateway to pathological pain (Amsterdam ; New York: Elsevier).

Lanyon, P., O'Reilly, S., Jones, A., and Doherty, M. (1998). Radiographic assessment of symptomatic knee osteoarthritis in the community: definitions and normal joint space. Ann Rheum Dis *57*, 595-601.

Larionov, A.A., Berstein, L.M., and Miller, W.R. (2002). Local uptake and synthesis of oestrone in normal and malignant postmenopausal breast tissues. J Steroid Biochem Mol Biol *81*, 57-64.

Laroche, M., Borg, S., Lassoued, S., De Lafontan, B., and Roche, H. (2007). Joint pain with aromatase inhibitors: abnormal frequency of Sjogren's syndrome. J Rheumatol *34*, 2259-2263.

Lawson, S.N., Crepps, B., and Perl, E.R. (2002). Calcitonin gene-related peptide immunoreactivity and afferent receptive properties of dorsal root ganglion neurones in guinea-pigs. J Physiol *540*, 989-1002.

Lawson, S.N., Crepps, B.A., and Perl, E.R. (1997). Relationship of substance P to afferent characteristics of dorsal root ganglion neurones in guinea-pig. J Physiol *505 (Pt 1)*, 177-191.

Lazzeroni, M., and DeCensi, A. (2013). Breast cancer prevention by antihormones and other drugs: where do we stand? Hematol Oncol Clin North Am *27*, 657-672, vii.

Lee, A.J., Kosh, J.W., Conney, A.H., and Zhu, B.T. (2001). Characterization of the NADPH-dependent metabolism of 17beta-estradiol to multiple metabolites by human liver microsomes and selectively expressed human cytochrome P450 3A4 and 3A5. J Pharmacol Exp Ther *298*, 420-432.

Leem, J.W., Willis, W.D., and Chung, J.M. (1993). Cutaneous sensory receptors in the rat foot. J Neurophysiol *69*, 1684-1699.

Leithner, C., Muller, S., Fuchtemeier, M., Lindauer, U., Dirnagl, U., and Royl, G. (2010). Determination of the brain-blood partition coefficient for water in mice using MRI. J Cereb Blood Flow Metab *30*, 1821-1824.

Lewis, C., Neidhart, S., Holy, C., North, R.A., Buell, G., and Surprenant, A. (1995). Coexpression of P2X2 and P2X3 receptor subunits can account for ATP-gated currents in sensory neurons. Nature *377*, 432-435.

Lin, C.Y., Vega, V.B., Thomsen, J.S., Zhang, T., Kong, S.L., Xie, M., Chiu, K.P., Lipovich, L., Barnett, D.H., Stossi, F.*, et al.* (2007). Whole-genome cartography of estrogen receptor alpha binding sites. PLoS Genet *3*, e87.

Lindsay, R.M., Lockett, C., Sternberg, J., and Winter, J. (1989). Neuropeptide expression in cultures of adult sensory neurons: modulation of substance P and calcitonin gene-related peptide levels by nerve growth factor. Neuroscience *33*, 53-65.

Lintermans, A., Laenen, A., Van Calster, B., Van Hoydonck, M., Pans, S., Verhaeghe, J., Westhovens, R., Henry, N.L., Wildiers, H., Paridaens, R.*, et al.* (2012). Prospective study to assess fluid accumulation and tenosynovial changes in the aromatase inhibitor-induced musculoskeletal syndrome: 2-year follow-up data. Ann Oncol.

Lintermans, A., Van Calster, B., Van Hoydonck, M., Pans, S., Verhaeghe, J., Westhovens, R., Henry, N.L., Wildiers, H., Paridaens, R., Dieudonne, A.S.*, et al.* (2011). Aromatase inhibitor-induced loss of grip strength is body mass index dependent: hypothesis-generating findings for its pathogenesis. Ann Oncol *22*, 1763-1769.

Liu, N.J., and Gintzler, A.R. (2000). Prolonged ovarian sex steroid treatment of male rats produces antinociception: identification of sex-based divergent analgesic mechanisms. Pain *85*, 273-281.

Liu, X.D., Xie, L., Zhong, Y., and Li, C.X. (2000). Gender difference in letrozole pharmacokinetics in rats. Acta Pharmacol Sin *21*, 680-684.

Livak, K.J., and Schmittgen, T.D. (2001). Analysis of relative gene expression data using real-time quantitative PCR and the 2(-Delta Delta C(T)) Method. Methods *25*, 402-408.

Longcope, C., Kato, T., and Horton, R. (1969). Conversion of blood androgens to estrogens in normal adult men and women. J Clin Invest *48*, 2191-2201.

Lonning, P.E., Helle, H., Duong, N.K., Ekse, D., Aas, T., and Geisler, J. (2009). Tissue estradiol is selectively elevated in receptor positive breast cancers while tumour estrone is reduced independent of receptor status. J Steroid Biochem Mol Biol *117*, 31-41.

Loprinzi, C.L., Duffy, J., and Ingle, J.N. (1993). Postchemotherapy rheumatism. J Clin Oncol *11*, 768-770.

Loprinzi, C.L., Reeves, B.N., Dakhil, S.R., Sloan, J.A., Wolf, S.L., Burger, K.N., Kamal, A., Le-Lindqwister, N.A., Soori, G.S., Jaslowski, A.J.*, et al.* (2011). Natural history of paclitaxel-associated acute pain syndrome: prospective cohort study NCCTG N08C1. J Clin Oncol *29*, 1472-1478.

Lu, Y., Jiang, Q., Yu, L., Lu, Z.Y., Meng, S.P., Su, D., Burnstock, G., and Ma, B. (2013). 17beta-estradiol rapidly attenuates P2X3 receptor-mediated peripheral pain signal transduction via ERalpha and GPR30. Endocrinology *154*, 2421-2433.

Lu, Y.C., Chen, C.W., Wang, S.Y., and Wu, F.S. (2009). 17Beta-estradiol mediates the sex difference in capsaicin-induced nociception in rats. J Pharmacol Exp Ther *331*, 1104-1110.

Lumpkin, E.A., and Caterina, M.J. (2007). Mechanisms of sensory transduction in the skin. Nature *445*, 858-865.

Lyon, C.J., Law, R.E., and Hsueh, W.A. (2003). Minireview: adiposity, inflammation, and atherogenesis. Endocrinology *144*, 2195-2200.

Ma, B., Yu, L.H., Fan, J., Cong, B., He, P., Ni, X., and Burnstock, G. (2011). Estrogen modulation of peripheral pain signal transduction: involvement of P2X(3) receptors. Purinergic Signal *7*, 73-83.

MacDonald, P.C., Rombaut, R.P., and Siiteri, P.K. (1967). Plasma precursors of estrogen. I. Extent of conversion of plasma delta-4-androstenedione to estrone in normal males and nonpregnant normal, castrate and adrenalectomized females. J Clin Endocrinol Metab *27*, 1103-1111.

MacLusky, N.J., Clark, C.R., Shanabrough, M., and Naftolin, F. (1987). Metabolism and binding of androgens in the spinal cord of the rat. Brain Res *422*, 83-91.

MacLusky, N.J., Walters, M.J., Clark, A.S., and Toran-Allerand, C.D. (1994). Aromatase in the cerebral cortex, hippocampus, and mid-brain: ontogeny and developmental implications. Mol Cell Neurosci *5*, 691-698.

Majithia, V., and Geraci, S.A. (2007). Rheumatoid arthritis: diagnosis and management. Am J Med *120*, 936-939.

Malfait, A.M., Little, C.B., and McDougall, J.J. (2013). A commentary on modelling osteoarthritis pain in small animals. Osteoarthritis Cartilage *21*, 1316-1326.

Mamet, J., Baron, A., Lazdunski, M., and Voilley, N. (2002). Proinflammatory mediators, stimulators of sensory neuron excitability via the expression of acid-sensing ion channels. J Neurosci *22*, 10662-10670.

Mannino, C.A., South, S.M., Quinones-Jenab, V., and Inturrisi, C.E. (2007). Estradiol replacement in ovariectomized rats is antihyperalgesic in the formalin test. J Pain *8*, 334-342.

Mao, J.J., Stricker, C., Bruner, D., Xie, S., Bowman, M.A., Farrar, J.T., Greene, B.T., and DeMichele, A. (2009). Patterns and risk factors associated with aromatase inhibitor-related arthralgia among breast cancer survivors. Cancer *115*, 3631-3639.

Mao, J.J., Su, H.I., Feng, R., Donelson, M.L., Aplenc, R., Rebbeck, T.R., Stanczyk, F.Z., and Demichele, A. (2011). Association of functional polymorphisms in CYP19A1 with aromatase inhibitor associated arthralgia in breast cancer survivors. Breast Cancer Res *13*, R8.

Martens, H.A., Schroder, C.P., van der Eerden, P.J., Willemse, P.H., and Posthumus, M.D. (2007). Severe disabling tendinopathy caused by anastrazole. Rheumatology (Oxford) *46*, 1619-1621.

Mauras, N., O'Brien, K.O., Klein, K.O., and Hayes, V. (2000). Estrogen suppression in males: metabolic effects. J Clin Endocrinol Metab *85*, 2370-2377.

McCarthy, M.M. (2008). Estradiol and the developing brain. Physiol Rev *88*, 91-124.

McCoy, E.S., Taylor-Blake, B., Street, S.E., Pribisko, A.L., Zheng, J., and Zylka, M.J. (2013). Peptidergic CGRPalpha primary sensory neurons encode heat and itch and tonically suppress sensitivity to cold. Neuron *78*, 138-151.

McGaraughty, S., Wismer, C.T., Zhu, C.Z., Mikusa, J., Honore, P., Chu, K.L., Lee, C.H., Faltynek, C.R., and Jarvis, M.F. (2003). Effects of A-317491, a novel and selective P2X3/P2X2/3 receptor antagonist, on neuropathic, inflammatory and chemogenic nociception following intrathecal and intraplantar administration. Br J Pharmacol *140*, 1381-1388.

McGonagle, D., Conaghan, P.G., Wakefield, R., and Emery, P. (2001). Imaging the joints in early rheumatoid arthritis. Best Pract Res Clin Rheumatol *15*, 91-104.

Mendelson, C.R., Wright, E.E., Evans, C.T., Porter, J.C., and Simpson, E.R. (1985). Preparation and characterization of polyclonal and monoclonal antibodies against human aromatase cytochrome P-450 (P-450AROM), and their use in its purification. Arch Biochem Biophys *243*, 480-491.

Meriggiola, M.C., Nanni, M., Bachiocco, V., Vodo, S., and Aloisi, A.M. (2012). Menopause affects pain depending on pain type and characteristics. Menopause *19*, 517-523.

Miller, T.W., Shin, I., Kagawa, N., Evans, D.B., Waterman, M.R., and Arteaga, C.L. (2008). Aromatase is phosphorylated in situ at serine-118. J Steroid Biochem Mol Biol *112*, 95-101.

Mo, G., Peleshok, J.C., Cao, C.Q., Ribeiro-da-Silva, A., and Seguela, P. (2013). Control of P2X3 channel function by metabotropic P2Y2 utp receptors in primary sensory neurons. Mol Pharmacol *83*, 640-647.

Moggs, J.G., and Orphanides, G. (2001). Estrogen receptors: orchestrators of pleiotropic cellular responses. EMBO Rep *2*, 775-781.

Molliver, D.C., Cook, S.P., Carlsten, J.A., Wright, D.E., and McCleskey, E.W. (2002). ATP and UTP excite sensory neurons and induce CREB phosphorylation through the metabotropic receptor, P2Y2. Eur J Neurosci *16*, 1850-1860.

Moradi-Azani, M., Ahmadiani, A., and Amini, H. (2011). Increase in formalin-induced tonic pain by 5alpha-reductase and aromatase inhibition in female rats. Pharmacol Biochem Behav *98*, 62-66.

Morales, L., Pans, S., Paridaens, R., Westhovens, R., Timmerman, D., Verhaeghe, J., Wildiers, H., Leunen, K., Amant, F., Berteloot, P.*, et al.* (2007). Debilitating musculoskeletal pain and stiffness with letrozole and exemestane: associated tenosynovial changes on magnetic resonance imaging. Breast Cancer Res Treat *104*, 87-91.

Morales, L., Pans, S., Verschueren, K., Van Calster, B., Paridaens, R., Westhovens, R., Timmerman, D., De Smet, L., Vergote, I., Christiaens, M.R.*, et al.* (2008). Prospective study to assess short-term intra-articular and tenosynovial changes in the aromatase inhibitor-associated arthralgia syndrome. J Clin Oncol *26*, 3147-3152.

Mowa, C.N., Usip, S., Collins, J., Storey-Workley, M., Hargreaves, K.M., and Papka, R.E. (2003a). The effects of pregnancy and estrogen on the expression of calcitonin gene-related peptide (CGRP) in the uterine cervix, dorsal root ganglia and spinal cord. Peptides *24*, 1163-1174.

Mowa, C.N., Usip, S., Storey-Workley, M., Amann, R., and Papka, R. (2003b). Substance P in the uterine cervix, dorsal root ganglia and spinal cord during pregnancy and the effect of estrogen on SP synthesis. Peptides *24*, 761-771.

Moxley, G. (2010). Rheumatic Disorders and Functional Disability With Aromatase Inhibitor Therapy. Clin Breast Cancer.

Multon, S., Pardutz, A., Mosen, J., Hua, M.T., Defays, C., Honda, S., Harada, N., Bohotin, C., Franzen, R., and Schoenen, J. (2005). Lack of estrogen increases pain in the trigeminal formalin model: a behavioural and immunocytochemical study of transgenic ArKO mice. Pain *114*, 257-265.

Muslimani, A.A., Spiro, T.P., Chaudhry, A.A., Taylor, H.C., Do, I.J., and Daw, H.A. (2009). Aromatase inhibitor-related musculoskeletal symptoms: is preventing osteoporosis the key to eliminating these symptoms? Clinical breast cancer *9*, 34-38.

Nabholtz, J.M., Buzdar, A., Pollak, M., Harwin, W., Burton, G., Mangalik, A., Steinberg, M., Webster, A., and von Euler, M. (2000). Anastrozole is superior to tamoxifen as first-line therapy for advanced breast cancer in postmenopausal women: results of a North American multicenter randomized trial. Arimidex Study Group. J Clin Oncol *18*, 3758-3767.

Naftolin, F., Horvath, T.L., Jakab, R.L., Leranth, C., Harada, N., and Balthazart, J. (1996). Aromatase immunoreactivity in axon terminals of the vertebrate brain. An immunocytochemical study on quail, rat, monkey and human tissues. Neuroendocrinology *63*, 149-155.

Naftolin, F., Ryan, K.J., Davies, I.J., Reddy, V.V., Flores, F., Petro, Z., Kuhn, M., White, R.J., Takaoka, Y., and Wolin, L. (1975). The formation of estrogens by central neuroendocrine tissues. Recent Prog Horm Res *31*, 295-319.

Najafi, S., Djavid, G.E., Mehrdad, N., Rajaii, E., Alavi, N., Olfatbakhsh, A., Najafi, M., Bahrami, A., and Heidari, K. (2011). Taxane-based regimens as a risk factor for chemotherapy-induced amenorrhea. Menopause *18*, 208-212.

Nakagawa, T., Wakamatsu, K., Zhang, N., Maeda, S., Minami, M., Satoh, M., and Kaneko, S. (2007). Intrathecal administration of ATP produces long-lasting allodynia in rats: differential mechanisms in the phase of the induction and maintenance. Neuroscience *147*, 445-455.

Nanayama, T., Kuraishi, Y., Ohno, H., and Satoh, M. (1989). Capsaicin-induced release of calcitonin gene-related peptide from dorsal horn slices is enhanced in adjuvant arthritic rats. Neurosci Res *6*, 569-572.

National Cancer Institute, N.C.I. (1999). Common Toxicity Criteria (CTC), version 2.0, April 30, 1999. Retreived September 1, 2013, from http://ctep.cancer.gov/protocolDevelopment/electronic_applications/docs/ctcv20_4-30-992.pdf.

Neugebauer, V., Han, J.S., Adwanikar, H., Fu, Y., and Ji, G. (2007). Techniques for assessing knee joint pain in arthritis. Mol Pain *3*, 8.

Neugut, A.I., Subar, M., Wilde, E.T., Stratton, S., Brouse, C.H., Hillyer, G.C., Grann, V.R., and Hershman, D.L. (2011). Association between prescription co-payment amount and compliance with adjuvant hormonal therapy in women with early-stage breast cancer. J Clin Oncol *29*, 2534-2542.

North, R.A. (2002). Molecular physiology of P2X receptors. Physiol Rev *82*, 1013-1067.

O'Brien, C., Woolf, C.J., Fitzgerald, M., Lindsay, R.M., and Molander, C. (1989). Differences in the chemical expression of rat primary afferent neurons which innervate skin, muscle or joint. Neuroscience *32*, 493-502.

Ockene, J.K., Barad, D.H., Cochrane, B.B., Larson, J.C., Gass, M., Wassertheil-Smoller, S., Manson, J.E., Barnabei, V.M., Lane, D.S., Brzyski, R.G*., et al.* (2005). Symptom experience after discontinuing use of estrogen plus progestin. JAMA *294*, 183-193.

Ogbonna, A.C., Clark, A.K., Gentry, C., Hobbs, C., and Malcangio, M. (2013). Pain-like behaviour and spinal changes in the monosodium iodoacetate model of osteoarthritis in C57Bl/6 mice. Eur J Pain *17*, 514-526.

Okada, M., Nakagawa, T., Minami, M., and Satoh, M. (2002). Analgesic effects of intrathecal administration of P2Y nucleotide receptor agonists UTP and UDP in normal and neuropathic pain model rats. J Pharmacol Exp Ther *303*, 66-73.

Osawa, Y., Yoshida, N., Fronckowiak, M., and Kitawaki, J. (1987). Immunoaffinity purification of aromatase cytochrome P-450 from human placental microsomes, metabolic switching from aromatization to 1 beta and 2 beta-monohydroxylation, and recognition of aromatase isozymes. Steroids *50*, 11-28.

Papadimitriou, K., Kountourakis, P., Morakis, E., Vassiliou, V., Barbounis, V., and Ardavanis, A. (2012). Bilateral de quervain syndrome after aromatase inhibitor administration: a case report and review of the literature. Case Rep Med *2012*, 810428.

Papka, R.E., and Storey-Workley, M. (2002). Estrogen receptor-alpha and -beta coexist in a subpopulation of sensory neurons of female rat dorsal root ganglia. Neurosci Lett *319*, 71-74.

Partridge, A.H., LaFountain, A., Mayer, E., Taylor, B.S., Winer, E., and Asnis-Alibozek, A. (2008). Adherence to initial adjuvant anastrozole therapy among women with early-stage breast cancer. J Clin Oncol *26*, 556-562.

Patel, A.S., Reigada, D., Mitchell, C.H., Bates, S.R., Margulies, S.S., and Koval, M. (2005). Paracrine stimulation of surfactant secretion by extracellular ATP in response to mechanical deformation. Am J Physiol Lung Cell Mol Physiol *289*, L489-496.

Peier, A.M., Moqrich, A., Hergarden, A.C., Reeve, A.J., Andersson, D.A., Story, G.M., Earley, T.J., Dragoni, I., McIntyre, P., Bevan, S.*, et al.* (2002). A TRP channel that senses cold stimuli and menthol. Cell *108*, 705-715.

Perl, E.R. (1996a). Cutaneous polymodal receptors: characteristics and plasticity. Prog Brain Res *113*, 21-37.

Perl, E.R. (1996b). Pain and the discovery of nociceptors. In Neurobiology of nociceptors, C. Belmonte, and F. Cervero, eds. (Oxford ; New York: Oxford University Press), pp. x, 531 p., [535] p. of plates.

Peterson, R.S., Yarram, L., Schlinger, B.A., and Saldanha, C.J. (2005). Aromatase is pre-synaptic and sexually dimorphic in the adult zebra finch brain. Proc Biol Sci *272*, 2089-2096.

Pfaff, D.W. (2002). Hormones, brain and behavior (San Diego, Calif.: Academic Press).

Pfister, C.U., Martoni, A., Zamagni, C., Lelli, G., De Braud, F., Souppart, C., Duval, M., and Hornberger, U. (2001). Effect of age and single versus multiple dose pharmacokinetics of letrozole (Femara) in breast cancer patients. Biopharm Drug Dispos *22*, 191-197.

Price, T.J., and Flores, C.M. (2007). Critical evaluation of the colocalization between calcitonin gene-related peptide, substance P, transient receptor potential vanilloid subfamily type 1 immunoreactivities, and isolectin B4 binding in primary afferent neurons of the rat and mouse. J Pain *8*, 263-272.

Raftogianis, R., Creveling, C., Weinshilboum, R., and Weisz, J. (2000). Estrogen metabolism by conjugation. J Natl Cancer Inst Monogr, 113-124.

Reddy, V.V., Rajan, R., and Daly, M.J. (1981). Oestrogen metabolism in adult rat's brain. Acta Endocrinol (Copenh) *96*, 7-14.

Remage-Healey, L., Dong, S., Maidment, N.T., and Schlinger, B.A. (2011). Presynaptic control of rapid estrogen fluctuations in the songbird auditory forebrain. J Neurosci *31*, 10034-10038.

Remage-Healey, L., Maidment, N.T., and Schlinger, B.A. (2008). Forebrain steroid levels fluctuate rapidly during social interactions. Nat Neurosci *11*, 1327-1334.

Remage-Healey, L., Oyama, R.K., and Schlinger, B.A. (2009). Elevated aromatase activity in forebrain synaptic terminals during song. J Neuroendocrinol *21*, 191-199.

Richardson, J.D., and Vasko, M.R. (2002). Cellular mechanisms of neurogenic inflammation. J Pharmacol Exp Ther *302*, 839-845.

Rosenfeld, M.G., Emeson, R.B., Yeakley, J.M., Merillat, N., Hedjran, F., Lenz, J., and Delsert, C. (1992). Calcitonin gene-related peptide: a neuropeptide generated as a consequence of tissue-specific, developmentally regulated alternative RNA processing events. Ann N Y Acad Sci *657*, 1-17.

Rossi, E., Morabito, A., Di Rella, F., Esposito, G., Gravina, A., Labonia, V., Landi, G., Nuzzo, F., Pacilio, C., De Maio, E.*, et al.* (2009). Endocrine effects of adjuvant letrozole compared with tamoxifen in hormone-responsive postmenopausal patients with early breast cancer: the HOBOE trial. J Clin Oncol *27*, 3192-3197.

Rowan, M.P., Berg, K.A., Milam, S.B., Jeske, N.A., Roberts, J.L., Hargreaves, K.M., and Clarke, W.P. (2010). 17beta-estradiol rapidly enhances bradykinin signaling in primary sensory neurons in vitro and in vivo. J Pharmacol Exp Ther *335*, 190-196.

Rowlands, I.W. (1944). The production of ovulation in the immature rat. J Endocrin *3*, 384.

Ryan, K.J. (1959). Biological aromatization of steroids. J Biol Chem *234*, 268-272.

Sanada, M., Yasuda, H., Omatsu-Kanbe, M., Sango, K., Isono, T., Matsuura, H., and Kikkawa, R. (2002). Increase in intracellular Ca(2+) and calcitonin gene-related peptide release through metabotropic P2Y receptors in rat dorsal root ganglion neurons. Neuroscience *111*, 413-422.

Sanoja, R., and Cervero, F. (2005). Estrogen-dependent abdominal hyperalgesia induced by ovariectomy in adult mice: a model of functional abdominal pain. Pain *118*, 243-253.

Sanoja, R., and Cervero, F. (2008). Estrogen modulation of ovariectomy-induced hyperalgesia in adult mice. Eur J Pain *12*, 573-581.

Santen, R.J., Brodie, H., Simpson, E.R., Siiteri, P.K., and Brodie, A. (2009). History of aromatase: saga of an important biological mediator and therapeutic target. Endocr Rev *30*, 343-375.

Santen, R.J., Demers, L., Ohorodnik, S., Settlage, J., Langecker, P., Blanchett, D., Goss, P.E., and Wang, S. (2007). Superiority of gas chromatography/tandem mass spectrometry assay (GC/MS/MS) for estradiol for monitoring of aromatase inhibitor therapy. Steroids *72*, 666-671.

Schaeffer, V., Meyer, L., Patte-Mensah, C., Eckert, A., and Mensah-Nyagan, A.G. (2010). Sciatic nerve injury induces apoptosis of dorsal root ganglion satellite glial cells and selectively modifies neurosteroidogenesis in sensory neurons. Glia *58*, 169-180.

Schaible, H.G., Schmidt, R.F., and Willis, W.D. (1986). Responses of spinal cord neurones to stimulation of articular afferent fibres in the cat. J Physiol *372*, 575-593.

Schieweck, K., Bhatnagar, A.S., Batzl, C., and Lang, M. (1993). Anti-tumor and endocrine effects of non-steroidal aromatase inhibitors on estrogen-dependent rat mammary tumors. J Steroid Biochem Mol Biol *44*, 633-636.

Schindler, A.E., Ebert, A., and Friedrich, E. (1972). Conversion of androstenedione to estrone by human tissue. J Clin Endocrinol Metab *35*, 627-630.

Schlinger, B.A., Amur-Umarjee, S., Shen, P., Campagnoni, A.T., and Arnold, A.P. (1994). Neuronal and non-neuronal aromatase in primary cultures of developing zebra finch telencephalon. J Neurosci *14*, 7541-7552.

Schnitt, S.J. (2006). Estrogen receptor testing of breast cancer in current clinical practice: what's the question? J Clin Oncol *24*, 1797-1799.

Schutz, B., Mauer, D., Salmon, A.M., Changeux, J.P., and Zimmer, A. (2004). Analysis of the cellular expression pattern of beta-CGRP in alpha-CGRP-deficient mice. J Comp Neurol *476*, 32-43.

Schwarzel, W.C., Kruggel, W.G., and Brodie, H.J. (1973). Studies on the mechanism of estrogen biosynthesis. 8. The development of inhibitors of the enzyme system in human placenta. Endocrinology *92*, 866-880.

Sestak, I., Cuzick, J., Sapunar, F., Eastell, R., Forbes, J.F., Bianco, A.R., and Buzdar, A.U. (2008). Risk factors for joint symptoms in patients enrolled in the ATAC trial: a retrospective, exploratory analysis. Lancet Oncol *9*, 866-872.

Sethumadhavan, K., Bellino, F.L., and Thotakura, N.R. (1991). Estrogen synthetase (aromatase). The cytochrome P-450 component of the human placental enzyme is a glycoprotein. Mol Cell Endocrinol *78*, 25-32.

Sherrington, C.S. (1906). The integrative action of the nervous system (New York,: C. Scribner's sons).

Shimizu, Y., Yarborough, C., and Osawa, Y. (1993). Competitive product inhibition of aromatase by natural estrogens. J Steroid Biochem Mol Biol *44*, 651-656.

Shu, X., and Mendell, L.M. (1999). Nerve growth factor acutely sensitizes the response of adult rat sensory neurons to capsaicin. Neurosci Lett *274*, 159-162.

Siiteri, P.K., and MacDonald, P.C. (1966). Placental estrogen biosynthesis during human pregnancy. J Clin Endocrinol Metab *26*, 751-761.

Sioufi, A., Gauducheau, N., Pineau, V., Marfil, F., Jaouen, A., Cardot, J.M., Godbillon, J., Czendlik, C., Howald, H., Pfister, C.*, et al.* (1997). Absolute bioavailability of letrozole in healthy postmenopausal women. Biopharm Drug Dispos *18*, 779-789.

Sluka, K.A., and Willis, W.D. (1998). Increased spinal release of excitatory amino acids following intradermal injection of capsaicin is reduced by a protein kinase G inhibitor. Brain Res *798*, 281-286.

Sodersten, P., Crews, D., Logan, C., and Soukup, R.W. (2014). Eugen Steinach: the first neuroendocrinologist. Endocrinology *155*, 688-695.

Sohrabji, F., Miranda, R.C., and Toran-Allerand, C.D. (1994). Estrogen differentially regulates estrogen and nerve growth factor receptor mRNAs in adult sensory neurons. J Neurosci *14*, 459-471.

Souslova, V., Cesare, P., Ding, Y., Akopian, A.N., Stanfa, L., Suzuki, R., Carpenter, K., Dickenson, A., Boyce, S., Hill, R.*, et al.* (2000). Warm-coding deficits and aberrant inflammatory pain in mice lacking P2X3 receptors. Nature *407*, 1015-1017.

Spitz, A., Young, J.M., Larsen, L., Mattia-Goldberg, C., Donnelly, J., and Chwalisz, K. (2012). Efficacy and safety of leuprolide acetate 6-month depot for suppression of testosterone in patients with prostate cancer. Prostate Cancer Prostatic Dis *15*, 93-99.

Staton, P.C., Wilson, A.W., Bountra, C., Chessell, I.P., and Day, N.C. (2007). Changes in dorsal root ganglion CGRP expression in a chronic inflammatory model of the rat knee joint: differential modulation by rofecoxib and paracetamol. Eur J Pain *11*, 283-289.

Steinach, E., and Kun, H. (1937). Transformation of male sex hormones into a substance with the action of a female hormone. Lancet *230*, 845.

Straub, R.H. (2007). The complex role of estrogens in inflammation. Endocr Rev *28*, 521-574.

Strom, J.O., Theodorsson, A., and Theodorsson, E. (2008a). Substantial discrepancies in 17beta-oestradiol concentrations obtained with three different commercial direct radioimmunoassay kits in rat sera. Scand J Clin Lab Invest *68*, 806-813.

Strom, J.O., Theodorsson, E., and Theodorsson, A. (2008b). Order of magnitude differences between methods for maintaining physiological 17beta-oestradiol concentrations in ovariectomized rats. Scand J Clin Lab Invest *68*, 814-822.

Takanami, K., Sakamoto, H., Matsuda, K., Hosokawa, K., Nishi, M., Prossnitz, E.R., and Kawata, M. (2010). Expression of G protein-coupled receptor 30 in the spinal somatosensory system. Brain Res *1310*, 17-28.

Taleghany, N., Sarajari, S., DonCarlos, L.L., Gollapudi, L., and Oblinger, M.M. (1999). Differential expression of estrogen receptor alpha and beta in rat dorsal root ganglion neurons. J Neurosci Res *57*, 603-615.

Tao, X., Brodie, A.M., and Nnane, I.P. (2006). The effect of tamoxifen on the pharmacokinetics of letrozole in female rats. Biopharm Drug Dispos *27*, 335-344.

Terner, J.M., Lomas, L.M., and Picker, M.J. (2005). Influence of estrous cycle and gonadal hormone depletion on nociception and opioid antinociception in female rats of four strains. J Pain *6*, 372-383.

Thorne, C. (2007). Management of arthralgias associated with aromatase inhibitor therapy. Curr Oncol *14 Suppl 1*, S11-19.

Thurlimann, B., Keshaviah, A., Coates, A.S., Mouridsen, H., Mauriac, L., Forbes, J.F., Paridaens, R., Castiglione-Gertsch, M., Gelber, R.D., Rabaglio, M.*, et al.* (2005). A comparison of letrozole and tamoxifen in postmenopausal women with early breast cancer. N Engl J Med *353*, 2747-2757.

Tjolsen, A., Berge, O.G., Hunskaar, S., Rosland, J.H., and Hole, K. (1992). The formalin test: an evaluation of the method. Pain *51*, 5-17.

Tominaga, M., Caterina, M.J., Malmberg, A.B., Rosen, T.A., Gilbert, H., Skinner, K., Raumann, B.E., Basbaum, A.I., and Julius, D. (1998). The cloned capsaicin receptor integrates multiple pain-producing stimuli. Neuron *21*, 531-543.

Toung, T.J., Traystman, R.J., and Hurn, P.D. (1998). Estrogen-mediated neuroprotection after experimental stroke in male rats. Stroke *29*, 1666-1670.

Tremere, L.A., Jeong, J.K., and Pinaud, R. (2009). Estradiol shapes auditory processing in the adult brain by regulating inhibitory transmission and plasticity-associated gene expression. J Neurosci *29*, 5949-5963.

Tsao, C.M., Ho, C.M., Tsai, S.K., and Lee, T.Y. (1999). Effects of estrogen on autotomy in normal and ovariectomized rats. Pharmacology *59*, 142-148.

Tsuda, M., Koizumi, S., Kita, A., Shigemoto, Y., Ueno, S., and Inoue, K. (2000). Mechanical allodynia caused by intraplantar injection of P2X receptor agonist in rats: involvement of heteromeric P2X2/3 receptor signaling in capsaicin-insensitive primary afferent neurons. J Neurosci *20*, RC90.

Tsuda, M., Ueno, S., and Inoue, K. (1999). Evidence for the involvement of spinal endogenous ATP and P2X receptors in nociceptive responses caused by formalin and capsaicin in mice. Br J Pharmacol *128*, 1497-1504.

Turner, K.J., Macpherson, S., Millar, M.R., McNeilly, A.S., Williams, K., Cranfield, M., Groome, N.P., Sharpe, R.M., Fraser, H.M., and Saunders, P.T. (2002). Development and validation of a new monoclonal antibody to mammalian aromatase. J Endocrinol *172*, 21-30.

U.S. Food and Drug Administration, C.D.E.R. (1996). Femara (Letrozole) NDA 20-726 Pharmacology Review Part 1, July 24, 1996. Retreived September 1, 2013, from http://www.accessdata.fda.gov/drugsatfda_docs/nda/97/20726_FEMARA%202.5MG_PHARMR_P1.PDF.

U.S. Food and Drug Administration, C.D.E.R. (1998a). Aromasin (Exemestane) NDA 20-753 Clinical Pharmacology Review Part 1, December 21, 1998. Retreived September 1, 2013, from http://www.accessdata.fda.gov/drugsatfda_docs/nda/99/20-753_Aromasin_biopharmr_P1.pdf.

U.S. Food and Drug Administration, C.D.E.R. (1998b). Aromasin (Exemestane) NDA 20-753 Pharmacology Review Part 1, November 30, 1998. Retreived September 1, 2013, from http://www.accessdata.fda.gov/drugsatfda_docs/nda/99/20-753_Aromasin_pharmr_P1.pdf.

Ueno, S., Tsuda, M., Iwanaga, T., and Inoue, K. (1999). Cell type-specific ATP-activated responses in rat dorsal root ganglion neurons. Br J Pharmacol *126*, 429-436.

Van Poznak, C., Hannon, R.A., Mackey, J.R., Campone, M., Apffelstaedt, J.P., Clack, G., Barlow, D., Makris, A., and Eastell, R. (2010). Prevention of aromatase inhibitor-induced bone loss using risedronate: the SABRE trial. J Clin Oncol *28*, 967-975.

Vanderhorst, V.G., Gustafsson, J.A., and Ulfhake, B. (2005). Estrogen receptor-alpha and -beta immunoreactive neurons in the brainstem and spinal cord of male and female mice: relationships to monoaminergic, cholinergic, and spinal projection systems. J Comp Neurol *488*, 152-179.

Vasko, M.R. (1995). Prostaglandin-induced neuropeptide release from spinal cord. Prog Brain Res *104*, 367-380.

Vasko, M.R., Campbell, W.B., and Waite, K.J. (1994). Prostaglandin E2 enhances bradykinin-stimulated release of neuropeptides from rat sensory neurons in culture. J Neurosci *14*, 4987-4997.

Vulchanova, L., Riedl, M.S., Shuster, S.J., Buell, G., Surprenant, A., North, R.A., and Elde, R. (1997). Immunohistochemical study of the P2X2 and P2X3 receptor subunits in rat and monkey sensory neurons and their central terminals. Neuropharmacology *36*, 1229-1242.

Wagner, C.K., and Morrell, J.I. (1996). Distribution and steroid hormone regulation of aromatase mRNA expression in the forebrain of adult male and female rats: a cellular-level analysis using in situ hybridization. J Comp Neurol *370*, 71-84.

Wagner, C.K., and Morrell, J.I. (1997). Neuroanatomical distribution of aromatase MRNA in the rat brain: indications of regional regulation. J Steroid Biochem Mol Biol *61*, 307-314.

Wang, E.C., Lee, J.M., Ruiz, W.G., Balestreire, E.M., von Bodungen, M., Barrick, S., Cockayne, D.A., Birder, L.A., and Apodaca, G. (2005). ATP and purinergic receptor-dependent membrane traffic in bladder umbrella cells. J Clin Invest *115*, 2412-2422.

Wang, J., Lu, K., Song, Y., Xie, L., Zhao, S., Wang, Y., Sun, W., Liu, L., Zhao, H., Tang, D*., et al.* (2013). Indications of clinical and genetic predictors for aromatase inhibitors related musculoskeletal adverse events in chinese han women with breast cancer. PLoS One *8*, e68798.

Warsame Afrah, A., Gustafsson, H., Olgart, L., Brodin, E., Stiller, C.O., and Taylor, B.K. (2004). Capsaicin-evoked substance P release in rat dorsal horn increases after peripheral inflammation: a microdialysis study. Neurosci Lett *368*, 226-230.

Weitzmann, M.N., and Pacifici, R. (2006). Estrogen deficiency and bone loss: an inflammatory tale. J Clin Invest *116*, 1186-1194.

Wempe, M.F., Buchanan, C.M., Buchanan, N.L., Edgar, K.J., Hanley, G.A., Ramsey, M.G., Skotty, J.S., and Rice, P.J. (2007). Pharmacokinetics of letrozole in male and female rats: influence of complexation with hydroxybutenyl-beta cyclodextrin. J Pharm Pharmacol *59*, 795-802.

Wheeler-Aceto, H., and Cowan, A. (1991). Standardization of the rat paw formalin test for the evaluation of analgesics. Psychopharmacology (Berl) *104*, 35-44.

Whelan, T.J., Goss, P.E., Ingle, J.N., Pater, J.L., Tu, D., Pritchard, K., Liu, S., Shepherd, L.E., Palmer, M., Robert, N.J.*, et al.* (2005). Assessment of quality of life in MA.17: a randomized, placebo-controlled trial of letrozole after 5 years of tamoxifen in postmenopausal women. J Clin Oncol *23*, 6931-6940.

Winter, J., Forbes, C.A., Sternberg, J., and Lindsay, R.M. (1988). Nerve growth factor (NGF) regulates adult rat cultured dorsal root ganglion neuron responses to the excitotoxin capsaicin. Neuron *1*, 973-981.

Wozniak, A., and Hutchison, J.B. (1993). Action of endogenous steroid inhibitors of brain aromatase relative to fadrozole. J Steroid Biochem Mol Biol *44*, 641-645.

Wu, M.V., Manoli, D.S., Fraser, E.J., Coats, J.K., Tollkuhn, J., Honda, S., Harada, N., and Shah, N.M. (2009). Estrogen masculinizes neural pathways and sex-specific behaviors. Cell *139*, 61-72.

Xia, J., Lim, J.C., Lu, W., Beckel, J.M., Macarak, E.J., Laties, A.M., and Mitchell, C.H. (2012). Neurons respond directly to mechanical deformation with pannexin-mediated ATP release and autostimulation of P2X7 receptors. J Physiol *590*, 2285-2304.

Xiang, Z., Bo, X., and Burnstock, G. (1998). Localization of ATP-gated P2X receptor immunoreactivity in rat sensory and sympathetic ganglia. Neurosci Lett *256*, 105-108.

Xu, G.Y., and Huang, L.Y. (2002). Peripheral inflammation sensitizes P2X receptor-mediated responses in rat dorsal root ganglion neurons. J Neurosci *22*, 93-102.

Xu, S., Cheng, Y., Keast, J.R., and Osborne, P.B. (2008). 17beta-estradiol activates estrogen receptor beta-signalling and inhibits transient receptor potential vanilloid receptor 1 activation by capsaicin in adult rat nociceptor neurons. Endocrinology *149*, 5540-5548.

Zaccheo, T., Giudici, D., Ornati, G., Panzeri, A., and di Salle, E. (1991). Comparison of the effects of the irreversible aromatase inhibitor exemestane with atamestane and MDL 18962 in rats with DMBA-induced mammary tumours. Eur J Cancer *27*, 1145-1150.

Zhang, L., Hoff, A.O., Wimalawansa, S.J., Cote, G.J., Gagel, R.F., and Westlund, K.N. (2001). Arthritic calcitonin/alpha calcitonin gene-related peptide knockout mice have reduced nociceptive hypersensitivity. Pain *89*, 265-273.

Zhao, H., Tian, Z., Cheng, L., and Chen, B. (2004). Electroacupuncture enhances extragonadal aromatization in ovariectomized rats. Reprod Biol Endocrinol *2*, 18.

Zhu, B.T., and Lee, A.J. (2005). NADPH-dependent metabolism of 17beta-estradiol and estrone to polar and nonpolar metabolites by human tissues and cytochrome P450 isoforms. Steroids *70*, 225-244.

Zimmermann, M. (1983). Ethical guidelines for investigations of experimental pain in conscious animals. Pain *16*, 109-110.

CURRICULUM VITAE

Jason Dennis Robarge

EDUCATION

B.S. Biochemistry	Purdue University	2001
M.S. Genetic Epidemiology	Washington University, School of Medicine	2005
	Advisor: Anne Bowcock, Ph.D.	
	Thesis: *Family-based association mapping for the identification of PSORS4, a psoriasis susceptibility gene mapping to the Epidermal Differentiation Complex on human chromosome 1q21*	
Ph.D. Pharmacology	Indiana University	2014
	Advisors: David Flockhart, M.D., Ph.D., Michael Vasko, Ph.D.	
	Dissertation: *Aromatase inhibitors produce hypersensitivity in experimental models of pain: Studies in vivo and in isolated sensory neurons*	

POSITIONS AND EXPERIENCE

Undergraduate Research – Purdue University, Department of Chemistry	1999 – 2001
Intern – Pharmacia, Structural/Analytical/Medicinal Chemistry R&D	2001
Intern – Purdue Research Foundation, Office of Technology Commercialization	2002
Intern – Pharmacia, Bioprocess and Formulation Technology	2002
M.S. Student – Washington University School of Medicine, Division of Biostatistics	2003 – 2005
Research Technician – Washington University School of Medicine, Division of Human Genetics	2003 - 2005
Biostatistician I – Indiana University School of Medicine, Division of Biostatistics	2005 – 2007
Ph.D. Student – Indiana University School of Medicine, Department of Pharmacology	2007 – 2014

DISTINCTIONS

Howard Hughes Research Internship Award	2000
Washington University, Genetic Epidemiology M.S. Scholarship	2003 – 2005
University Fellowship, Indiana University School of Medicine ($24,000)	2007
Indiana Clinical and Translational Research Institute – Pre-Doctoral Fellowship in Translational Research ($51,500)	2008 – 2010
Department of Defense (DoD) Breast Cancer Research Program – Pre-Doctoral Traineeship Award ($118,544)	2010 – 2013

PROFESSIONAL ASSOCIATIONS

American Society for Clinical Pharmacology and Therapeutics

Society for Neuroscience

Golden Key National Honor Society

Phi Beta Kappa Scholastic Honor Society

ADDITIONAL EXPERIENCE AND PROFESSIONAL TRAINING

"Scientific Writing from the Reader's Perspective" – writing workshop by George Gopen	2009, 2012
spInUp Fellow – Program in intellectual property and technology commercialization offered by the Indiana University Research and Technology Corporation (IURTC)	2012

PUBLICATIONS

In preparation

1. **Robarge JD**, Shariati B, Duarte DB, Skaar TC, Flockhart DA, Vasko MR. Aromatase inhibitors cause mechanical, but not thermal hypersensitivity and augment ATP-induced nociception in rats. *Target journal: Experimental Neurology*
2. **Robarge JD**, Skaar TC, Desta Z, Li L, Nguyen AT, Henry NL, Storniolo AM, Hayes DF, Stearns V, Flockhart DA. Effects of exemestane and letrozole therapy on plasma concentrations of estrogens in postmenopausal women with breast cancer. *Target journal: Journal of Clinical Oncology*

Peer reviewed

3. Henry NL, Chan H, Dantzer J, Goswami CP, Li L, Skaar TC, Rae JM, Desta Z, Khouri N, Pinsky R, Oesterreich S, Zhou C, Hadjiyski L, Philips S, **Robarge J**, Nguyen A, Storniolo AM, Flockhart DA, Hayes DF, Helvie M, Stearns V. Aromatase inhibitor-induced modulation of breast density: Clinical and genetic effects. Br J Cancer 2013; 109:2331-2339.
4. Kim KM, Murray MD, Tu W, **Robarge J**, Ding Y, Brater DC, Flockhart DA. Neurohormonal pharmacogenetics and healthcare outcomes in patients with chronic heart failure. Eur J Clin Pharmacol. 2012; 68(11):1483-91.
5. Henry NL, Nguyen A, Azzouz F, Li L, **Robarge J**, Philips S, Cao D, Skaar TC, Rae JM, Storniolo AM, Flockhart DA, Hayes DF, Stearns V. Lack of association between oestrogen receptor polymorphisms and change in bone mineral density with tamoxifen therapy.. Br J Cancer. 2010; 102(2):294-300.
6. Li L, Borges-Gonzales S, **Robarge J**, Shen C, Desta Z, Flockhart DA. A Penalized Mixture Model Approach in Genotype/Phenotype Association Analysis for Quantitative Phenotypes. Cancer Inform. 2010; 9:93-103.
7. Borges S, Desta Z, Jin Y, Faouzi A, **Robarge JD**, Philip S, Nguyen A, Stearns V, Hayes D, Rae JM, Skaar TC, Flockhart DA, Li L. Composite Functional Genetic and Comedication CYP2D6 Activity Score in Predicting Tamoxifen Drug Exposure Among Breast Cancer Patients. J Clin Pharmacol. 2010; 50(4):450-8.
8. de Cid R*, Riveira-Munoz E*, Zeeuwen PL*, **Robarge J***, Liao W, Dannhauser EN, Giardina E, Stuart PE, Nair R, Helms C, Escaramís G, Ballana E, Martín-Ezquerra G, den Heijer M, Kamsteeg M, Joosten I, Eichler EE, Lázaro C, Pujol RM, Armengol L, Abecasis G, Elder JT, Novelli G, Armour JA, Kwok PY, Bowcock A, Schalkwijk J, Estivill X. Deletion of the late cornified envelope LCE3B and LCE3C genes as a susceptibility factor for psoriasis. Nat Genet. 2009; 41(2):211-5. *** co-first authors**
9. Schneider BP, Radovich M, Flockhart DA, Carpenter JS, Li L, **Robarge JD**, Storniolo AM, Hancock BA, Skaar TC, Sledge GW. Exploratory study evaluating the association of polymorphisms of angiogenesis genes with hot flashes. Breast Cancer Res Treat. 2009; 116(3):543-9.
10. Jin Y, Hayes DF, Li L, **Robarge JD**, Skaar TC, Philips S, Nguyen A, Schott A, Hayden J, Lemler S, Storniolo AM, Flockhart DA, Stearns V. Estrogen receptor genotypes influence hot flash prevalence and composite score before and after tamoxifen therapy. J Clin Oncol, 2008; 26(36):5849-54.
11. Li L, Yu M, **Robarge JD**, Shen C, Azzouz F, McLeod HL, Borges-Gonzales S, Nguyen A, Skaar T, Desta Z, Sweeney CJ, Flockhart DA. A mixture model approach in gene-gene and gene-environmental interactions for binary phenotypes. J Biopharm Stat. 2008; 18(6):1150-77.
12. Henry NL, Giles JT, Ang D, Mohan M, Dadabhoy D, **Robarge J**, Hayden J, Lemler S, Shahverdi K, Powers P, Li L, **Flockhart D**, Stearns V, Hayes DF, Storniolo AM, Clauw DJ. Prospective characterization of musculoskeletal symptoms in early stage breast cancer patients treated with aromatase inhibitors. Breast Cancer Res Treat. 2008; 111(2):365-72.

13. Schneider BP, Radovich M, Sledge GW, **Robarge JD**, Li L, Storniolo AM, Lemler S, Nguyen AT, Hancock BA, Stout M, Skaar T, Flockhart DA. Association of polymorphisms of angiogenesis genes with breast cancer. Breast Cancer Res Treat. 2008; 111(1):157-63.
14. **Robarge JD**, Li L, Desta Z, Nguyen A, Flockhart DA. The Star-Allele Nomenclature: Retooling for Translational Genomics. Clin Pharmacol Ther. 2007; 82(3):244–248.
15. Knoderer HM, **Robarge J**, and Flockhart DA. Predicting asparaginase-associated pancreatitis. Pediatric Blood and Cancer. 2007; 49(5):634-9.
16. Li L, Cheng AS, Jin VX, Paik HH, Fan M, Li X, Zhang W, **Robarge J**, Davuluri RV, Balch C, Kim S, Huang TH-M, Nephew KP. A mixture model-based discriminate analysis for identifying new ordered motif pairs in gene motif modules directly regulated by estrogen receptor-alpha. Bioinformatics. 2006 22(18):2210-6.
17. Dobbs MB, Gurnett CA, Pierce B, Exner GU, **Robarge J**, Morcuende JA, Cole WG, Templeton PA, Foster B, Bowcock AM. HOXD10 M319K mutation in a family with isolated congenital vertical talus. J Orthop Res. 2006; 24(3):448-453.
18. Dobbs MB, Gurnett CA, **Robarge J**, Gordon JE, Morcuende JA, Bowcock AM. Variable hand and foot abnormalities in family with congenital vertical talus and CDMP-1 gene mutation. J Orthop Res. 2005; 23(6):1490-4.
19. **Robarge J**. Electric blanket use and breast cancer. Epidemiology. 2004 15(3):375.
20. Helms C, Cao L, Krueger JG, Wijsman EM, Chamian F, Gordon D, Heffernan M, Daw JA, **Robarge J**, Ott J, Kwok PY, Menter A, Bowcock AM. A putative RUNX1 binding site variant between SLC9A3R1 and NAT9 is associated with susceptibility to psoriasis. Nat Genet. 2003; 35(4):349-56.
21. Shin J, Qualls MM, Boomer JA, **Robarge J**, Thompson DH. An efficient new route to plasmenyl-type lipids: synthesis and cytotoxicity of a plasmenylcholine analogue of the antitumor ether lipid ET-18-OMe. J Am Chem Soc. 2001; 123(3):508-9.

ABSTRACTS

Peer Reviewed

1. Troy C. Quigg, Brian D. Pope, Courtney B. Spiegel, David L. Thacker, **Jason D. Robarge**, Todd C. Skaar, W. Scott Goebel, Jamie Renbarger. Indoleamine 2,3-dioxygenase (IDO) activity is associated with acute graft-versus-host Disease (GVHD) in human allogeneic HSCT. American Society for Blood and Marrow Transplantation/Center for International Blood and Marrow Transplant Research 2013 Tandem Meeting (Salt Lake City, UT).
2. **Jason Robarge**, Djane Duarte, Todd Skaar, Jill Fehrenbacher, David Flockhart, Michael Vasko. The aromatase inhibitor letrozole produces mechanical hypernociception in the rat. Society for Neuroscience 2012 Meeting (Washington, D.C.).
3. **Jason Robarge**, Djane Duarte, Todd Skaar, Michael Vasko, David Flockhart. Investigating the Mechanism of Aromatase Inhibitor-induced Hypernociception. DOD BCRP Era of Hope 2011 Meeting (Orlando, FL).

4. Silvana Borges, Lang Li , **Jason Robarge**, Anne Nguyen, Faouzi Azzouz, Todd C. Skaar, Zeruesenay Desta, David A. Flockhart. A novel CYP2D6 Scoring System for the Prediction of CYP2D6 activity: Application to tamoxifen metabolism. American Society for Clinical Pharmacology and Therapeutics April 2008 (Orlando, FL)
5. N. Lynn Henry, Anne Nguyen, **Jason Robarge**, Lang Li, Jill Hayden, Suzanne Lemler, Anne Schott, Todd C Skaar, David A Flockhart, Daniel F Hayes, Vered Stearns, Consortium on Breast Cancer Pharmacogenomics (COBRA) Investigators. Association of chemotherapy and estrogen receptor genotype with change in bone mineral density after one year of tamoxifen therapy. San Antonio Breast Cancer Symposium December 2007 (San Antonio, TX).
6. N. Lynn Henry, Monika Mohan, Dina Dadabhoy, Vered Stearns, Daniel F. Hayes, Anna Maria Storniolo, Jon T. Giles, Dennis C. Ang, Daniel J. Clauw, Consortium on Breast Cancer Pharmacogenomics (COBRA) Investigators. Aromatase Inhibitor-Induced Musculoskeletal Toxicity in a Prospective Clinical Trial. American Society of Clinical Oncology, Breast Cancer Symposium September 2007 (San Francisco, CA).
7. Vered Stearns, Daniel Hayes, Lang Li, **Jason Robarge**, Todd Skaar, Anne Nguyen, Anne Schott, Anna Maria Storniolo, David Flockhart, Yan Jin. Tamoxifen-Induced Hot Flashes are Associated with Estrogen Receptor Polymorphisms. American Society of Clinical Oncology June 2007 (Chicago, IL).
8. Jia Miao, Yan Jin, Rita Marunde, Milan Radovich, **Jason Robarge**, Lang Li, Stephen D. Hall. Genotypes of CYP3A Cluster were Associated with Midazolam Disposition In Vivo. American Society for Clinical Pharmacology and Therapeutics March 2007 (Anaheim, CA).
9. Allison Taraska, Silvana Borges, Milan Radovich, Santosh Philips, Anne Nguyen, Lang Li, **Jason Robarge**, Bryan Schneider, Suzanne Lemler, David Flockhart, Todd Skaar. Effect of CYP2D6 genotype on antidepressant use patterns. American Society for Clinical Pharmacology and Therapeutics March 2007 (Anaheim, CA).
10. Bryan Schneider, Milan Radovich, George Sledge, Lang Li, **Jason Robarge**, Todd Skaar, Anna Maria Storniolo, Kathy Miller, David Flockhart. Association of genetic polymorphisms of angiogenesis genes and breast cancer risk. San Antonio Breast Cancer Symposium December 2006 (San Antonio, TX).
11. Bryan Schneider, Milan Radovich, David Flockhart, Janet Carpenter, Lang Li, **Jason Robarge**, Anna Maria Storniolo, Suzanne Lemler, Anne Nguyen, Todd Skaar, Kathy Miller, George Sledge. Exploratory study evaluating the association of polymorphisms of angiogenesis genes with hot flashes. San Antonio Breast Cancer Symposium December 2006 (San Antonio, TX).
12. **Jason Robarge,** Lang Li, David Flockhart. A Mixture Model Approach in Analyzing Genotype-Phenotype Association. Presentation. Joint Statistical Meetings August 2006 (Seattle, WA).

Additional

13. **Jason Robarge**, Djane Duarte, Todd Skaar, Michael Vasko, David Flockhart. Investigating the Mechanism of Aromatase Inhibitor-induced Hypernociception. Indiana Clinical and Translational Science Institute 2009 Annual Meeting (Indianapolis, IN).

14. **Jason Robarge**, Todd Skaar, Djane Duarte, Michael Vasko, David Flockhart. Aromatase Inhibitor-induced musculoskeletal Symptoms (AIMSS): Identification of genetic predictors and causative mechanisms. Presentation. Indiana Clinical and Translational Science Institute, Pre-Doctoral Fellows in Translational Research Meeting 2009 (Indianapolis, IN).
15. **Jason Robarge**, Todd Skaar, Djane Duarte, Michael Vasko, David Flockhart. Aromatase Inhibitor-induced musculoskeletal Symptoms (AIMSS): Identification of genetic predictors and causative mechanisms. Indiana Clinical and Translational Science Institute 2009 Annual Meeting (Indianapolis, IN).
16. Rebecca Fletcher, Kirthi Krishnamraju, Anne Nguyen, **Jason Robarge**, Lang Li, Mark Crowder, D Rao, Todd Skaar, David Flockhart, Sean Mooney. Facilitating pharmacogenetic association studies using an extensible genotype information management system. Indiana Bioinformatics Conference May 2007 (Indianapolis, IN).
17. David Bond, Milan Radovich, **Jason Robarge**, Daniel Hayes, David Flockhart, Bryan Schneider. A Retrospective Analysis of Association Between Polymorphisms in Angiogenesis Genes and Incidence of Hot Flashes. Consortium on Breast Cancer Pharmacogenomics. Indiana University Cancer Center Summer Research Program Conference, IUPUI August 2006 (Indianapolis, IN).
18. David Bond, Milan Radovich, **Jason Robarge**, Daniel Hayes, David Flockhart, Bryan Schneider. A Retrospective Analysis of Association Between Polymorphisms in Angiogenesis Genes and Incidence of Hot Flashes. Consortium on Breast Cancer Pharmacogenomics. Committee on Institutional Cooperation Conference Summer Research Opportunities Program, Univ. of Illinois July 2006 (Champaign-Urbana, IL).
19. Lang Li, Sujuan Gao, Silvana Borges-Gonzales, **Jason Robarge**, Anne Nguyen, Zeruesenay Desta, Skaar Todd, Yan Jin, Stephen Hall, and David Flockhart. A Binomial Mixture Model Approach in Analyzing Genotype/Phenotype Association For Binary Phenotypes. Abstract. National Institute of General Medical Sciences, Pharmacogenetics Research Network Annual Meeting, Washington University School of Medicine November 2005 (Saint Louis, MO).
20. Lang Li, Jin Yan, Menggang Yu, **Jason Robarge**, Silvana Borges-Gonzales, Anne Nguyen, Zeruesenay Desta, Skaar Todd, Christopher J. Sweeney, and David Flockhart. A Normal Mixture Model Approach in Analyzing Genotype/Phenotype Association For Continutous Phenotypes. Abstract. National Institute of General Medical Sciences, Pharmacogenetics Research Network Annual Meeting, Washington University School of Medicine November 2005 (Saint Louis, MO).
21. Junhwa Shin, **Jason Robarge**, David Thompson. Development of New Routes to Plasmenylcholines: Facile Synthesis of Plasmalogens and a Plasmenylcholine Analog of the Antitumor Ether Lipid ET-18-OCH_3. Howard Hughes Summer Research Internship Conference, Purdue Univ. July 2000 (W. Lafayette, IN).